Development and Characterization of Chemical Modifications for siRNA Strand Selection

by

Andrew J. Varley

A thesis submitted to the
School of Graduate and Postdoctoral Studies in partial
fulfillment of the requirements for the degree of

Doctor of Philosophy in Applied Biosciences

Faculty of Science

University of Ontario Institute of Technology (Ontario Tech University)

Oshawa, Ontario, Canada

December 2021

THESIS EXAMINATION INFORMATION

Submitted by: **Andrew Varley**

Doctor of Philosophy in **Applied Bioscience**

Thesis title: Development and Characterization of Chemical Modifications for siRNA Strand Selection

An oral defense of this thesis took place on December 13, 2021 in front of the following examining committee:

Examining Committee:

Chair of Examining Committee	
Research Supervisor	Dr. Jean-Paul Desaulniers
Examining Committee Member	Dr. Dario Bonetta
Examining Committee Member	Dr. Sean Forrester
Thesis Examiner	Dr. Olena Zenkina
External Examiner	Dr. Hongbin (Tony) Yan

The above committee determined that the thesis is acceptable in form and content and that a satisfactory knowledge of the field covered by the thesis was demonstrated by the candidate during an oral examination. A signed copy of the Certificate of Approval is available from the School of Graduate and Postdoctoral Studies.

ABSTRACT

Small interfering RNA (siRNA) are non-coding, double-stranded RNA that enable efficient gene silencing through RNA interference (RNAi) mechanisms. The primary effector of RNAi is an RNA-guided nuclease, Ago2, which selects one of the two strands as a guide to form the RNA induced silencing complex (RISC). Incorporation of the antisense, rather than the sense, strand is crucial for potency and safety siRNA therapeutics. Thermodynamic stability, phosphorylation status, and nucleotide sequence play a role in canonical strand selection; however, chemical modifications can improve strand selection and activity. To evaluate the impact of novel chemical modifications on strand activity, an RT-qPCR-based target cleavage assay was developed and validated. Dose-response analysis highlighted the consequence of overdosing, as dosages over 8 pM (for our siRNA sequence) resulted in significant sense strand activity without any on-target benefit. This assay was then used to characterize strand activity for siRNAs carrying azobenzene linkers, propargyl linkers, triazole-bound folate linkers, cubane linkers, hydrophobic phosphotriester modifications, or a 5’ phosphorofluoridate. Antisense vs. sense strand profiles revealed that nucleic acid substitutions (linkers) tend to reduce overall potency, likely due to an altered helical conformation and impaired recognition, but can effectively limit sense strand uptake when placed within the central region. These non-nucleotidyl linkers lack key hydrogen bond interactions between the guide RNA and both Ago2 and target mRNA, which are important for orienting the mRNA for cleavage. Surprisingly, placing a folic acid linker at the sense 3’ end was highly effective at limiting 3’ activity. Hydrophobic phosphate triester modifications have been shown to facilitate carrier-free uptake and are well tolerated. Profiles revealed that small phenethyl linkers had a limited

impact of strand activity while larger octadecyloxy hydrophobic tails were more deactivating, likely due to steric constraints. Lastly, phosphorofluoridate analogues were also developed for their first introduction to siRNA. They exhibited a limited impact on strand activity. This may be the result of enzymatic hydrolysis and replacement with a natural phosphate, or efficient uptake of the modification within Ago2.

Keywords: siRNA; Strand Selection; Chemical Modifications; Gene Therapy; Gene Silencing

AUTHOR'S DECLARATION

I hereby declare that this thesis consists of original work of which I have authored. This is a true copy of the thesis, including any required final revisions, as accepted by my examiners.

I authorize the University of Ontario Institute of Technology (Ontario Tech University) to lend this thesis to other institutions or individuals for the purpose of scholarly research. I further authorize University of Ontario Institute of Technology (Ontario Tech University) to reproduce this thesis by photocopying or by other means, in total or in part, at the request of other institutions or individuals for the purpose of scholarly research. I understand that my thesis will be made electronically available to the public.

_____ ANDREW VARLEY

STATEMENT OF CONTRIBUTIONS

The work described in Chapter III required the synthesis of several siRNAs, performed by Dr. Matt Hammill, Dr. Lidya Salim, and Dr. Kouta Tsubaki. Credit to relevant individuals is stated within each section. Additionally, Afrodet Giorgees performed mass spectrometry analysis on purified phosphorofluoridate modified strands. DNA sequencing was performed by BioBasic (Markham, Ontario). Much of the work described in Chapter III has been published in three publications, with another publication in preparation. 1) "Hammill, ML, Salim, L, Tsubaki, K, Varley, AJ, Kitamura, M, Okauchi, T, and Desaulniers, JP. *ChemBioChem*. **2021**, in press". I performed strand activity assays, contributed ideas, and writing of the manuscript. 2) "Tsubaki, K, Hammill, ML, Varley, AJ, Kitamura, M, Okauchi, T, and Desaulniers, JP. *ACS Medicinal Chemistry Letters*. **2020** 11(7), 1457-1462". I performed strand activity assays and contributed to writing of the manuscript. 3) "Varley, AJ, Hammill, ML, Salim L, and Desaulniers JP. *Nucleic Acid Ther.* **2020,** 30(4), 229-236". As part of an undergraduate thesis project, Shreya Jain contributed towards screening transformants and confirming inactivity of a mutant luciferase enzyme in Chapter II. I performed the majority of the development and design of constructs, subsequent assays required for the publication, the phosphorofluoridate chemistry, and writing of the manuscript. I have used standard referencing practices to acknowledge ideas, research techniques, or other materials that belong to others.

ACKNOWLEDGEMENTS

I would like to thank all of those in my life who have contributed towards the completion of this milestone. First, I would like to extend a special thank you to my supervisor, Dr. Jean-Paul Desaulniers, for not only the opportunity, support, encouragement, and patience he showed as a mentor, but also for redefining what it means to be a graduate student. The time spent in the lab has been far more valuable than just an educational experience, with opportunities to network, present, and travel all while maintaining a healthy work-life balance. You took me in at the brink of leaving academia and am forever thankful for showing me what it could be.

I would also like to thank my committee members Dr. Dario Bonetta and Dr. Sean Forrester. Dr. Bonetta has been a sounding board for difficult experiments with meaningful feedback and support through my PhD, Master's, and even undergraduate studies at Ontario Tech University. Dr. Forrester also provided meaningful suggestions and feedback during and in-between meetings. Thank you both for the time and usage of your lab equipment to make this research possible. I would like to thank Dr. Olena Zenkina, Dr. Tony Yan, faculty members, and staff, especially those who have taught, provided guidance, or otherwise spent their precious time to help produce or examine this work. I would like to thank Dr. Julia Green-Johnson for use of their lab space, equipment, and support through my graduate studies.

I would like to thank my lab mates for their friendship, guidance, and support. Dr. Matthew Hammill, you taught me the ropes as I entered the world of nucleic acid chemistry. Dr. Golam Islam, Ifrodet Giorgees, Charlene Fernandez, Autumn Collins, and Dr. Lidya Salim, you have all contributed to the lab experience and thank you for being

part of it. A special shout out to Ifrodet for running countless MS samples while I try to make sense of my HPLC woes.

To my mother and father, I cannot express enough the gratitude I have for the endless support you've provided throughout my entire academic experience. When I needed to reboot my life, you were there to help and give me not only a place to live, but also instill the mindset needed to persevere through the long journey towards a PhD.

Lastly, I would like to thank my wife, Sierra Varley, for everything she's done in keeping me sane, supported, and healthy throughout my studies. Going through a similar path, you know what I need when I need it, often better than I do. You have taught me a new perspective of what it means to be successful and can't thank you enough to picking up the slack when things get busy.

TABLE OF CONTENTS

LIST OF FIGURES

LIST OF ABBREVIATIONS AND SYMBOLS

A – Adenosine

ACN - Acetonitrile

ASO – Antisense oligonucleotide

C – Cytidine

DMEM-FBS – Dulbecco's modified Eagle's medium with 10% (v/v) fetal bovine serum

DNA – Deoxyribonucleic acid

FDA – U.S. food and drug administration

G – Guanosine

LDL – Low-density lipoprotein

mRNA – Messenger RNA

PCR – Polymerase chain reaction

PIWI – P-element induced wimpy testis

PP – Phenethyl phosphotriester

qRT-PCR – Quantitative real time PCR

RISC – RNA induced silencing complex

RNA – Ribonucleic acid

RNAi – RNA interference

T – Thymidine

TLC – Thin layer chromatography

TRBP - Transactivation response element RNA-binding protein

U – Uridine

UTR – Untranslated region

Chapter I.

Introduction

I.I **Gene Regulation**

Protein expression is the result of two major processes: first, a deoxyribonucleic acid (DNA) sequence is used to transcribe a messenger ribonucleic acid (mRNA), and second, the mRNA transcript is used to translate a polypeptide. The resulting polypeptide then folds into a functional molecule such as an enzyme or structural protein. Once formed, a protein's half-life in the body can range from as short as a few minutes to several years. For simplicity, gene expression can be broken down into three distinct processes: transcription, translation, and post-translational events (Figure 1). Some genes are not protein coding, but rather the RNA itself is the final product with its own cellular functions.

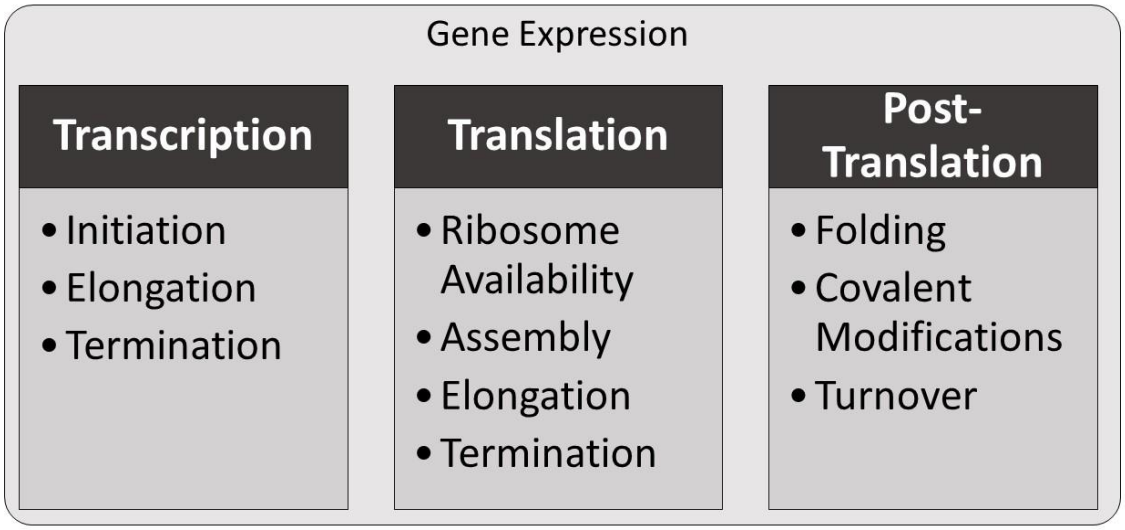

Figure 1: Overview of gene regulation, from transcription to post-translational events.

Nearly all cellular functions rely, at least at some point, on RNA. Therefore, RNA synthesis is tightly controlled at all three stages: initiation, elongation, and termination; however, initiation represents the most important regulatory checkpoint. Transcription factors and regulatory factors are responsible for initiation of transcription and mediating

upstream promoter elements, respectively.[1] The immature transcript then undergoes splicing to remove introns prior to export into the cytoplasm.

Translation is the conversion of the genetic code in mRNA to a protein sequence. This is enabled through sequence pairing of mRNA codons and transfer RNA (tRNA) anticodons. Translational regulation is primarily controlled by ribosomal assembly to mRNA through recognition of the 5' end[2], although elongation, termination, and ribosome availability also play a role. The human ribosome is composed of four RNA strands and 80 proteins[3], divided into two major subunits named 60S and 40S for their sedimentation coefficients in Svedberg units. The 40S subunit binds to the 5' end of mRNA and scans in the 3' direction for the start codon. Once found, the 60S subunit is recruited and translation begins. Elongation continues until the stop codon is reached, at which point release factors bind, and the complex disassembles.

The resulting polypeptide sequence is then folded into a fully functional unit, often with covalent post-translational modifications. For any given synthetic rate of a protein, an adequate degradation rate is also required to maintain optimal protein concentrations within the cell and prevent damaged proteins from persisting. Degradation is regularly controlled by the ubiquitin-proteasome system, a process in which proteins are labelled with a polypeptide tag and subsequently degraded by a corresponding proteasome.[4] Protein degradation plays an important role in many biological functions and the regulation of such is especially important for processes such as the cell cycle.[5]

Protein concentrations are therefore an outcome of transcription, translation, and protein degradation. The improper regulation of any of these processes can lead to diseases such as cancer, autoimmunity disorders, diabetes, neurological disorders and/or obesity. In

particular, gene over-expression can lead to diseases such as Parkinson's[6], Alzheimer's[7], and cancer[8], and are excellent candidates for gene silencing therapies such as RNA interference (RNAi).

I.II Oligonucleotides Therapeutics: Antisense RNA and RNA Interference

I.II.I Brief History of Oligonucleotide Therapy

Oligonucleotide therapy is an approach with over four decades of history. Prior to the discovery of RNAi, antisense RNA (asRNA) was the primary focus of oligonucleotide therapy and was the first antisense oligonucleotide (ASO) approach (Figure 2). asRNA are generally small, untranslated RNA transcripts that pair to complementary messenger RNA (mRNA) to arrest translation.[9] The ability to use these molecules therapeutically was realized in 1978 when eukaryotic RNA induced immunity against a viral pathogen by inhibiting viral protein synthesis.[10] Notably, a similar mechanism occurs when cells are treated with antisense DNA (asDNA); however, DNA-RNA hybrids are also recognized by RNase H, leading to a much more potent therapeutic via cleavage of the hybridized RNA stand.[11]

Theoretically, ASO drugs could be designed to downregulate the expression of nearly any target gene, providing a dramatic advantage over traditional drug design. Six years after the discovery of asRNA, targeted knockdown was achieved through *in vivo* studies in prokaryotic and eukaryotic models (Figure 2).[12–14] Of note, these studies relied on asRNA synthesis from artificially introduced plasmids. However, the difficulty of introducing large plasmids, coupled with an inability to regulate a permanently maintained plasmid, is a concern for clinical trials. Therefore, oligonucleotides were an appealing alternative to plasmid-based therapy, resulting in a major push towards ASO drugs. At the time, the

expertise and labor-intensive synthesis required for ASO drugs was a major roadblock to the design and development of any synthetic oligonucleotide. However, in the early 1980, the development of solid-state oligonucleotide chemistry led to a paradigm shift for both the time and expertise required for synthesis as yield, time, and simplicity of the process was dramatically improved.[15,16] Many steps of RNA synthesis are now automated, and while careful handling of phosphoramidites requires highly qualified personnel, the refined control over reaction conditions have improved reproducibility and costs.

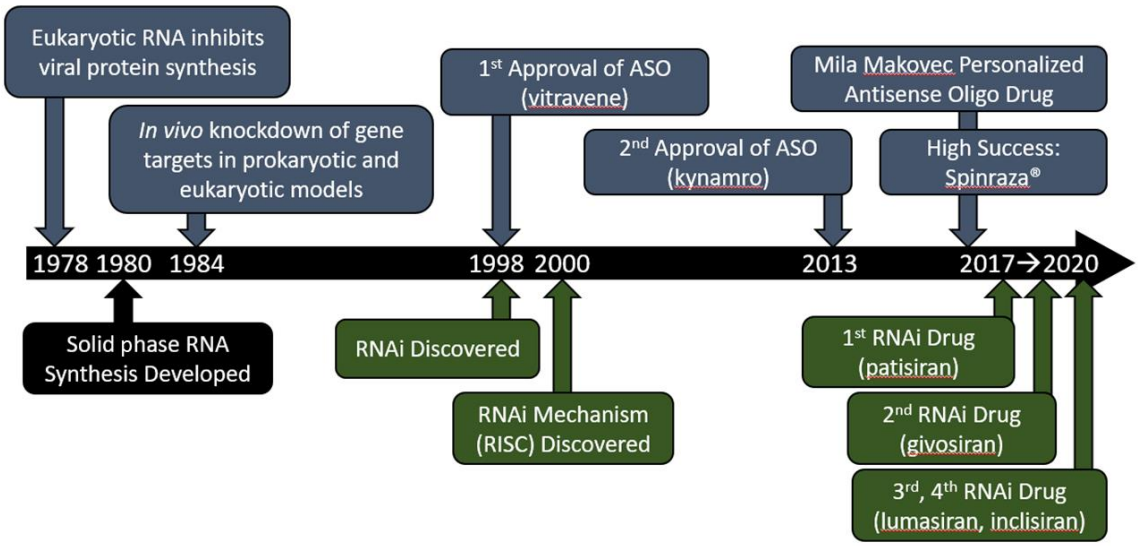

Figure 2: Brief history of antisense oligonucleotides (blue) and siRNA (green). Note that while several other ASOs have been approved since 2013, only the first two are mentioned here.

With the ability to synthesize oligonucleotides and a successful proof of concept, optimism was high for oligonucleotide therapeutics, but clinical approval came slower than anticipated. The first FDA approved antisense drug, Vitravene, wasn't approved until 1998 (Figure 2).[17] This 21 nt phosphorothioate asDNA hybridizes to *Cytomegalovirus retinitis* RNA (a retina-infecting virus which causes blindness) for knockdown via RNase H, particularly important for immunocompromised patients. Although the landmark Vitravene ASO is no longer in production, several ASO have been FDA approved since, with

Spinraza being particularly exciting. Spinraza is an 18 nt phosphorothioate 2'-O-methoxyethoxy antisense oligo carrying 5-methylcytidine monomers that block a splicing site in SMN1 and SMN2 mRNA to treat infants with types 1, 2, and 3 spinal muscular atrophy.[17,18] This drug has had high clinical success, encouraging optimism for RNA drug therapies.

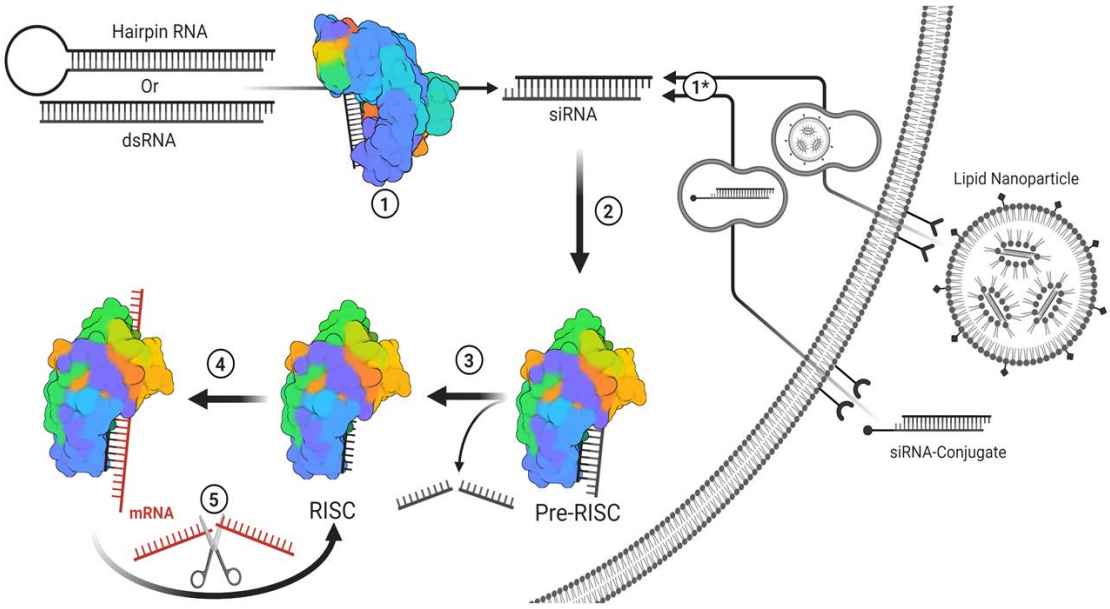

Figure 3: Outline of siRNA mechanisms. (1) Fully complementary endogenous hairpin RNA or double stranded RNA (dsRNA) within the cytoplasm are recognized and cleaved into ~19 bp long RNA with an additional two nucleotide-long overhang on each end. (1) Lipid nanoparticles or conjugated siRNA facilitate cell entry of therapeutic siRNAs. (2) The distinct siRNA structure is recognized by Ago2, forming the pre-RNA induced silencing complex (pre-RISC). (3) The passenger strand is sliced and released from AGO2 to form a mature RISC. (4) The RISC will search for mRNA sequences that are complimentary to the guide strand sequence. The seed sequence (bases 2–8) act as a primer for hybridization of the rest of the strand. Once the seed region is bound, hybridization propagates down the strand. (5) Once completely hybridized with a complementary mRNA sequence, the mRNA is cleaved and released. The RISC is then free to repeat this process to target mRNA in a catalytic fashion. Reproduced with permission.*[126]

One oligonucleotide therapy that has been particularly exciting in recent years is RNAi. The first scientific report of the RNAi phenomenon was by Napoli and Jorgensen in 1990, in which the administration of RNA in an effort to deepen the violet colour in

petunias resulted to in the inexplicable suppression of colour.[19] The term RNAi was coined by Fire and colleagues in 1998 during gene expression experiments in *Caenorhabditis elegans,* when they discovered the dependency of double stranded RNA for activity.[20] Two years later, the RNA-guided nuclease activity of the RNA induced silencing complex (RISC) was discovered in *Drosophila,* outlining the general mechanism for RNAi (Figure 3).[21] Much like ASOs, the discovery of RNAi was met with enthusiasm. The chemical modifications and delivery methods used for ASO technology were equally as applicable to RNAi; however, it still took nearly two decades for RNAi technology to reach therapeutic success. The first FDA approved RNAi drug, patisiran, by Alnylam Pharmaceuticals, was accepted in August of 2018. Patisiran is a double stranded, short interfering RNA (siRNA) that carries several 2'-O-methyl modifications and deoxythymidine overhangs at the 3' ends.[22] Intravenous delivery of patisiran to target tissues is achieved using a lipid nanoparticle (see I.IV for details on siRNA delivery), protecting the siRNA from serum nucleases during transport and facilitating cell entry.[22,23] At this time, three other siRNA therapeutics, givosiran, lumasiran, and inclisran, have been approved by federal health organizations. Notably, these three siRNAs are heavily chemically modified and use a trivalent GalNAc conjugate rather than a lipid nanoparticle for hepatic delivery (see I.IV for details).

I.II.II Personalized Medicine

Oligonucleotide therapeutics are unique in the drug world for the separation of their 'pharmacophore' and 'dianophore' features that determine target specificity and tissue distribution/metabolism, respectively.[24] Once the ideal dianophore for a particular tissue or cell type is defined, the pharmacophore can be selected based on the sequence alone. This

facilitates the possibility of rapid drug development and personalized medicine. Examples have already been seen as in the case of Mila Makovec, a child suffering from a fatal neurodegenerative disorder. In 2017, her genome was sequenced, the detrimental ~2000 base pair repeating insertion was identified, and an ASO drug named milasen was developed.[25] This treatment significantly improved quality of life for the patient until their unfortunate passing in Feb 2021; however, financial, labor, and ethical constraints limit similar treatments for most individuals. Novel breakthroughs in oligonucleotide therapeutics aim to improve delivery methods, specificity, potency, and costs of these drugs.

I.III **Mechanisms and Proteins of the RNAi Pathway**

I.III.I Small RNA Biogenesis

There are three principal modes for mammalian small RNA biogenesis: microRNA (miRNA), small interfering RNA (siRNA), and Piwi-interacting RNA (piRNA) pathways.[26] For each small RNA category, multiple biogenesis pathways exist.

The miRNA biogenesis pathway begins with imperfectly paired RNA hairpins.[27] This transcript is recognized by the nuclear protein DiGeorge Syndrome Critical Region 8 (DGCR8) and associates with the nuclease Drosha to form the microprocessor complex.[28] In the canonical pathway, the complex cleaves the 5' cap and 3' poly-A tail, allowing export of the hairpin pre-miRNA.[29] Notably, about half of all pre-miRNA molecules are generated from spliceosome cleavage and therefore intragenic regions.[30] Once within the cytoplasm, pre-miRNA hairpins are cleaved by the nuclease Dicer, forming a mature double stranded miRNA duplex.[31]

siRNA biogenesis is like that of miRNA, and forms as the result of endogenous or exogenous (viral) sources. Endogenous pre-siRNA originates from either inverted repeat sequences (forming hairpin-siRNA), *trans* derived loci, or a *cis* derived locus (Figure 4).[32] Like miRNA, siRNA is also cleaved by Dicer once exported to the cytoplasm.

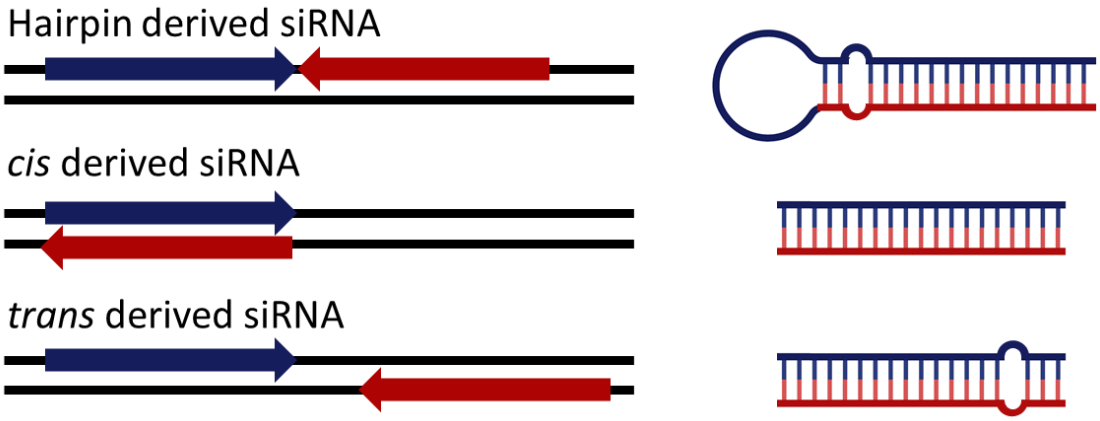

Figure 4: Origins and resulting structures of endogenous siRNA.

Much of what is known about piRNA biogenesis has been derived from *Drosophila melanogaster*, with few only some parallels seen in mammals. piRNA biogenesis is markedly different than siRNA, both for using ssRNA as a precursor and its independence from Dicer, relying instead on the single stranded phosphodiesterase named Zucchini.[33,34] Once hydrolyzed, the piRNA products contain a 5'-phosphate and 3'-hydroxyl group which is loaded into a Piwi-clade Argonaute protein. piRNA pathways are restricted to germline cells and not pertinent for this study.

I.III.II Dicer

The nuclease Dicer is essential for canonical siRNA and miRNA processing. Dicer is an RNase III family ribonuclease that cleaves siRNA and miRNA into ~19 base pair dsRNA with two nucleotide 3' overhangs on either end (Figure 5).[35] Post-cleavage, Dicer

facilitates efficient loading of the siRNA into Argonaute 2 (Ago2) during a hand-off event. This is exemplified by a 100-fold increase in potency of a 27 nt long precursor dsRNA (compared to conventional 21 nt long siRNA), which must act as a substrate for Dicer prior to uptake by Ago2.[36]

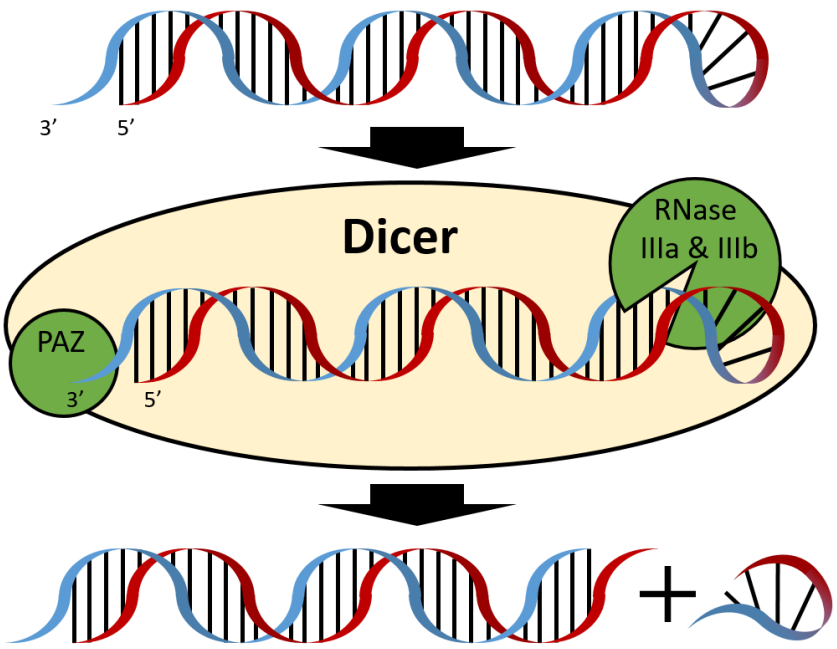

Figure 5: Dicer mediated cleavage of siRNA. Dicer recognizes 3' overhands on dsRNA via the PAZ domain and cleaves ~19 bp upstream via RNase IIIa and RNase IIIb domains, releasing short hairpins (shown) or longer dsRNA strands (not shown).

The siRNA hand-off is facilitated by recognition between the PIWI box (within the PIWI domain) of human Argonautes and an RNase III domain of Dicer.[37] Additionally, the RNA-binding cofactor of Dicer, transactivation response element RNA-binding protein (TRBP), improves Dicer processing of precursor miRNA (and possibly precursor siRNA) in RNA-crowded environments.[38] Unlike *D. melanogaster*, human Dicer is not essential for asymmetric RISC loading[39] (see section **I.III.IV** for more details on asymmetrical

loading). It is also worth noting that although Dicer plays an important role in small RNA biogenesis, Dicer independent siRNA and miRNA pathways also exist.[40,41]

I.III.III Argonaute

The term Argonaute was named after an *Arabidopsis thaliana* mutant which resembled the small squid *Argonauta argo*.[42] Argonaute proteins are classified into three major paralogous groups: Argonaute-like proteins (similar to *Arabidopsis thaliana* AGO1), Piwi-like proteins (closely related to *Drosophila melanogaster* PIWI), and the *Caenorhabditis elegans* specific group 3 Argonautes.[43] Humans carry eight Argonaute genes: four Argonaute-like and four Piwi-like. Piwi-like proteins function distinctly from Argonaute proteins and are primarily restricted to germ line cells where they function in a Dicer independent manner (reviewed elsewhere[53]).

Argonaute (Ago) proteins are the central effector molecules across RNAi pathways and programmed for their targets by guide RNA. The system is widespread across animals and responsible for regulating gene-expression networks, development, proliferation, metabolism, and the DNA-damage response.[45] Of the four Ago proteins (Ago1-Ago4) in humans, only Ago2 is nuclease active and capable of target mRNA cleavage.[46] This nuclease activity is also essential for efficient maturation of the RISC. The immature RISC is formed when double stranded siRNA is loaded within Ago2 and will become fully functional once the passenger strand is cleaved. Notably, the nuclease domain is responsible for cleavage of both target mRNA and passenger strand RNA. This cleavage occurs between nucleotides opposite position 10 and 11 relative of the 5’ end of the guide strand.[47] Once the passenger strand is cleaved, the two short strands no longer form a

thermodynamically stable hybrid and are released from the complex (aided by the N-terminal domain[48]), forming a mature RISC.

The miRNA pathway is also mediated by Argonaute proteins. miRNA is a common mechanism for endogenous gene regulation and small RNAs are predicted to regulate over 60% of human genes.[49,50] Unlike siRNA, miRNA mechanisms do not result in target cleavage, but instead, downregulation is due to the inhibition of initiation or elongation.[51] Many miRNA-guided Argonautes target the 3' untranslated region (UTR) of genes where they exhibit silencing via translational repression, deadenylation, and/or mRNA decay.[52–

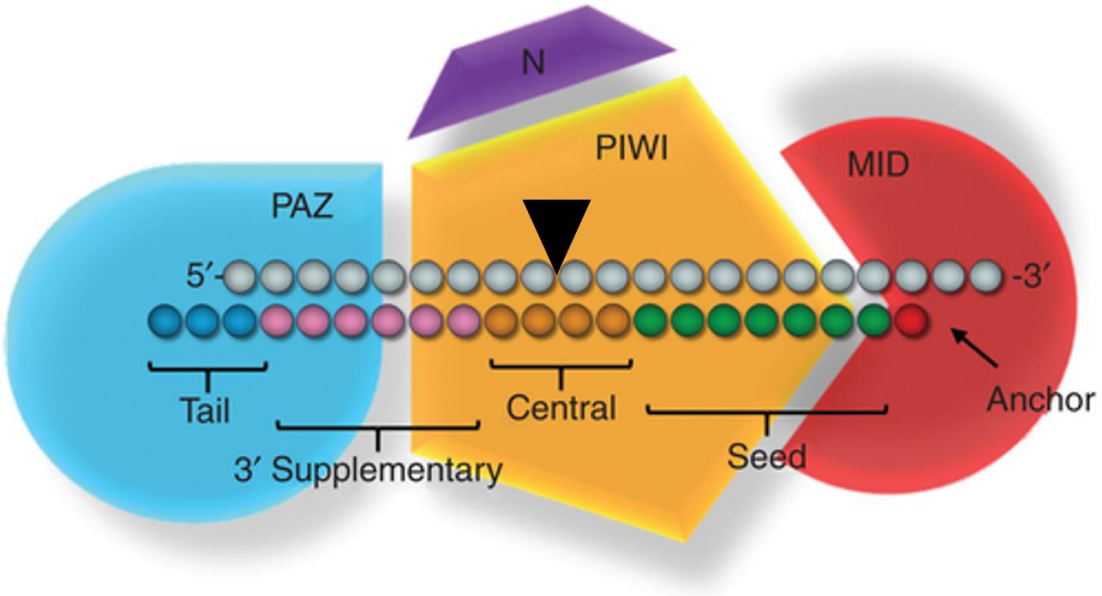

Figure 6: Argonaute 2 (Ago2) domains and RNA regions. Black arrow indicates passenger/target strand cleavage site. Adapted with permission.[117]

[54] Notably, Argonaute proteins are also responsible for roles outside of RNAi, with functions ranging from heterochromatin silencing[55] to upregulating translation.[56]

Argonaute proteins contain four distinct functional domains: the N (terminal), PAZ, MID, and PIWI domains (Figure 6). While both Argonaute and Dicer contain a 3' sensing

PAZ domain, Argonaute is distinct from Dicer for the absence of a large extended loop.[57] The PAZ domain is essential for binding the 3' overhangs in a sequence independent manner with low affinity, enabled by an oligonucleotide/oligosaccharide binding like fold.[58,59] The ability to bind 3' overhangs is a distinguishing factor that preferentially selects small regulatory RNAs (which carry 3' overhangs) against degraded RNAs in non-related pathways.[43]

The nuclease activity of Ago2 is found within a P-element Induced Wimpy testis (PIWI) domain, a highly conserved RNA-binding motif which adopts an RNase H type fold associated with RNA cleavage.[60,61] Notably, the PIWI domain contains a divalent metal ion and carries a slightly more degenerative catalytic core (Asp-Asp-Asp/Glu/His/Lys) than RNase H.[62] The MID domain anchors the 5'-nucleotide of an siRNA or miRNA with a bias for U or A.[63] The deep binding pocket shields the 5' nucleotide of small RNA, separating it from the target strand. This is in agreement with previous reports suggesting that the 5'-end nucleotide plays a no significant role in substrate mRNA recognition.[64,65]

Studies have found that targeting mutant alleles with a single nucleotide polymorphism proposes challenges as downregulation of the wildtype and disease allele is often observed.[66] Improved discrimination between alleles can be achieved by introducing a mismatch to destabilize binding between the guide and target; explained by the excess energy model which can be applied to all RNA-guided nucleases.[66]

I.III.IV Asymmetric Loading of siRNA

This section focuses on mechanisms behind endogenous asymmetric loading of siRNA and do not widely apply to therapeutic siRNA, which do not depend on Dicer.

Asymmetrical sensing refers to the ability for the RISC to preferentially load one strand of the miRNA/siRNA over the other, known as the asymmetry rule. Preferential selection of a strand relies on three primary factors: phosphorylation of the 5' end, an A or U at the 5' terminal[67], and overall thermodynamic stability of the 5' end (Figure 7).[68,69] Once bound to Ago2, the passenger strand of the RNA duplex is cleaved by the PIWI domain and the N terminal assists in release from the RISC.[48] While *Drosophila* requires Dicer for

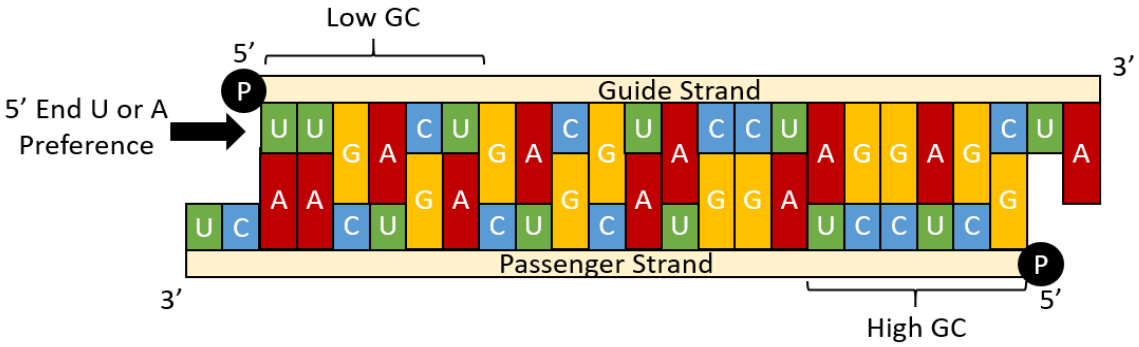

Figure 7: Major factors for guide strand selection by human Ago2. A 5' uridine or adenosine are preferentially chosen as well as the end with overall lower thermodynamic stability (lower GC). A 5' monophosphate group must be present for strand incorporation.

asymmetrical sensing, the mechanisms behind Dicer-independent strand selection in human Ago2 are less understood.[70] Importantly, Dicer is not necessary for asymmetrical loading therapeutic siRNAs.

Dicer-dependent asymmetrical sensing relies on interactions with TRBP, which aids an internal Dicer domain in sensing of the least thermostable 5' end.[71] The free 3' end of the guide strand is then free for Ago2 to bind and incorporate into Ago2 during Dicer/Ago2/TRBP interactions. Other reports suggest that TRBP alone could recognize siRNA asymmetrically.[72]

I.III.V Ago2-Guide RNA Interaction

The human Ago2 crystal structure reveals extensive hydrogen bonding between Ago2 and the first several residues of the 5' guide RNA within a central cleft.[73] The terminal 5' phosphate is anchored within a conserved basic pocket (consisting of tyrosine, two lysine, and a glutamine residue), containing the carboxy-terminal carboxylate and the divalent cation, Mg^{2+}.[61,63,74] The Mg^{2+} atom is octahedrally coordinated to three amino acid oxygens, two phosphate-group oxygens, and a water molecule.[74] The binding pocket preferentially selects bases U or A at the 5' terminal nucleotide due to hydrogen bonding at the Watson-Crick edge. This sequesters the nucleobase such that it does not contribute to target recognition.[75,76] Bases 2-8 of the 5' end are responsible for initial hybridization during target recognition and positions the target mRNA for eventual cleavage.[73,74]

Interactions between the PAZ domain of Ago2 and the 3' end tail of the gRNA are mediated through hydrogen bonds and salt linkages to the RNA backbone with no sequence preference.[77] Stable anchoring of the 3' end is essential for unwinding and passenger release.[78] Interestingly, complete target recognition displaces the 3' end of the guide strand from the PAZ cleft, likely leaving it vulnerable to nuclease activity. Upon release, the PAZ domain again fastens the 3' end of the guide strand.

I.IV **siRNA Chemistry, Delivery, and Development**

I.IV.I RNA Structure and Stability

Ribonucleic acid (RNA) and deoxyribonucleic acid (DNA) monomers are composed of three key parts: a nucleobase, D-ribose carrying one or two hydroxyl groups, and a phosphate. The nucleobase is covalently bound to the anomeric carbon of β-D-ribofuranose (RNA) or β-2-deoxyribofuranose (DNA), with each sugar coupled by a 3'-5' phosphodiester bond to form polymers. Both DNA and RNA contain the nucleobases adenine (A), cytosine (C), and guanine (G), while thymine (T) is only found in DNA and uracil (U) is only found in RNA. A 2' hydroxyl on RNA distinguishes it from DNA, which imparts instability due to nucleophilic attack to the tetracoordinated phosphate backbone, hydrolytically cleaving (or isomerization) of the RNA (Figure 8). High pH and temperatures facilitate this reaction, with higher stability found at pH 4-6[79], and long term

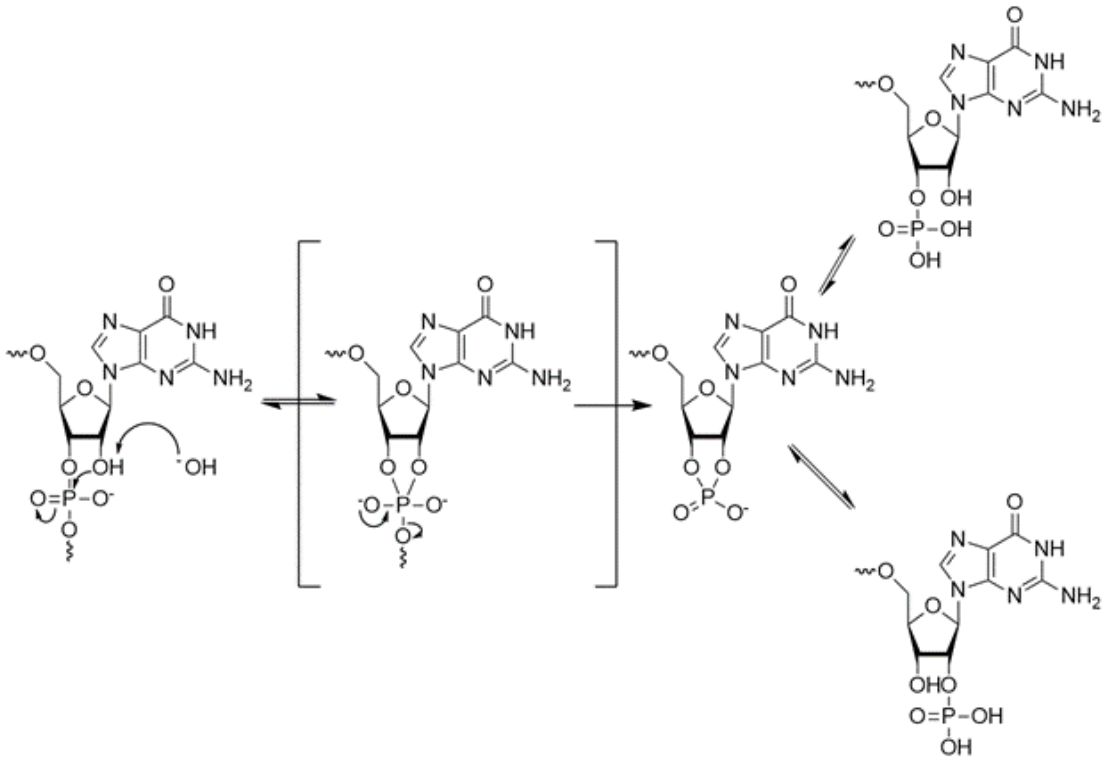

Figure 8: Hydrolysis of RNA due to nucleophilic attack from the 2' hydroxyl group.

RNA storage solutions are typically slightly acidic. Auto-hydrolysis is promoted by Mg^{2+} at temperatures above 37 °C, therefore buffers often contain ethylenediaminetetraacetic acid (EDTA) to chelate the divalent cation.[80]

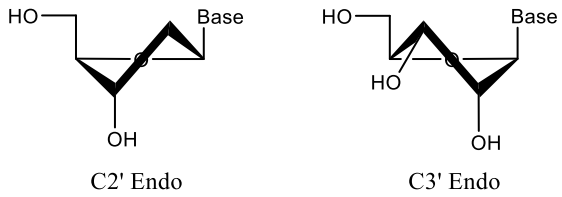

Figure 9: Sugar pucker conformations of dsDNA (left) and dsRNA (right)

In nature, DNA is usually found as a double stranded helix, whereas RNA can fold upon itself to form complex secondary structures and partially hybridize to multiple strands. Double stranded DNA forms a right-handed B-form duplex due to the preference for C2' endo sugar conformations. Double stranded RNA forms a similar, but thicker A-form duplex with a shorter distance between base pairs due to the preference for C3' endo sugar conformation (Figure 9). DNA-RNA hybrids generally exist as A-form. A third and radically different structure, Z-form, is characterized by a left-handed helix with 'zig-zag' pattern in the phosphodiester backbone. The cellular roles for Z-form DNA and RNA is poorly understood and few protein interactions have been described.[81]

I.IV.I Solid Phase RNA Synthesis

High efficiency, reactant availability, and ease of automation have made nucleoside phosphoramidite solid-phase synthesis the gold standard to produce synthetic oligonucleotides. A phosphoramidite is a monoamide of a phosphite diester. When a nucleoside or artificial spacer phosphoramidite must be synthesized in-house, the commercially available 2-cyanoethyl N,N-diisopropylchlorophosphoramidite can act as a

phosphitylating reagent for the 3'-hydroxyl group. Controlled-pore glass or polystyrene are two widely used solid supports for oligonucleotide synthesis, the prior being the support most used in the Desaulniers lab. Aminopropyl groups attached to the supports covalently bind a non-nucleosidic linker or a nucleoside succinate to act as a starting point for synthesis.

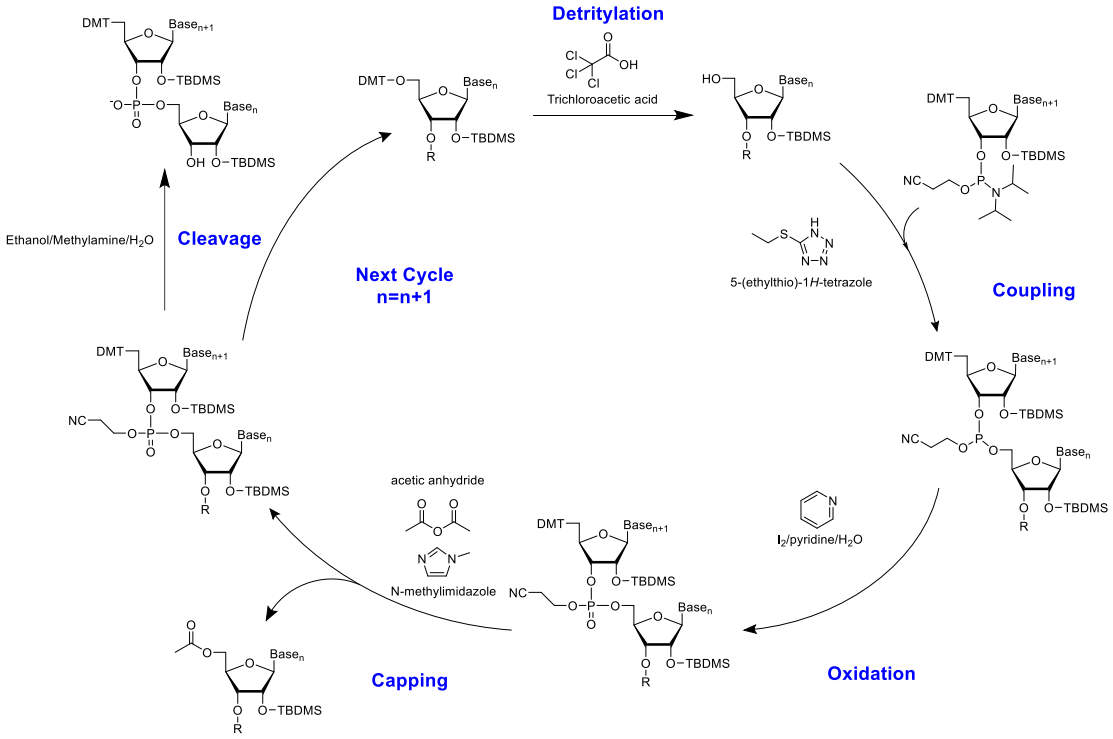

Figure 10: Solid-state DMT-phosphoramidite oligonucleotide RNA synthesis.

Oligonucleotide synthesis occurs in the 3' to 5' direction through the stepwise addition of nucleotide residues to the 5' terminus of the growing chain (Figure 10). Four distinct chemical reactions occur for each nucleotide addition, which repeat in a cyclical fashion. First, the 4,4'-dimethoxytrityl chloride (DMT) group is removed with trichloroacetic acid (TCA) in acetonitrile. Second, the nucleoside phosphoramidite is activated with 5-(ethylthio)-1*H*-tetrazole, which couples with a 5'-hydroxyl group to afford a phosphite triester linkage. Third, acetic anhydride is used to cap unreacted 5'-hydroxyl

groups, preventing downstream extension of coupling-failed oligos. Lastly, I_2 is added in water with pyridine to oxidize the tricoordinated phosphite triester linkage into a tetracoordinated phosphate triester. The non-linking phosphate ester bond carries a cyanoethyl group, protecting the oxygen from reactions until the RNA is cleaved from the support and deprotected.

Once the desired RNA sequence is synthesized, it must be cleaved from the linker, deprotected, and purified. Cleavage from the solid support and deprotection of base-labile protecting groups is facilitated by 40% methylamine in 1:1 water:ethanol and the soluble RNA is collected. Finally, the 2' hydroxyl is deprotected using hydrogen fluoride at 65 °C in DMSO to remove the *tert*-butyldimethylsilyl protecting groups. RNA is precipitated, desalted, and can be purified via HPLC or PAGE.

I.IV.II Lipid Nanoparticle Delivery

Effective delivery of siRNA faces several major challenges. These large (~14kDa), hydrophilic polyanions electrostatically resist passage through the plasma membrane and they must evade nuclease degradation prior to cell entry. They must also gain cell entry to the desired tissue type while avoiding immune and elimination systems which effectively clear siRNA from the body.[82]

Lipid nanoparticle (LNP) delivery was the method of choice for the first accepted siRNA therapeutic, patisiran. LNPs have proven effective for hepatic delivery and protect RNA from degradation by ribonucleases present in the plasma. Hepatic delivery is particularly effective due to the fenestration of the liver and recognition of LNPs by ApoE, an apolipoprotein that associates with lipid particles for recognition by hepatic low-density lipoprotein (LDL) receptors.[83] LNP formulations can be modified for extrahepatic delivery,

but current designs carry a prohibitively high cost for transfection competency.[84] Once recognized by target cells, LNPs are engulfed within the cell and proceed through the conventional endocytic route (early endosome, late endosome, lysosome). The process in which RNA is released from both the LNP and cellular container is poorly understood, and only a small fraction (1-2%) are expected to evade lysosomal degradation.[85] However, late endosome/lysosome formation may be essential for the functional delivery of oligonucleotides.[86]

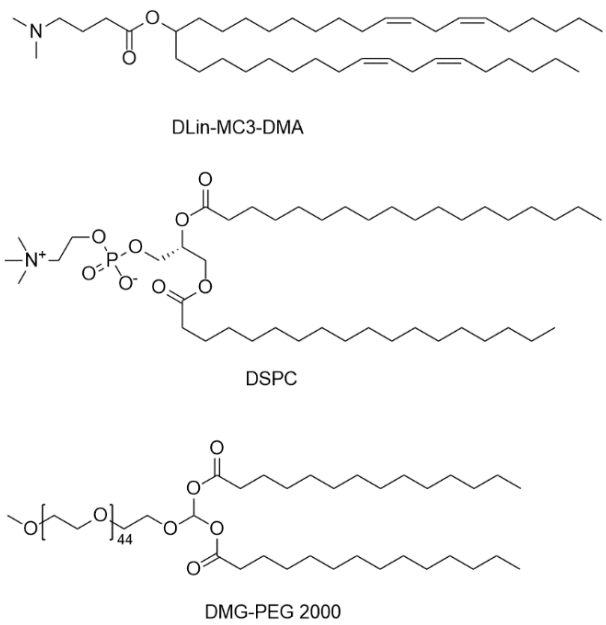

Figure 11: Lipids used in the assembly of the lipid nanoparticle used in patisiran/Onpattro.

The composition of the lipid nanoparticle facilitates effective cellular uptake after intravenous delivery of the drug. While many formulations exist, patisiran is encapsulated and delivered within an LNP composed of cholesterol, 1,2-distearoyl-sn-glycero-3-phosphocholine (DSPC), (6Z,9Z,28Z,31Z)-heptatriaconta-6,9,28,31 tetraen-19-yl-4-(dimethylamino) butanoate (DLin-MC3-DMA), and 1,2-dimyristoyl-rac-glycero-3-methoxypolyethylene glycol-2000 (PEG_{2000}-C-DMG) (Figure 11). Cholesterol and DSPC

are included to improve physicochemical stability of the LNP.[87,88] DLin-MC3-DMA is a neutral ionizable lipid that is predicted to aid in particle formation, fusogenicity, cellular uptake, and endosomal release of the siRNA.[88,89] PEG_{2000}-C-DMG also aids in stability, but also increases circulation time.[88,90] The ratio of each of these components dramatically impact the overall success of the LNP; patisiran used a ratio (by weight) of 1 siRNA: 3.1 cholesterol: 6.5 DLin-MC3-DMA: 1.65 DSPC: 0.8 PEG_{2000}-C-DMG.

A discussion of LNPs would not be complete with discussing the role they have played in the ongoing SARS-CoV-2 global pandemic. At the time of writing, only four vaccines are approved for use in Canada, and two of them (Moderna's SpikeVax and Pfizer-BioNTech's Comirnaty) utilize LNP for delivery of an mRNA vaccine. LNP-mRNA formulations for cancer therapies have been in clinical trials since 2014, while clinical trials for LNP-mRNA formulations for influenza vaccines and protein replacement therapies began in 2017.[91] This set the stage well for the rapid development of anti-SARS-CoV-2 LNP-mRNA vaccines, and without the LNP delivery system, these vaccines would not be possible. The massive funding influx for these technologies will likely result in substantial advancements in LNP formulations, including efficiency of delivery and extrahepatic targeting.

I.IV.III Conjugate Delivery

Systemic delivery of unprotected (naked), unmodified siRNA is not feasible due to the rapid degradation and clearance of serum RNA from nucleases and elimination systems. However, recent advancements in siRNA chemistry have opened the possibility of delivering extensively modified, naked siRNA. Instead of an LNP for delivery to target tissues, these siRNA are conjugated to membrane-permeating molecules or receptor ligands. Early work with siRNA conjugates focused on membrane-permeant peptides, polyethylene glycol, or cholesterol-modified siRNAs[92], with cholesterol-modified siRNAs gaining significant attention. Both cholesterol-formulated LNPs and cholesterol-modified siRNAs are readily taken up by the liver, but siRNA conjugates can go a step further to effectively target extrahepatic tissues. For example, Biscans and colleagues[93] measured tissue specific uptake and retention of various lipid-conjugated siRNA with markedly increased uptake by the heart and lung for docosanoic acid-conjugated siRNA. Also, folic acid modified siRNAs facilitate uptake into key cell types, such as macrophages and folate receptor alpha over-expressing cancers.[94–96] Currently, only a single siRNA conjugate, the trivalent GalNAc (Figure 12), has achieved market approval and is currently used in three of the four approved siRNA therapeutics. The GalNAc conjugate binds with high specificity to the asialoglycoprotein receptor on hepatocytes, demonstrating the efficacy of a functional tissue delivery system.[97–100]

Unlike LNP encapsulated siRNA, naked siRNA must tolerate nuclease assault in the blood. Therefore, the success of siRNA conjugates depends on well tolerated modifications that avoid rapid nuclease hydrolysis during systemic transport. These modifications also provide significant benefit for length of activity, as persistence within intracellular

components can serve as a long-term depot for siRNA conjugates with duration of therapeutic effect of up to a year.[101]

I.IV.IV Current siRNA Therapeutics

The FDA approval of Onpattro® (patisiran) by Alnylam Pharmaceuticals in 2018 marked the introduction of a new class of therapeutics: siRNA drugs.[102] Not only was this a breakthrough for siRNA therapeutics, but also for the field of antisense oligonucleotides and LNP delivery as the fundamental science behind many aspects of these drugs are alike. Administration of patisiran activates the RNAi pathway and leads to >85% knockdown of transthyretin (TTR), substantially improving outcomes for patients with hereditary amyloidogenic transthyretin (ATTRv) amyloidosis.[103] This disease is caused by mutant TTR proteins which results in the deposition of amyloid fibrils in multiple organs, leading

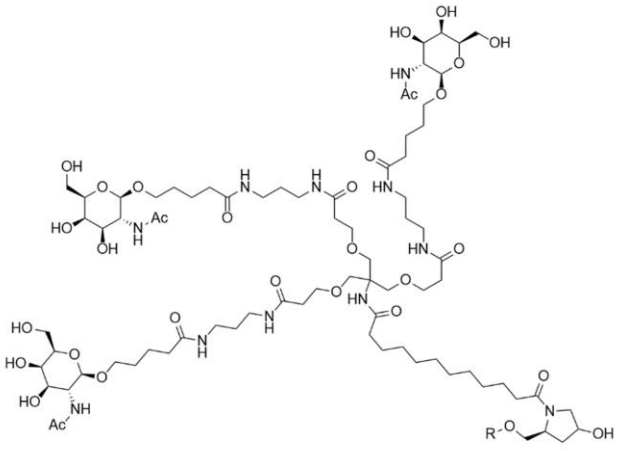

Figure 12: Trivalent GalNAc cluster. R designates 3' end of the sense strand.

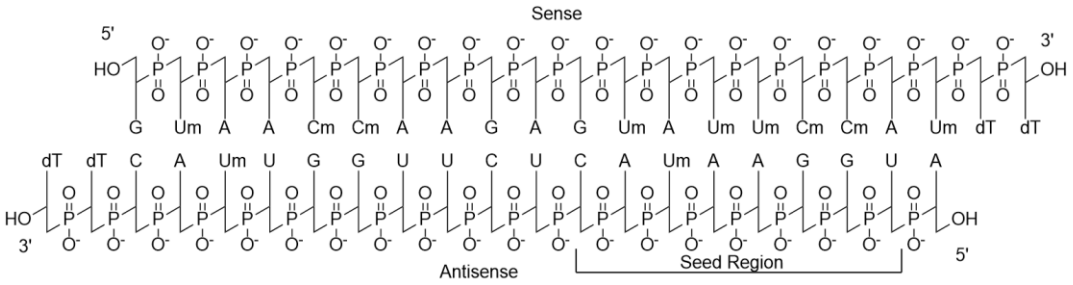

Figure 13: Structure and chemical modifications used in patisiran/Onpattro®. Abbreviations include A, adenosine; C, cytidine; G, guanosine; U, uridine; Cm, 2'-O-methylcytidine; Um, 2'-O-methyluridine; and dT, thymidine.

to neurodegeneration.[104] While patisiran was novel as the first approved drug to utilize siRNA or lipid nanoparticles, the chemical nature of patisiran was primarily that of natural RNA monomers, with roughly a quarter of them carrying the 2'-O-methyl nucleotide analogues (Figure 13). These modifications are well studied and synthetic oligonucleotides containing these modifications are commercially available.

The second FDA approved siRNA drug was givosiran/Givlaari® in 2019, which treats hepatic porphyria. This rare disorder leads to a buildup of toxic porphyrin molecules which form during heme production. Givosiran targets hepatic *ALAS1*, effectively preventing the accumulation of neurotoxic heme intermediates.[105] Instead of an LNP, givosiran uses a GalNAc conjugate bound to the 3' end of the sense strand for targeted uptake to hepatocytes (discussed in **I.IV.III**). Without the protection of an LNP, givosrian was extensively chemically modified for protection from serum nucleases. Phosphorothioate linkers were used at the non-conjugated termini, and every nucleotide carried either a 2'-O-methyl or 2'-fluoro ribose modification (Figure 14).

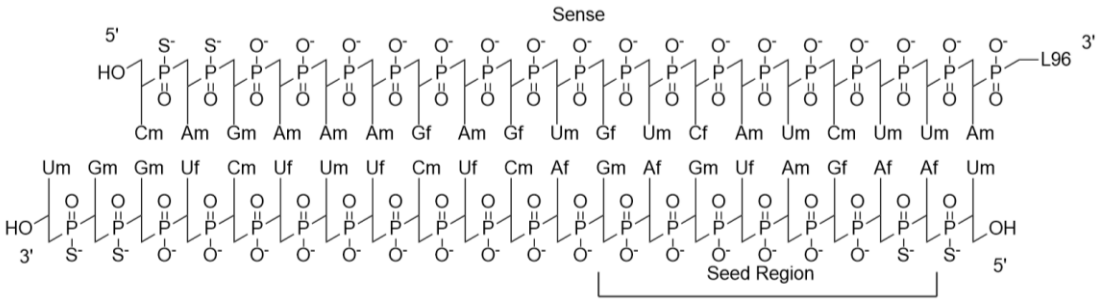

Figure 14: Structure and chemical modifications used in givosiran/Gilvaari®. Abbreviations used include: Am, 2'-O-methyladenosine; Gm, 2'-O-methylguanosine; Cm, 2'-O-methylcytidine; Um, 2'-O-methyluridine; Af, 2'-fluoroadenosine; Gf, 2'-fluoroguanosine ;Cf, 2'-fluorocytidine;Uf, 2'-fluorouridine; and L96, the GalNAc cluster depicted in Figure 12.

Two other siRNA therapeutics developed by Alnylam have been approved: lumasiran/Oxlumo (FDA approval, 2020) and inclisiran/Leqvio® (EU approval, 2020, currently owned by Novartis). Both siRNAs use a similar design to givosiran, targeting the liver via a trivalent GalNAc and use the same chemical modifications with similar designs. Lumasiran treats primary hyperoxaluria, characterized by high oxalate production resulting in urinary obstruction and kidney damage.[106] This drug silences the HAO1 mRNA, responsible for glycolate oxidase. Inclisiran is the first approved siRNA to target a wider population, which treats atherosclerotic cardiovascular disease due by reducing LDL cholesterol but has not achieved FDA approval at this time.

I.IV.V Considerations for Cell Culture

Mammalian cell cultures provide an essential tool to study cellular responses, including those of siRNA treatments. While these studies provide consistency and reproducibility in results, researchers cannot assume that cells function in a similar manner within organs of a multicellular organism. The absence of a proper mechanical environment[107], physiological oxygen concentrations[108], and removal of waste products[109] represents considerable limitations of cell culture and responses are generally studied

within a narrow scope of cell types. Lastly, the cultures are grown in media that do not perfectly mimic serum composition, and the medium chosen can have significant consequences. For instance, a recent study by van Essen and colleagues discovered that the culture medium used during siRNA transfection experiments determined the maturation status of dendritic cells.[110] Therefore, organism outcomes from siRNA treatments are not well predicted by cell culture, and some research groups opt to limit or omit cell culture treatments in favour of small mammals studies.

I.V **Strand Selection for Therapeutic siRNAs**

During RISC maturation, either the antisense or the sense strand is selected as the guide strand. Incorporation of the sense strand is a major concern for therapeutic siRNAs for two reasons. Firstly, any strand that is incorporated into Ago2 may exhibit miRNA-like off-target effects. These are typically the result of recognition within the seed region (nucleotides 2–8) to the 3′UTR of mRNAs, which leads to widespread gene down regulation in an miRNA-like fashion.[111–113] Therefore, limiting siRNA uptake to a single strand limits the number of possible off-target gene targets. If sense strand uptake is unavoidable, its activity can be mitigated through chemical modifications and design strategies which reduce seed-region binding and possible matches in the 3'UTR, respectively.[114–116] Secondly, the selection of the sense strand leads to the degradation and/or removal of the antisense strand, rendering it ineffective. This means more siRNAs must be added to achieve the desired knockdown efficiency, typically contributing to more impactful immune responses. Additionally, therapeutic siRNAs compete with the endogenous miRNA pool, potentially leading to saturation of the RNAi machinery.[117] High siRNA payloads can therefore lead to global de-repression of miRNA-repressed genes.

The extensive coordination of the 5'-phosphate MID domain binding pocket provides little room for tolerated chemical modifications, and this region is typically the most important for strand selection. The presence of a 5' phosphate is essential for uptake of the associated strand[118,119]; however, Clp1 (kinase) and phosphatases maintain a balance of 5' phosphorylated and free hydroxyl ends.[120,121] An effective 5' phosphate mimic must (1) sterically fit within the deep binding pocket of Ago2; (2) permit interactions with Ago2 side chains without significant distortion to the attached nucleoside; and (3) prevent hydrolysis by phosphatases within the cell.[122–126] The 5' (*E)*-vinylphosphonate moiety at meets these criteria and is well tolerated (Figure 15).[76] This modification is particularly useful for chemically modified antisense 5' ends, as several 5' modifications are more readily recognized by phosphatases than kinases, ultimately leading to a decrease in the phosphorylation status of the strand.[127,128] In contrast, siRNA benefit from non-hydrolyzable sense strand modifications that block 5' phosphorylation, such as the 5'-O-methyl or 5' morpholino (Figure 15).[129]

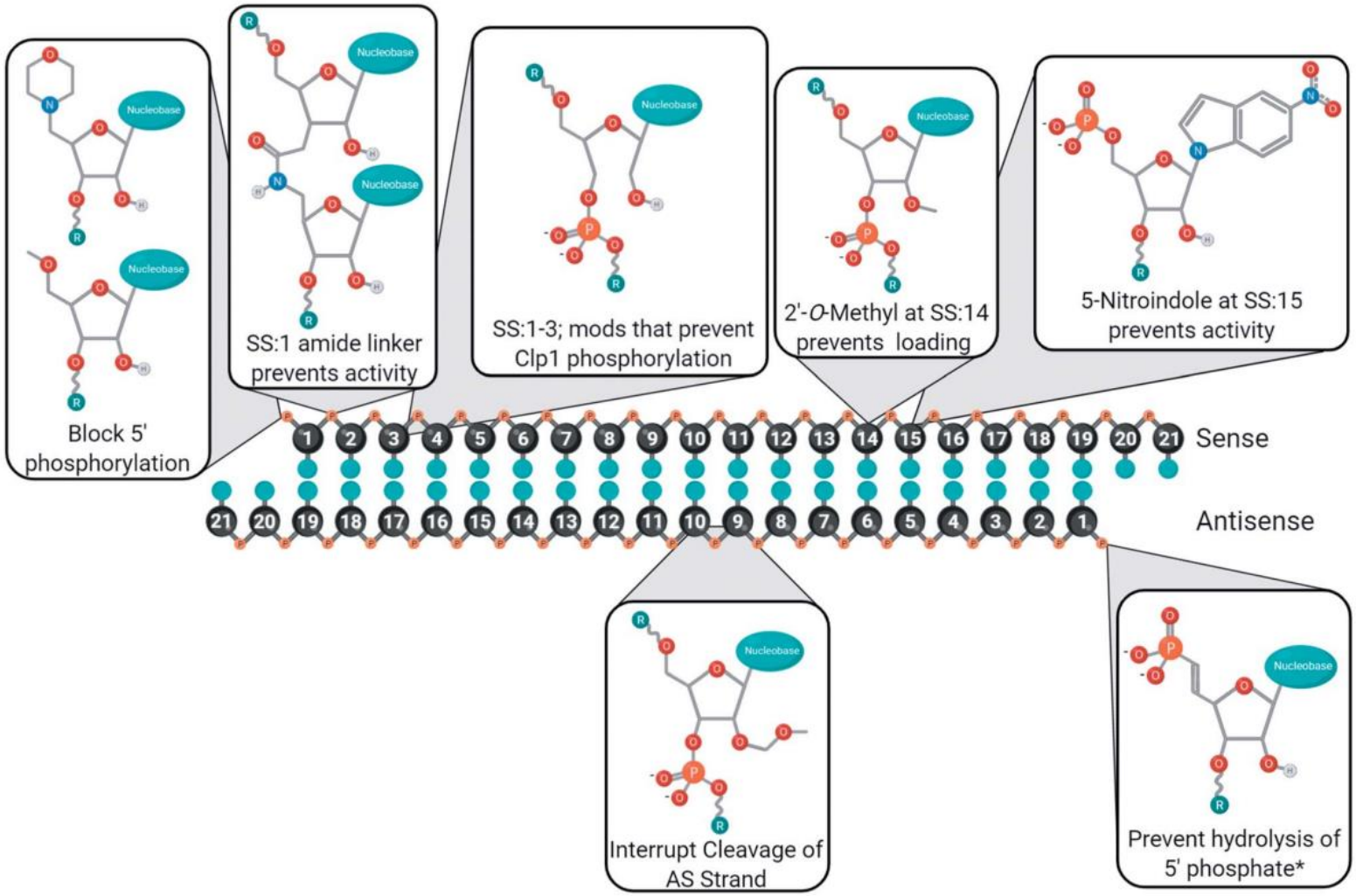

Figure 15: Strategies for limiting sense strand uptake of siRNA.

While many internal modifications exist, relatively few have shown promise for improving strand selection. This is partly due to a lack of characterization of these modifications, as the impact that many modifications have on strand activity have not been evaluated. The utility of investigating such modifications is evident from the unexpectedly effective strand silencing effect of an amide linker. Replacement of the first phosphodiester linkage from the 5' end with a single amide linker is sufficient to completely inactive the modified strand (Figure 15).[130] A deactivating effect is also present when the same modification is placed at the second or third linker, but not the fourth.[130] A similarly surprising modification was that of placing a 2'-O-methoxylethyl at position 9 or 10 of the antisense strand (Figure 15), possibly due to poor cleavage of the modified strand when placed in the passenger position of the RISC, preventing RISC maturation with the currently selected guide strand.[131]

A 2'-O-methyl at position 14 of the sense strand dramatically reduces its own activity (Figure 15).[132] This modification was shown to abolish interactions between the RNA and a highly conserved amino acid sequence across the Argonaute family proteins. Notably, this modification is widely applied and is compatible with the 2'-O-methoxylethyl at position 9 and 10.[131] Lastly, replacing the nucleobase at position 15 with the universal base, 5-nitroindole, inhibits activity of the modified strand.[133]

I.VI **Research Goals**

I.VI.I Develop a Method to Measure Strand Activity

Our lab utilizes a well-studied antisense siRNA sequence (5'-UCG AAG UAC UCA GCG UAA GdTdT-3') for silencing experiments[94,134–145]; however, no assay exists for this sequence to measure sense strand activity. Therefore, the development of such an assay

would be beneficial for all siRNA carrying this sequence. Chapter II discusses the design and validation of a quantitative reverse transcription polymerase chain reaction (RT-qPCR) based assay built upon the Dual Luciferase Assay (Promega) platform.

I.VI.II Characterize the Impact of Novel Chemical Modifications on Strand Activity

The Desaulniers lab has several promising chemical modifications for siRNA experiments and/or therapeutics. The utility of these modifications depends on the role they play in all aspects of siRNA efficacy, including potency, specificity, and safety. Comparing mRNA-level (provided through a strand activity assay) and protein-level (Dual Luciferase Assay from Promega) knockdown will also provide insights into the impact that these modifications have on siRNA mechanisms. Therefore, measuring strand specific potency for all chemically modified siRNA is valuable and will improve our understanding of these molecules. Analysis of several types of modifications, placed at several locations, will eventually lead to general conclusions for limiting sense strand activity through chemical modifications. Chapter III and Chapter IV discusses and characterizes the impact of several chemical modifications.

I.VII **References**

1. Conaway, R. C. & Conaway, J. W. General initiation factors for RNA polymerase II. *Annu. Rev. Biochem*. 62, 161–190 (1993).

2. Pfingsten, J. S. & Kieft, J. S. RNA structure-based ribosome recruitment: lessons from the Dicistroviridae intergenic region IRESes. *RNA* 14, 1255–1263 (2008).

3. Khatter, H., Myasnikov, A. G., Natchiar, S. K. & Klaholz, B. P. Structure of the human 80S ribosome. *Nature* 520, 640 (2015).

4. Glickman, M. H. & Ciechanover, A. The ubiquitin-proteasome proteolytic pathway: destruction for the sake of construction. *Physiol. Rev.* 82, 373–428 (2002).

5. Parry, D. H. & O'Farrell, P. H. The schedule of destruction of three mitotic cyclins can dictate the timing of events during exit from mitosis. *Curr. Biol.* 11, 671–683 (2001).

6. Phan, J.-A. et al. Early synaptic dysfunction induced by α-synuclein in a rat model of Parkinson's disease. *Sci. Rep*. 7, 6363 (2017).

7. Harris, C. D., Ermak, G. & Davies, K. J. A. RCAN1-1L is overexpressed in neurons of Alzheimer's disease patients. *FEBS J.* 274, 1715–1724 (2007).

8. McDonnell, T. J. et al. Expression of the protooncogene bcl-2 in the prostate and its association with emergence of androgen-independent prostate cancer. *Cancer Res*. 52, 6940–6944 (1992).

9. Hastie, N. D. & Held, W. A. Analysis of mRNA populations by cDNA.mRNA hybrid-mediated inhibition of cell-free protein synthesis. *Proc. Natl. Acad. Sci. U. S. A.* 75, 1217–1221 (1978).

10. Stephenson, M. L. & Zamecnik, P. C. Inhibition of Rous sarcoma viral RNA translation by a specific oligodeoxyribonucleotide. *Proc. Natl. Acad. Sci.* 75, 285–288 (1978).

11. Crooke, S. T. *Antisense Drug Technology: Principles: Strategies, and Applications*. (CRC press, 2001).

12. Pestka, S., Daugherty, B. L., Jung, V., Hotta, K. & Pestka, R. K. Anti-mRNA: specific inhibition of translation of single mRNA molecules. *Proc. Natl. Acad. Sci*. 81, 7525–7528 (1984).

13. Izant, J. G. & Weintraub, H. Inhibition of thymidine kinase gene expression by anti-sense RNA: a molecular approach to genetic analysis. *Cell* 36, 1007–1015 (1984).

14. Mizuno, T., Chou, M.-Y. & Inouye, M. A unique mechanism regulating gene expression: translational inhibition by a complementary RNA transcript (micRNA). *Proc. Natl. Acad. Sci.* 81, 1966–1970 (1984).

15. Gait, M. J. et al. Rapid synthesis of oligodeoxyribonucleotides IV. Improved solid phase synthesis of oligodeoxy-ribonucleotides through phosphotriester intermediates. *Nucleic Acids Res.* 8, 1081–1096 (1980).

16. Gait, M. J., Matthes, H. W. D., Singh, M., Sproat, B. S. & Titmas, R. C. Rapid synthesis of oligodeoxyribonucleotides VII. Solid phase synthesis of oligodeoxyribonucleo-tides by a continuous flow phosphotriester method on a kieselguhr-polyamide support. *Nucleic Acids Res*. 10, 6243–6254 (1982).

17. Stein, C. A. & Castanotto, D. FDA-Approved Oligonucleotide Therapies in 2017. *Mol. Ther*. 25, 1069–1075 (2017).

18. Corey, D. R. Nusinersen, an antisense oligonucleotide drug for spinal muscular atrophy. *Nat. Neurosci.* 20, 497 (2017).

19. Napoli, C., Lemieux, C. & Jorgensen, R. Introduction of a chimeric chalcone synthase gene into petunia results in reversible co-suppression of homologous genes in trans. *Plant Cell* 2, 279–289 (1990).

20. Fire, A. et al. Potent and specific genetic interference by double-stranded RNA in Caenorhabditis elegans. *Nature* 391, 806 (1998).

21. Hammond, S. M., Bernstein, E., Beach, D. & Hannon, G. J. An RNA-directed nuclease mediates post-transcriptional gene silencing in Drosophila cells. *Nature* 404, 293 (2000).

22. Garber, K. Alnylam launches era of RNAi drugs. (2018).

23. Jayaraman, M. et al. Maximizing the potency of siRNA lipid nanoparticles for hepatic gene silencing in vivo. *Angew. Chem. Int. Ed. Engl*. 51, 8529–8533 (2012).

24. Khvorova, A. & Watts, J. K. The chemical evolution of oligonucleotide therapies of clinical utility. *Nat. Biotechnol.* 35, 238–248 (2017).

25. Kim, J. et al. Patient-customized oligonucleotide therapy for a rare genetic disease. *N. Engl. J. Med*. 381, 1644–1652 (2019).

26. Ipsaro, J. J. & Joshua-Tor, L. From guide to target: molecular insights into eukaryotic RNA-interference machinery. *Nat. Struct. Mol. Biol.* 22, 20 (2015).

27. Rodriguez, A., Griffiths-Jones, S., Ashurst, J. L. & Bradley, A. Identification of mammalian microRNA host genes and transcription units. *Genome Res.* 14, 1902–1910 (2004).

28. Lee, Y. et al. The nuclear RNase III Drosha initiates microRNA processing. *Nature* 425, 415 (2003).

29. O'Brien, J., Hayder, H., Zayed, Y. & Peng, C. Overview of microrna biogenesis, mechanisms of actions, and circulation. *Front. Endocrinol. (Lausanne).* 9, 402 (2018).

30. De Rie, D. et al. An integrated expression atlas of miRNAs and their promoters in human and mouse. *Nat. Biotechnol*. 35, 872 (2017).

31. Lund, E. & Dahlberg, J. E. Substrate selectivity of exportin 5 and Dicer in the biogenesis of microRNAs. in *Cold Spring Harbor symposia on quantitative biology* vol. 71 59–66 (Cold Spring Harbor Laboratory Press, 2006).

32. Carthew, R. W. & Sontheimer, E. J. Origins and Mechanisms of miRNAs and siRNAs. *Cell* 136, 642–655 (2009).

33. Brennecke, J. et al. Discrete small RNA-generating loci as master regulators of transposon activity in Drosophila. *Cell* 128, 1089–1103 (2007).

34. Ipsaro, J. J., Haase, A. D., Knott, S. R., Joshua-Tor, L. & Hannon, G. J. The structural biochemistry of Zucchini implicates it as a nuclease in piRNA biogenesis. *Nature* 491, 279 (2012).

35. Bernstein, E., Caudy, A. A., Hammond, S. M. & Hannon, G. J. Role for a bidentate ribonuclease in the initiation step of RNA interference. *Nature* 409, 363 (2001).

36. Kim, D.-H. et al. Synthetic dsRNA Dicer substrates enhance RNAi potency and efficacy. *Nat. Biotechnol*. 23, 222 (2005).

37. Tahbaz, N. et al. Characterization of the interactions between mammalian PAZ PIWI domain proteins and Dicer. *EMBO Rep.* 5, 189–194 (2004).

38. Fareh, M. et al. TRBP ensures efficient Dicer processing of precursor microRNA in RNA-crowded environments. *Nat. Commun.* 7, 13694 (2016).

39. Betancur, J. G. & Tomari, Y. Dicer is dispensable for asymmetric RISC loading in mammals. *RNA* 18, 24–30 (2012).

40. Ye, R. et al. A Dicer-independent route for biogenesis of siRNAs that direct DNA methylation in Arabidopsis. *Mol. Cell* 61, 222–235 (2016).

41. Yang, J.-S., Maurin, T. & Lai, E. C. Functional parameters of Dicer-independent microRNA biogenesis. *RNA* (2012).

42. Bohmert, K. et al. AGO1 defines a novel locus of Arabidopsis controlling leaf development. *EMBO J.* 17, 170–180 (1998).

43. Hutvagner, G. & Simard, M. J. Argonaute proteins: key players in RNA silencing. *Nat. Rev. Mol. Cell Biol*. 9, 22 (2008).

44. Ku, H.-Y. & Lin, H. PIWI proteins and their interactors in piRNA biogenesis, germline development and gene expression. *Natl. Sci. Rev*. 1, 205–218 (2014).

45. Gurtan, A. M. & Sharp, P. A. The role of miRNAs in regulating gene expression networks. *J. Mol. Biol*. 425, 3582–3600 (2013).

46. Meister, G. et al. Human Argonaute2 mediates RNA cleavage targeted by miRNAs and siRNAs. *Mol. Cell* 15, 185–197 (2004).

47. Liu, J. et al. Argonaute2 is the catalytic engine of mammalian RNAi. *Science* 305, 1437–1441 (2004).

48. Kwak, P. B. & Tomari, Y. The N domain of Argonaute drives duplex unwinding during RISC assembly. *Nat. Struct. Mol. Biol.* 19, 145 (2012).

49. Friedman, R. C., Farh, K. K.-H., Burge, C. B. & Bartel, D. P. Most mammalian mRNAs are conserved targets of microRNAs. *Genome Res.* 19, 92–105 (2009).

50. Berezikov, E., Chung, W.-J., Willis, J., Cuppen, E. & Lai, E. C. Mammalian mirtron genes. *Mol. Cell* 28, 328–336 (2007).

51. Humphreys, D. T., Westman, B. J., Martin, D. I. K. & Preiss, T. MicroRNAs control translation initiation by inhibiting eukaryotic initiation factor 4E/cap and poly (A) tail function. *Proc. Natl. Acad. Sci.* 102, 16961–16966 (2005).

52. Huntzinger, E. & Izaurralde, E. Gene silencing by microRNAs: contributions of translational repression and mRNA decay. *Nat. Rev. Genet.* 12, 99 (2011).

53. Tritschler, F., Huntzinger, E. & Izaurralde, E. Role of GW182 proteins and PABPC1 in the miRNA pathway: a sense of deja vu. *Nat. Rev. Mol. Cell Biol*. 11, 379 (2010).

54. Ameres, S. L. & Zamore, P. D. Diversifying microRNA sequence and function. *Nat. Rev. Mol. Cell Biol*. 14, 475 (2013).

55. Zilberman, D., Cao, X. & Jacobsen, S. E. ARGONAUTE4 control of locus-specific siRNA accumulation and DNA and histone methylation. *Science* 299, 716–719 (2003).

56. Vasudevan, S. & Steitz, J. A. AU-rich-element-mediated upregulation of translation by FXR1 and Argonaute 2. *Cell* 128, 1105–1118 (2007).

57. MacRae, I. J. et al. Structural Basis for Double-Stranded RNA Processing by Dicer. *Science* 311, 195–198 (2006).

58. Ma, J.-B., Ye, K. & Patel, D. J. Structural basis for overhang-specific small interfering RNA recognition by the PAZ domain. *Nature* 429, 318 (2004).

59. Lingel, A., Simon, B., Izaurralde, E. & Sattler, M. Nucleic acid 3′-end recognition by the Argonaute2 PAZ domain. *Nat. Struct. Mol. Biol.* 11, 576 (2004).

60. Song, J.-J., Smith, S. K., Hannon, G. J. & Joshua-Tor, L. Crystal structure of Argonaute and its implications for RISC slicer activity. *Science* 305, 1434–1437 (2004).

61. Parker, J. S., Roe, S. M. & Barford, D. Crystal structure of a PIWI protein suggests mechanisms for siRNA recognition and slicer activity. *EMBO J.* 23, 4727–4737 (2004).

62. Tolia, N. H. & Joshua-Tor, L. Slicer and the argonautes. *Nat. Chem. Biol.* 3, 36 (2007).

63. Frank, F., Sonenberg, N. & Nagar, B. Structural basis for 5′-nucleotide base-specific recognition of guide RNA by human AGO2. *Nature* 465, 818 (2010).

64. Doench, J. G. & Sharp, P. A. Specificity of microRNA target selection in translational repression. *Genes Dev.* 18, 504–511 (2004).

65. Lewis, B. P., Shih, I., Jones-Rhoades, M. W., Bartel, D. P. & Burge, C. B. Prediction of mammalian microRNA targets. *Cell* 115, 787–798 (2003).

66. Bisaria, N., Jarmoskaite, I. & Herschlag, D. Lessons from enzyme kinetics reveal specificity principles for RNA-guided nucleases in RNA interference and CRISPR-based genome editing. *Cell Syst*. 4, 21–29 (2017).

67. Lisowiec-Wąchnicka, J., Bartyś, N. & Pasternak, A. A systematic study on the influence of thermodynamic asymmetry of 5′-ends of siRNA duplexes in relation to their silencing potency. *Sci. Rep*. 9, 2477 (2019).

68. Tomari, Y., Matranga, C., Haley, B., Martinez, N. & Zamore, P. D. A protein sensor for siRNA asymmetry. *Science* 306, 1377–1380 (2004).

69. Okamura, K., Ishizuka, A., Siomi, H. & Siomi, M. C. Distinct roles for Argonaute proteins in small RNA-directed RNA cleavage pathways. *Genes Dev*. 18, 1655–1666 (2004).

70. Suzuki, H. I. et al. Small-RNA asymmetry is directly driven by mammalian Argonautes. *Nat. Struct. Mol. Biol*. 22, 512 (2015).

71. Noland, C. L., Ma, E. & Doudna, J. A. siRNA repositioning for guide strand selection by human Dicer complexes. *Mol. Cell* 43, 110–121 (2011).

72. Gredell, J. A., Dittmer, M. J., Wu, M., Chan, C. & Walton, S. P. Recognition of siRNA asymmetry by TAR RNA binding protein. *Biochemistry* 49, 3148–3155 (2010).

73. Schirle, N. T. & MacRae, I. J. The crystal structure of human Argonaute2. *Science* 336, 1037–1040 (2012).

74. Ma, J.-B. et al. Structural basis for 5′-end-specific recognition of guide RNA by the A. fulgidus Piwi protein. *Nature* 434, 666 (2005).

75. Hu, H. Y. et al. Sequence features associated with microRNA strand selection in humans and flies. *BMC Genomics* 10, 413 (2009).

76. Elkayam, E. et al. siRNA carrying an (E)-vinylphosphonate moiety at the 5′ end of the guide strand augments gene silencing by enhanced binding to human Argonaute-2. *Nucleic Acids Res.* 45, 3528–3536 (2016).

77. Jinek, M. et al. A programmable dual-RNA–guided DNA endonuclease in adaptive bacterial immunity. *Science* 1225829 (2012).

78. Deerberg, A., Willkomm, S. & Restle, T. Minimal mechanistic model of siRNA-dependent target RNA slicing by recombinant human Argonaute 2 protein. *Proc. Natl. Acad. Sci.* 110, 17850–17855 (2013).

79. Jarvinen, P., Oivanen, M., & Lönnberg, H. Interconversion and phosphoester hydrolysis of 2',5'- and 3',5'-dinucleoside monophosphates: kinetics and mechanisms. *J. Org. Chem*. 56, 5396-5401 (1991).

80. AbouHaidar, M. G. & Ivanov, I. G. Non-enzymatic RNA hydrolysis promoted by the combined catalytic activity of buffers and magnesium ions. *Zeitschrift für Naturforsch*. C 54, 542–548 (1999).

81. Herbert, A. Z-DNA and Z-RNA in human disease. *Commun. Biol*. 2, 7 (2019).

82. Roberts, T. C., Langer, R. & Wood, M. J. A. Advances in oligonucleotide drug delivery. *Nat. Rev. Drug Discov*. 19, 673–694 (2020).

83. Haute, D. Van & Berlin, J. M. Challenges in realizing selectivity for nanoparticle biodistribution and clearance: lessons from gold nanoparticles. *Ther. Deliv*. 8, 763–774 (2017).

84. Kulkarni, J. A., Cullis, P. R. & Van Der Meel, R. Lipid nanoparticles enabling gene therapies: from concepts to clinical utility. *Nucleic Acid Ther*. 28, 146–157 (2018).

85. Guevara, M. L., Persano, F. & Persano, S. Advances in Lipid Nanoparticles for mRNA-Based Cancer Immunotherapy. *Frontiers in Chemistry* vol. 8 963 (2020).

86. Patel, S. et al. Boosting intracellular delivery of lipid nanoparticle-encapsulated mRNA. *Nano Lett.* 17, 5711–5718 (2017).

87. Cheng, X. & Lee, R. J. The role of helper lipids in lipid nanoparticles (LNPs) designed for oligonucleotide delivery. *Adv. Drug Deliv. Rev.* 99, 129–137 (2016).

88. Cullis, P. R. & Hope, M. J. Lipid nanoparticle systems for enabling gene therapies. *Mol. Ther*. 25, 1467–1475 (2017).

89. Leung, A. K. K. et al. Lipid nanoparticles containing siRNA synthesized by microfluidic mixing exhibit an electron-dense nanostructured core. *J. Phys. Chem. C* 116, 18440–18450 (2012).

90. Mui, B. L. et al. Influence of polyethylene glycol lipid desorption rates on pharmacokinetics and pharmacodynamics of siRNA lipid nanoparticles. *Mol. Ther. Acids* 2, e139 (2013).

91. Hou, X., Zaks, T., Langer, R. & Dong, Y. Lipid nanoparticles for mRNA delivery. *Nat. Rev. Mater*. (2021) doi:10.1038/s41578-021-00358-0.

92. Whitehead, K. A., Langer, R. & Anderson, D. G. Knocking down barriers: advances in siRNA delivery. *Nat. Rev. Drug Discov.* 8, 129–138 (2009).

93. Biscans, A. et al. Diverse lipid conjugates for functional extra-hepatic siRNA delivery in vivo. *Nucleic Acids Res.* 47, 1082–1096 (2019).

94. Salim, L., Islam, G. & Desaulniers, J.-P. Targeted delivery and enhanced gene-silencing activity of centrally modified folic acid–siRNA conjugates. *Nucleic Acids Res*. 48, 75–85 (2020).

95. Yang, C., Gao, S. & Kjems, J. Folic acid conjugated chitosan for targeted delivery of siRNA to activated macrophages in vitro and in vivo. *J. Mater. Chem. B* 2, 8608–8615 (2014).

96. Dohmen, C. et al. Defined folate-PEG-siRNA conjugates for receptor-specific gene silencing. *Mol. Ther. Acids* 1, e7 (2012).

97. Rajeev, K. G. et al. Hepatocyte-specific delivery of siRNAs conjugated to novel non-nucleosidic trivalent N-acetylgalactosamine elicits robust gene silencing in vivo. *ChemBioChem* 16, 903–908 (2015).

98. Matsuda, S. et al. siRNA conjugates carrying sequentially assembled trivalent N-acetylgalactosamine linked through nucleosides elicit robust gene silencing in vivo in hepatocytes. *ACS Chem. Biol*. 10, 1181–1187 (2015).

99. Prakash, T. P. et al. Targeted delivery of antisense oligonucleotides to hepatocytes using triantennary N-acetyl galactosamine improves potency 10-fold in mice. *Nucleic Acids Res.* 42, 8796–8807 (2014).

100. Tanowitz, M. et al. Asialoglycoprotein receptor 1 mediates productive uptake of N-acetylgalactosamine-conjugated and unconjugated phosphorothioate antisense oligonucleotides into liver hepatocytes. *Nucleic Acids Res.* 45, 12388–12400 (2017).

101. Brown, C. R. et al. Investigating the pharmacodynamic durability of GalNAc–siRNA conjugates. *Nucleic Acids Res.* 48, 11827–11844 (2020).

102. Mullard, A. FDA approves landmark RNAi drug. *Nat. Rev. Drug Discov.* 17, 613 (2018).

103. Suhr, O. B. et al. Efficacy and safety of patisiran for familial amyloidotic polyneuropathy: a phase II multi-dose study. *Orphanet J. Rare Dis*. 10, 109 (2015).

104. Adams, D. et al. Patisiran, an RNAi therapeutic, for hereditary transthyretin amyloidosis. *N. Engl. J. Med.* 379, 11–21 (2018).

105. Chan, A. et al. Preclinical development of a subcutaneous ALAS1 RNAi therapeutic for treatment of hepatic porphyrias using circulating RNA quantification. *Mol. Ther. Acids* 4, e263 (2015).

106. Scott, L. J. & Keam, S. J. Lumasiran: First Approval. *Drugs* 81, 277–282 (2021).

107. Pampaloni, F., Reynaud, E. G. & Stelzer, E. H. K. The third dimension bridges the gap between cell culture and live tissue. *Nat. Rev. Mol. Cell Biol.* 8, 839–845 (2007).

108. Ivanovic, Z. Hypoxia or in situ normoxia: The stem cell paradigm. *J. Cell. Physiol.* 219, 271–275 (2009).

109. Halldorsson, S., Lucumi, E., Gómez-Sjöberg, R. & Fleming, R. M. T. Advantages and challenges of microfluidic cell culture in polydimethylsiloxane devices. *Biosens. Bioelectron.* 63, 218–231 (2015).

110. van Essen, M. F. et al. Culture medium used during small interfering RNA (siRNA) transfection determines the maturation status of dendritic cells. *J. Immunol. Methods* 479, 112748 (2020).

111. Jackson, A. L. et al. Expression profiling reveals off-target gene regulation by RNAi. *Nat. Biotechnol.* 21, 635 (2003).

112. Birmingham, A. et al. 3′ UTR seed matches, but not overall identity, are associated with RNAi off-targets. *Nat. Methods* 3, 199 (2006).

113. Lin, X. et al. siRNA-mediated off-target gene silencing triggered by a 7 nt complementation. *Nucleic Acids Res.* 33, 4527–4535 (2005).

114. Jackson, A. L. et al. Position-specific chemical modification of siRNAs reduces "off-target" transcript silencing. *RNA* 12, 1197–1205 (2006).

115. Vaish, N. et al. Improved specificity of gene silencing by siRNAs containing unlocked nucleobase analogs. *Nucleic Acids Res.* 39, 1823–1832 (2011).

116. Dua, P., Yoo, J. W., Kim, S. & Lee, D. Modified siRNA structure with a single nucleotide bulge overcomes conventional siRNA-mediated off-target silencing. *Mol. Ther.* 19, 1676–1687 (2011).

117. Alagia, A. & Eritja, R. siRNA and RNAi optimization. *Wiley Interdiscip. Rev. RNA* 7, 316–329 (2016).

118. Chen, P. Y. et al. Strand-specific 5′-O-methylation of siRNA duplexes controls guide strand selection and targeting specificity. *RNA* 14, 263–274 (2008).

119. Nykänen, A., Haley, B. & Zamore, P. D. ATP requirements and small interfering RNA structure in the RNA interference pathway. *Cell* 107, 309–321 (2001).

120. Weitzer, S. & Martinez, J. The human RNA kinase hClp1 is active on 3′ transfer RNA exons and short interfering RNAs. *Nature* 447, 222 (2007).

121. Weitzer, S. & Martinez, J. hClp1, A Novel Kinase Revitalizes RNA Metabolism. *Cell Cycle* 6, 2133–2137 (2007).

122. Shah, S. & Friedman, S. H. Tolerance of RNA interference toward modifications of the 5′ antisense phosphate of small interfering RNA. *Oligonucleotides* 17, 35–43 (2007).

123. Chiu, Y.-L. & Rana, T. M. RNAi in human cells: basic structural and functional features of small interfering RNA. *Mol. Cell* 10, 549–561 (2002).

124. Czauderna, F. et al. Structural variations and stabilising modifications of synthetic siRNAs in mammalian cells. *Nucleic Acids Res*. 31, 2705–2716 (2003).

125. Schwarz, D. S., Hutvágner, G., Haley, B. & Zamore, P. D. Evidence that siRNAs function as guides, not primers, in the Drosophila and human RNAi pathways. *Mol. Cell* 10, 537–548 (2002).

126. Varley, A. J. & Desaulniers, J.-P. Chemical strategies for strand selection in short-interfering RNAs. *RSC Adv*. 11, 2415–2426 (2021).

127. Kenski, D. M. et al. Analysis of acyclic nucleoside modifications in siRNAs finds sensitivity at position 1 that is restored by 5′-terminal phosphorylation both in vitro and in vivo. *Nucleic Acids Res.* 38, 660–671 (2010).

128. Parmar, R. et al. 5′-(E)-Vinylphosphonate: A Stable Phosphate Mimic Can Improve the RNAi Activity of siRNA–GalNAc Conjugates. *ChemBioChem* 17, 985–989 (2016).

129. Kumar, P. et al. 5′-Morpholino modification of the sense strand of an siRNA makes it a more effective passenger. *Chem. Commun*. 55, 5139–5142 (2019).

130. Hardcastle, T. et al. A Single Amide Linkage in the Passenger Strand Suppresses Its Activity and Enhances Guide Strand Targeting of siRNAs. *ACS Chem. Biol.* 13, 533–536 (2018).

131. Song, X. et al. Site-specific modification using the 2′-methoxyethyl group improves the specificity and activity of siRNAs. *Mol. Ther. Acids* 9, 242–250 (2017).

132. Zheng, J. et al. Single modification at position 14 of siRNA strand abolishes its gene-silencing activity by decreasing both RISC loading and target degradation. *FASEB J*. 27, 4017–4026 (2013).

133. Zhang, J. et al. Modification of the siRNA Passenger Strand by 5-Nitroindole Dramatically Reduces its Off-Target Effects. *ChemBioChem* 13, 1940–1945 (2012).

134. Hammill, M. L., Islam, G. & Desaulniers, J.-P. Reversible control of RNA interference by siRNAzos. *Org. Biomol. Chem*. 18, 41–46 (2019).

135. Hammill, M. L., Isaacs-Trépanier, C. & Desaulniers, J.-P. siRNAzos: A New Class of Azobenzene-Containing siRNAs that Can Photochemically Regulate Gene Expression. *ChemistrySelect* 2, 9810–9814 (2017).

136. Varley, A. J., Hammill, M. L., Salim, L. & Desaulniers, J.-P. Effects of Chemical Modifications on siRNA Strand Selection in Mammalian Cells. *Nucleic Acid Ther*. 30, 229–236 (2020).

137. Tsubaki, K. et al. Synthesis and Evaluation of Neutral Phosphate Triester Backbone-Modified siRNAs. *ACS Med. Chem. Lett*. (2020).

138. Hammill, M. L., Islam, G. & Desaulniers, J.-P. Synthesis, Derivatization and Photochemical Control of ortho-Functionalized Tetrachlorinated Azobenzene-Modified siRNAs. *ChemBioChem* (2020).

139. Hammill, M. L. et al. Building siRNAs with cubes: synthesis and evaluation of cubane-modified siRNAs. *ChemBioChem* (2021).

140. Salim, L., McKim, C. & Desaulniers, J.-P. Effective carrier-free gene-silencing activity of cholesterol-modified siRNAs. *RSC Adv.* 8, 22963–22966 (2018).

141. Zhu, L. & Mahato, R. I. Targeted delivery of siRNA to hepatocytes and hepatic stellate cells by bioconjugation. *Bioconjug. Chem*. 21, 2119–2127 (2010).

142. Lorenzer, C. et al. Targeted delivery and endosomal cellular uptake of DARPin-siRNA bioconjugates: Influence of linker stability on gene silencing. *Eur. J. Pharm. Biopharm.* 141, 37–50 (2019).

143. Elbashir, S. M. et al. Duplexes of 21-nucleotide RNAs mediate RNA interference in cultured mammalian cells. *Nature* 411, 494 (2001).

144. Sardo, C., Craparo, E. F., Porsio, B., Giammona, G. & Cavallaro, G. Improvements in rational design strategies of inulin derivative polycation for siRNA delivery. *Biomacromolecules* 17, 2352–2366 (2016).

145. Chen, Q. et al. Lipophilic siRNAs mediate efficient gene silencing in oligodendrocytes with direct CNS delivery. *J. Control. Release* 144, 227–232 (2010).

Chapter II.

Development of Strand Target Cleavage Assay

II.I **Plasmid Design**

siRNA strand activity can be measured through two primary outcomes: target mRNA cleavage or reduction in protein abundance. This assay was developed to measure activity through mRNA cleavage via RT-qPCR, built upon the Dual Luciferase Reporter Assay[1] platform. This assay utilizes both the firefly and *Renilla* luciferase enzymes, expressed from pGL3-Control and pRLSV40, respectively. Bioluminescence can be separately measured from each enzyme through the addition of ATP and either luciferin (firefly) or coelenterazine (*Renilla*). The antisense strand of most of the Desaulniers Lab's siRNA library targets the firefly luciferase coding sequence within pGL3-Control, while the *Renilla* luciferase from pRLSV40 is used as a reference control. Specifically, the siRNA targets nineteen nucleotides at position 155 to 173 of the coding sequence (CT TAC GCT GAG TAC TTC GA; contributing to codons for Thr-Tyr-Ala-Glu-Tyr-Phe-Glu). Modifying pGL3-Control by replacing the antisense target sequence with the reverse compliment sequence (TC GAA GTA CTC AGC GTA AG; contributing to codons for Ile-Glu-Val-Leu-Ser-Val-Arg) allowed this new gene to be an effective sense strand target

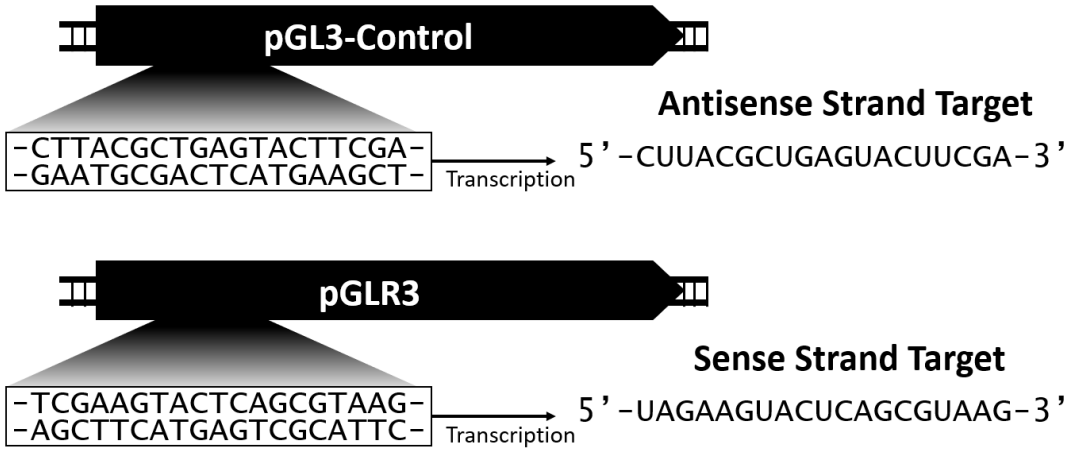

Figure 16: Design of pGLR3. The antisense strand of siRNA targets pGL3-Control, while the sense strand of siRNA targets the reverse compliment sequence in pGLR3.

(Figure 16). The new plasmid is named pGLR3 and is expected to express the modified luciferase gene at the same abundance as the pGL3-Control derived luciferase. However, the dramatic change of seven amino acids is expected to disrupt protein function.

The plasmid pGLR3 was developed using a unique application of the NEBuilder® HiFi DNA Assembly (Gibson Assembly).[2] While this method is typically used to assemble multiple DNA strands, here it was used to replace the 19 bp region within pGL3-Control without the need for an insert. This was achieved through the amplification of nearly the entire pGL3-Control plasmid using primers with the desired replacement sequence on the 5' end. PCR amplification was performed using an annealing temperature gradient with New England Biolabs' Q5 DNA Polymerase (98 °C for 1:00; 35 cycles of 98 °C for 0:10, 60-70.1 °C for 0:30, and 72 °C for 3:20; 72 °C for 5:00). Gel electrophoresis identified 70.1 °C as the ideal annealing temperature (Figure 17). The PCR products from this sample were purified using BioBasic PCR Cleanup Kit. NEBuilder® HiFi DNA Assembly was then used to circularize the plasmid (0.1 pmol DNA in 10 µl reaction; 50 °C for 15

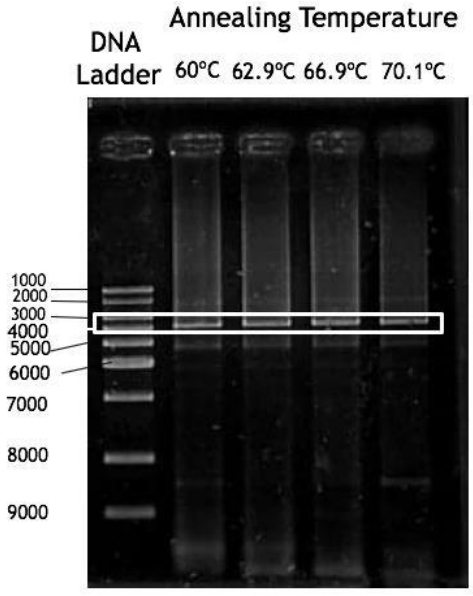

Figure 17: Gel electrophoresis of pGLR3 precursor amplification.

minutes), which was transformed into *E. coli* DH5α via electroporation and chemical transformation.

Electroporation and chemical transformation were performed to deliver the assembled plasmids into *E. coli* DH5α. Electrocompetent cells were prepared using a 5 ml starter culture grown in LB overnight at 37 °C. The starter culture was then diluted into 500 ml of prewarmed LB and grown until an OD600 of 0.4 was reached. The culture was then quick cooled on ice, harvested by centrifugation and washed thrice with cold 10% glycerol. Cells were resuspended to an OD600 of 100-200 in cold 10% glycerol and immediately stored at -80 °C. Chemically competent cells were prepared with the same starter culture preparation, then washed once with cold 30 mM $CaCl_2$ and resuspended in cold 30 mM $CaCl_2$ to an OD600 of approximately 50. All centrifugation steps were performed at 8000g for 1 minute at 0 to 4 °C.

Electroporation and chemical transformation were performed using 1 µl of assembled pGLR3 and 50 µl of thawed cells. Electroporation was performed at 2500 V applied over 5 to 5.5 ms. Chemical transformation was performed by Shreya Jain, by placing the pGLR3 and cell mixture on ice for 30 minutes, followed by 42 °C heat shock for 30 seconds and immediately returned to ice. Cells were recovered in 1 ml LB at 37 °C under agitation for one hour prior to plating on prewarmed LB agar with 100 µg/ml ampicillin for selection. After one day's growth, well isolated colonies were selected for screening by colony PCR using Taq 2x Master Mix from New England Biolabs (95 °C for 0:30; 35 cycles of 95 °C for 0:25, 55 °C for 0:30, and 68 °C for 0:20; 68 °C for 5:00) using seq_forward and seq_reverse (Appendix A). Screening identified sixteen colonies with the desired amplicon size, which were grown in 5 ml LB overnight at 37 °C under agitation. Plasmids were

extracted using QIAprep Spin Miniprep Kit – Plasmid DNA (Qiagen). Screening PCR was re-performed on twelve randomly selected plasmids to produce high purity amplicons for sequencing. Several steps of the screening processes were performed by Shreya Jain. Sanger sequencing was completed by BioBasic (Markham, ON). Of these, a single sample was found to have the desired pGLR3 sequence. Glycerol stocks of *E. coli* DH5α/pGLR3 were prepared in 10% glycerol in LB and frozen at -80 °C for long-term storage.

The modified luciferase in pGLR3 was tested using the Dual Luciferase Assay (Promega) by Shreya Jain for whether it retained bioluminescent properties. As expected, the pGLR3 plasmid did not produce a functionally bioluminescent luciferase.

II.II **HeLa Cell Culture**

Culture media, solutions, and chemicals were obtained from MilliporeSigma. HeLa cells were obtained from American Type Culture Collection and maintained at 37 °C in an atmosphere of 5% CO_2 and 100% humidity in Dulbecco's modified Eagle's medium supplemented with 10% (v/v) fetal bovine serum (DMEM-FBS). For routine cell passaging, 500 U/ml penicillin and 100 mg/ml streptomycin was added to the media. When cultures reached 80%–90% confluence, the cells were washed twice with phosphate-buffered saline, treated with trypsin ethylenediaminetetraacetic acid solution for up to 5 min, and harvested using two volumes of DMEM-FBS. The cells were centrifuged at 200 g for 5 min then resuspended in DMEM-FBS. Cells were then counted on a hemocytometer using trypan blue exclusion to test for cell viability and used for seeding cultures.

II.III **siRNA Treatment and cDNA Synthesis**

In a 24-well culture dish, 500 ml of 10^5 cells/ml (50,000 cells per well) were dispensed and grown until 50-70% confluency. For siRNA treatments, 50 ml of Opti-MEM

was mixed with 2.0 µl of Lipofectamine 2000 (both from ThermoFisher) and incubated at room temperature for at least 5 min. This mixture was added to a separately prepared mixture of 50 ml OptiMEM containing 100 ng pGL3-Control, 100 ng pGL3-Reverse, 25 ng pRLSV40, and an appropriate mass of siRNA for the desired culture concentration. The combined mixture was incubated at room temperature for 20 to 30 min then added to 50-70% confluent cultures to yield a final volume of 600 ml and incubated for an additional 24 h. RNA was then extracted from cells using an RNA Purification Plus Kit, including the supplementary on-column DNase I treatment, according to the manufacturer's instructions (Norgen Biotek). RNA was spectrophotometrically analyzed on a Bio-Drop DUO (BioDrop) to measure nucleic acid concentration, A260/A280, and A260/A230. First-strand cDNA was synthesized using 100 to 250 ng RNA in 10.0 µl reactions using the iScript Reverse Transcription Supermix according to the manufacturer's instructions (Bio-Rad) and diluted to 2.5 ng/µl to 5.0 ng/µl for qPCR amplification. Assays performed for azobenzene, propargyl, and folic acid modified siRNAs were subject to randomly sampling of 10% of RNA samples for DNA through reverse transcriptase-free cDNA synthesis mixtures; no significant DNA contamination was found in these samples.

II.IV **qPCR Design and Validation**

Measuring target cleavage requires efficient RNA extraction, first strand cDNA synthesis, highly specific primer sets, and optimized amplification conditions. Each of these aspects were carefully considered and validated to provide a robust and specific assay system. Where possible, the assay design closely followed Minimum Information for Publication of Quantitative Real-Time PCR Experiments (MIQE) guidelines.

Primers pairs were designed using a combination of primerBLAST (NCBI), SnapGene Viewer (GSL Biotech LLC), and/or NetPrimer (Premier Biosoft), to evaluate specificity, melting temperature, self/cross complementarity, and predicted secondary structures. To validate primer sets, three cDNA samples were prepared and pooled. qPCR amplification was performed in 96 well plates in 10 µl using SsoAdvanced™ Universal SYBR® Green Supermix (Bio-Rad) on a CFX96 Connect Real-Time PCR System (Bio-Rad). Four primer sets for firefly luciferase and two primer sets (See Appendix A1 for primers) for *Rinella* luciferase were evaluated by annealing temperature gradient (98 °C for 0:30; 40 cycles of 96 °C for 0:05 and 55-65 °C for 0:10) and melt curve analysis (65 °C to 95 °C, 0.5 °C increment per 0:05). Ideal primers were identified by those with the lowest C_q values and single amplicon. For firefly luciferase, Luc_qPCR2.F and Luc_qPCR2.R were selected at 58 °C. For *Rinella* luciferase, Rluc_qPCR1.F and Rluc_qPCR1.R were also selected at 58 °C. Two antisense and two sense specific forward primers were analyzed using Luc_qPCR2.R as the reverse primer. Similar analysis identified AS_qPCR2.F and SS_qPCR2.F as the ideal primers for the antisense and sense target, respectively. Due to significant similarity between these primer sets, specificity between pGL3-Control and pGLR3 was confirmed by qPCR. These target-specific primers were selected for standard curve analysis, identifying the linear dynamic range of 95%-105% efficiency for each gene (Appendix B). These results confirmed that the same conditions (98 °C for 0:30; 40 cycles of 96 °C for 0:05, then 57 °C for 0:25) efficiently amplified each gene, simplifying the assay design by allowing each gene target to be simultaneously quantified with a single, highly specific amplification protocol. Statistical

significance for gene expression experiments was determined by t-test comparison of three biological replicates at a 95% confidence level.

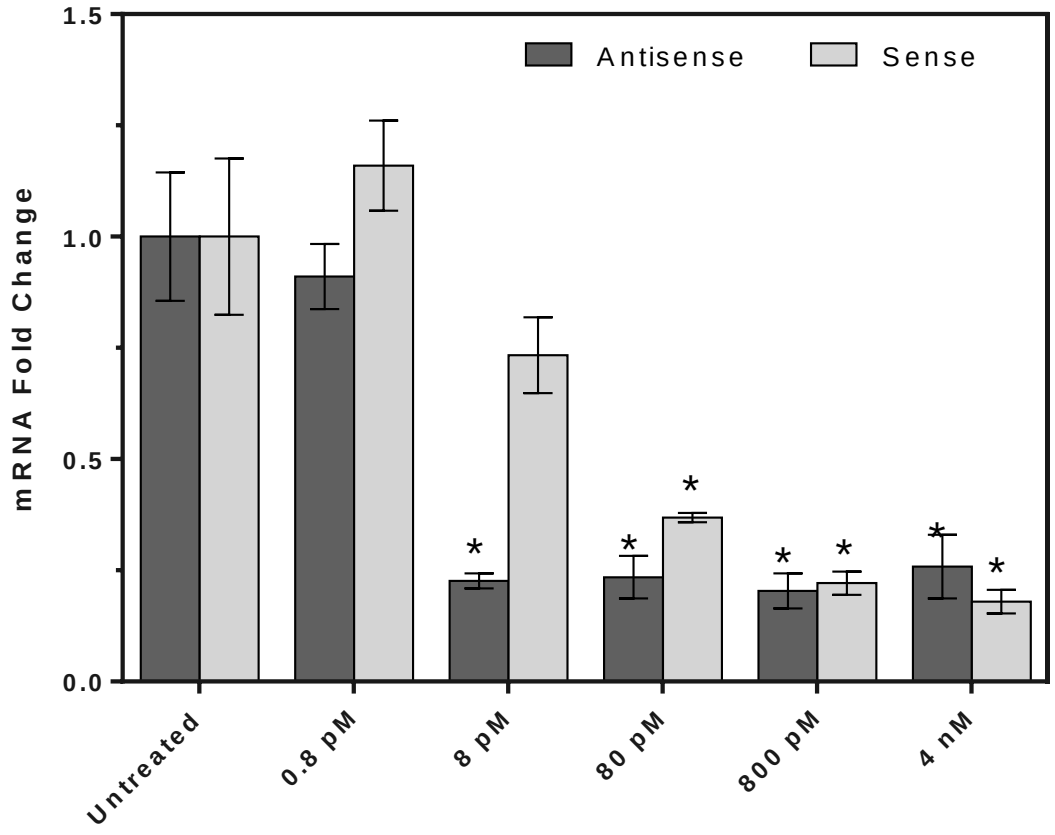

Figure 18: The antisense strand is more active than the sense strand in siRNA. Luciferase mRNA expression was measured in HeLa cells 24 hours after treatment with wildtype siRNA. Mean ± SEM values of independent triplicates are shown. (*) indicates a statistically significant difference ($p < 0.05$) between the untreated and treated sample.

Strand activity was measured using 0.8 pM to 4 nM wildtype siRNA to measure the natural knockdown potency of either strand. As expected, greater knockdown was observed for the antisense strand than the sense strand (Figure 18). No significant gene silencing occurred at 0.8 pM; however, the antisense strand reached maximum potency of 78% knockdown at 8 pM indicating an optimal dosage within the 0.8 pM to 8 pM range. Importantly, the sense strand did not reach statistically significant silencing by 8 pM. These

results also suggest that approximately 20% of mRNA is protected from the RNAi machinery. This may be immature mRNA in the nucleus, mature mRNA that has not yet left the nucleus, or possibly a subset of cells that receive the expression plasmids, but no the siRNA. To ensure that gene expression was not altered by any unexpected variables, a scrambled siRNA was also tested at 8 pM, 800 pM, and 4nM (Figure 19). No significant changes in gene expression were observed.

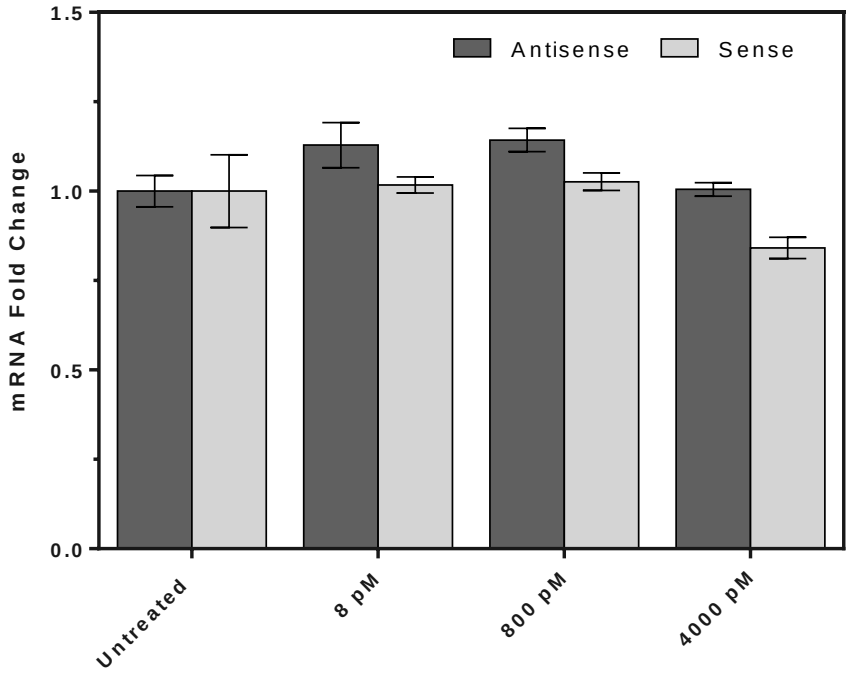

Figure 19: Luciferase gene expression is not altered by scramble siRNA. Mean ± SEM values of independent triplicates are shown. (*) indicates a statistically significant difference ($p < 0.05$) between the untreated and treated sample.

II.V **References**

1. Sherf, B. A., Navarro, S. L., Hannah, R. R. & Wood, K. V. Dual-luciferase reporter assay: an advanced co-reporter technology integrating firefly and Renilla luciferase assays. *Promega Notes* 57, 2–8 (1996).

2. Gibson, D. G., et al. Enzymatic assembly of DNA molecules up to several hundred kilobases. *Nature Methods* 6, 343-345 (2009).

Chapter III.

Characterizing the Impact of Modifications on Strand Activity

III.I **Azobenzene Modified siRNAs**

The azobenzene modification was first introduced into siRNA by Dr. Matt Hammill[1], imparting novel photo-switchable properties. The azobenzene linker is about 9.9 Å long when in *trans* form; however, the extra length provided by the ethyl linkage increases this distance to be similar to that of two A-form (3' endo sugar pucker) nucleotides (12 Å).[2,3] Isomerization to the *cis* form decreases this distance by about 4.4 Å, disrupting the siRNA structure and preventing uptake by the RISC (Figure 20).[1,4-6] The transition between these states is easily controlled by light, as irradiation by ultraviolet or visible light causes photoisomerization to the *cis* or *trans* form, respectively. These characteristics are promising for limiting activation of therapeutic siRNA in off-target tissues or facilitating developmental studies where timely activation/deactivation of gene silencing is essential.

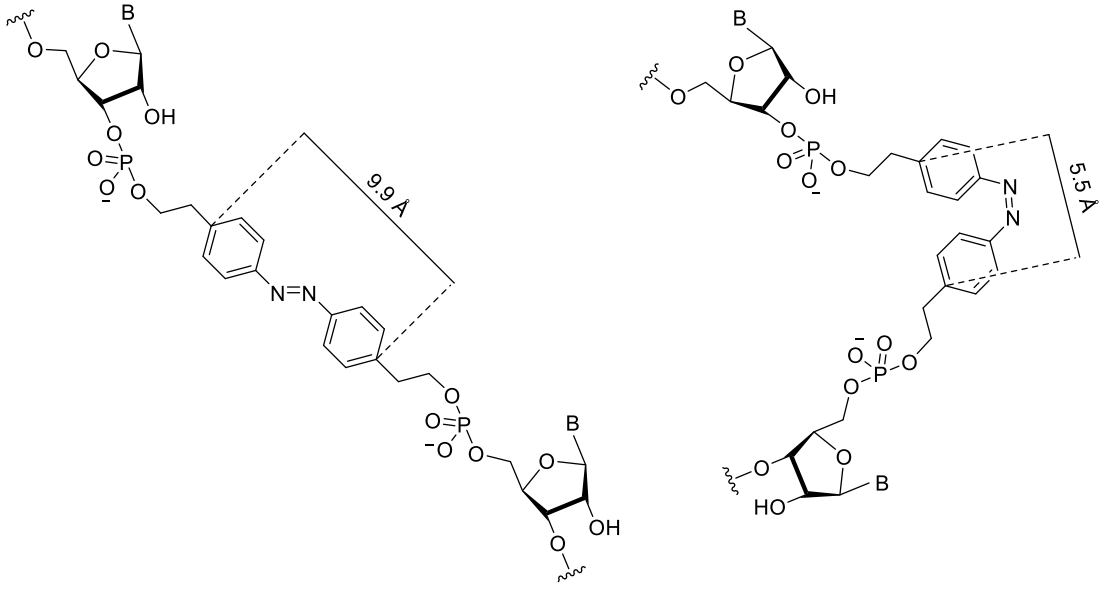

Figure 20: The azobenzene linker isomerizes between the trans (left) and cis (right) form under visible or ultraviolet light, respectively. Within siRNA, the isomerization from trans to cis disrupts the helical conformation and prevents uptake by the RISC.

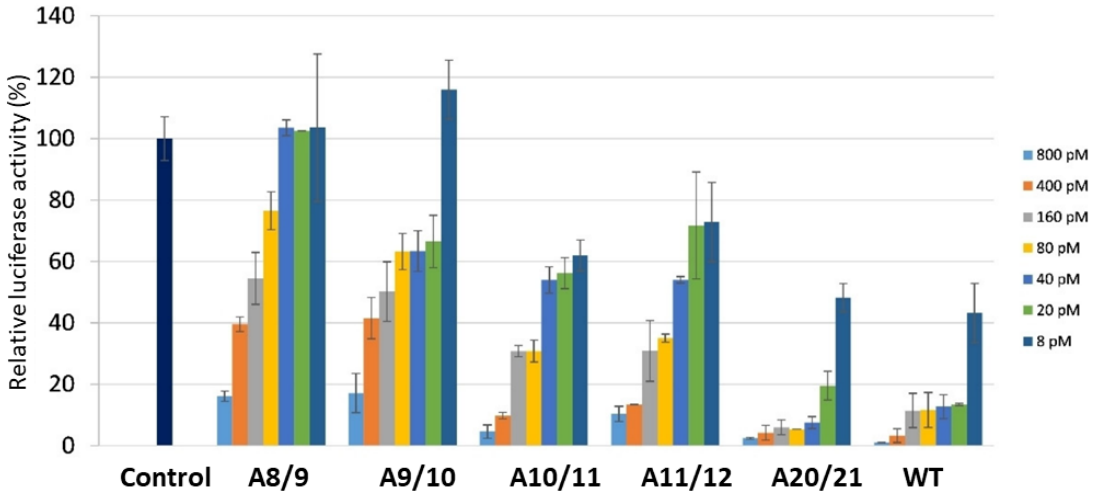

Figure 21: Reduction in normalized firefly luciferase protein expression for siRNAs bearing an azobenzene linker on the sense strand, performed by Dr. Hammill. The two sense strand nucleotides replaced by the azobenzene linker are indicated as #/# from the 5' end. Each siRNA was treated at a concentration of 8, 20, 40, 80, 160, 400 or 800 pM HeLa cells and lysed 22 hr post transfection.

Centrally located sense strand azobenzene modifications impart uptake tolerance or inhibition when in the *trans* or *cis* form, respectively, with a reduction in overall antisense potency (siRNA synthesis and assays performed my Dr. Hammill; Figure 21).[4] However, the modification is likely to have a substantial impact on the activity of the modified strand. Therefore, strand activity assays were performed to characterize target cleavage by each strand. To facilitate these studies, Dr. Hammill introduced an azobenzene at nucleotide one, eight, ten, or twenty on the sense strand (Table 1). These positions provide an opportunity to evaluate the impact of 5', central, or 3' modifications. Additionally, an azobenzene control was also investigated through placement of the azobenzene within the sense strand of an siRNA which targets the endogenous gene *bcl-2*.

Table 1. Azobenzene modified siRNAs used in this study.

siRNA	Sequence and Location of Azobenzene
WT[a]	5' CUUACGCUGAGUACUUCGAtt 3' 3' ttGAAUGCGACUCAUGAAGCU 5'
A1/2	5' ******UACGCUGAGUACUUCGAtt 3' 3' ttGAAUGCGACUCAUGAAGCU 5'
A8/9	5' CUUACGC******AGUACUUCGAtt 3' 3' ttGAAUGCGACUCAUGAAGCU 5'
A10/11	5' CUUACGCUG******UACUUCGAtt 3' 3' ttGAAUGCGACUCAUGAAGCU 5'
A20/21	5' CUUACGCUGAGUACUUCGA****** 3' 3' ttGAAUGCGACUCAUGAAGCU 5'
Abcl2[b]	5' GCCUUCUUU******GUUCGGUGtt 3' 3' ttGAAUGCGACUCAUGAAGCU 5'

[a] The top and bottom strands correspond to the sense and antisense strand, respectively. Deoxynucleotides indicated with lower case.
[b] Endogenous target (*bcl-2*) and azobenzene negative control
* Indicates modification location

As expected, azobenzene modified siRNAs potency for mRNA cleavage was substantially reduced compared to the wildtype (Figure 22). Modification of the 5' end (A1/2) led to dramatic loss in both antisense and sense strand activity, suggesting poor recognition by Ago2. Antisense activity for centrally modified sense strand siRNA was tolerated (A8/9 & A10/11) and managed to reach maximum potency of up to 85% silencing by 4 nM. Although the antisense potency was reduced up to 500-fold for these siRNAs, sense strand activity was dramatically lower with a maximum of target reduction of only 35%, suggesting either limited uptake or poor target recognition. Central modifications may interrupt recognition by Ago2 but may also prevent cleavage of the passenger strand due to misaligned phosphodiester linkages at the cleavage site. In contrast, siRNA modified

at the 3’ end (A20/21) retained good antisense strand potency, but also carried relatively high sense strand activity. At the 3’ end, the azobenzene is not expected to have a large impact on RISC uptake. Modifications at the 3’ end are generally well tolerated for either strand but preferred for the sense strand. Examples include the large GalNAc trimer present on the siRNA therapeutic givosiran[7], or asymmetrical siRNA which lack several sense strand nucleotides at the 3’ end altogether.[8]

In conclusion, sense strand azobenzene modifications improve antisense vs sense strand activity; however, there is also a loss in overall potency. Since the azobenzene modification was developed for control of siRNA activity, rather than strand selection properties, these assays have characterized an additional benefit for the modification, therefore increasing the value of the azobenzene modification.

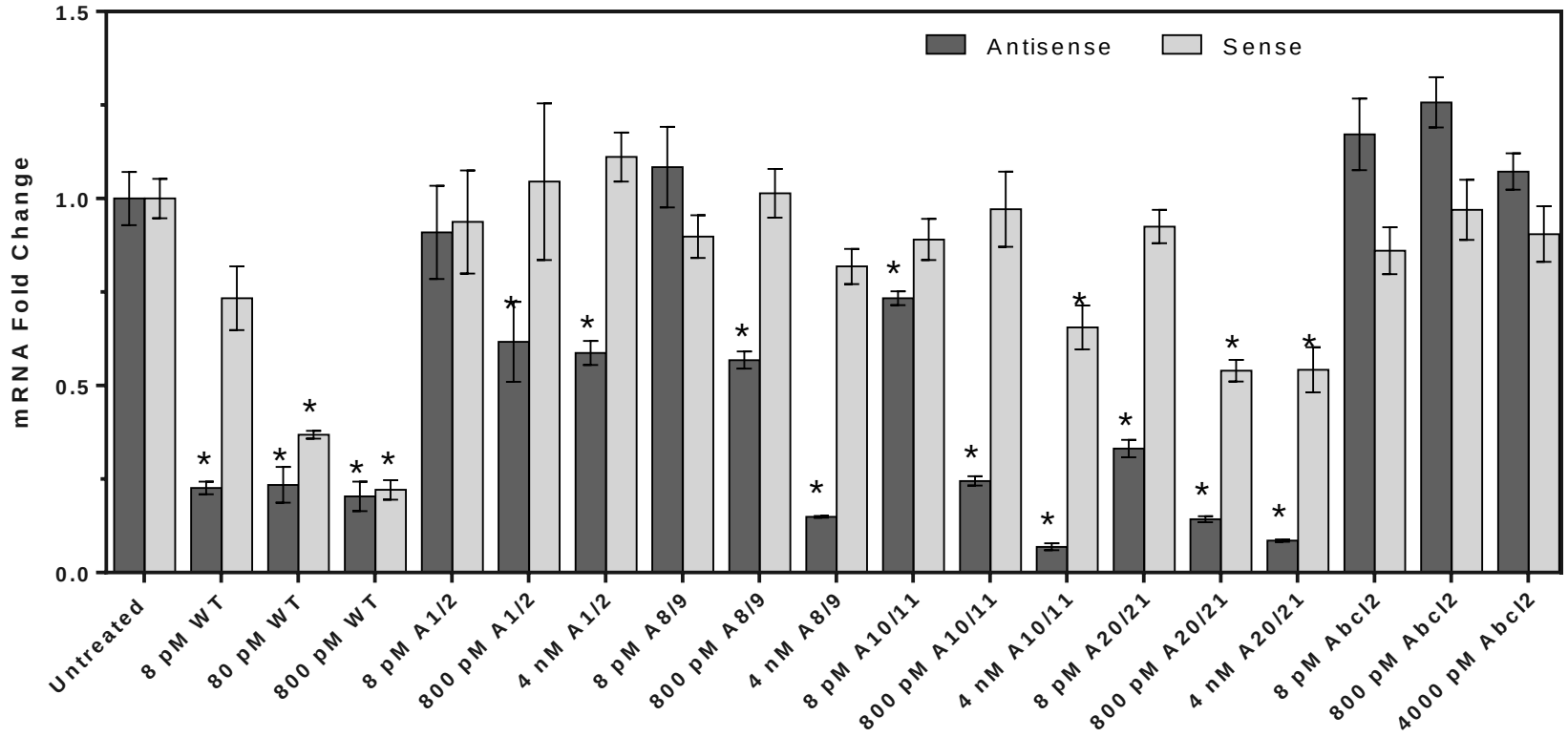

Figure 22: Reduction in antisense or sense strand target mRNA expression for siRNAs bearing an azobenzene linker on the sense strand. Expression was measured in HeLa cells 24 hr after transfection. Mean ± SEM values of independent triplicates are shown. (*) indicates a statistically significant difference ($p < 0.05$) between the untreated and treated sample.

III.II **Propargyl and Folic Acid Modified siRNAs**

The propargyl linker and triazole-linked folic acid modifications were introduced into siRNA by Dr. Lidya Salim (Figure 23). The propargyl linker acts as a convenient handle for the copper catalyzed click reaction addition of molecules of interest, such as folic acid. Folic acid is an important vitamin for the healthy growth and function of cells, and particularly important for pregnant women. Several types of cancer are associated with increased folate uptake and will over express folate receptor alpha.[9] This provides the opportunity for carrier free, semi-selective uptake of a folic-acid conjugated siRNA into

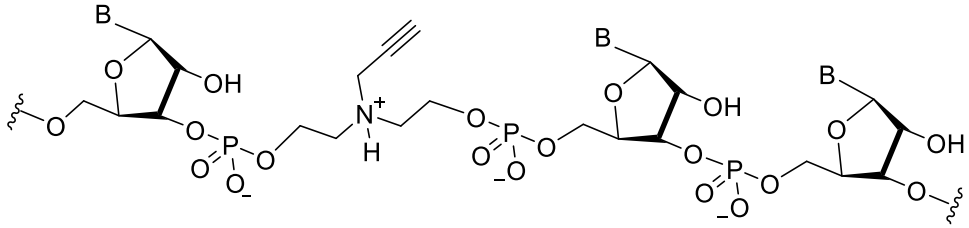

Propargyl Linker

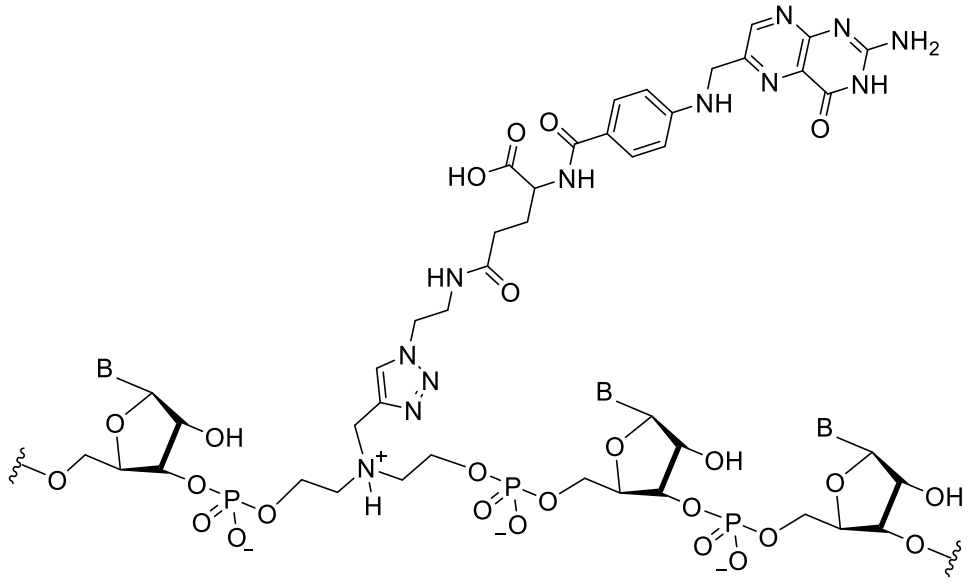

Folic Acid Linker

Figure 23: The propargyl linker (top) and triazole-bound folic acid linker (bottom). The propargyl linker acts as a convenient handle for click-chemistry, for molecules such as folic acid.

cancerous cells. This approach is particularly well suited for cancers which overexpress both the folate receptor alpha and an identified oncogene. Notably, click chemistry has previously been used to attach folic acid to an siRNA; however, previous work involved long linkers such as PEG[10] rather than the proximal attachment developed by Dr. Salim.

Dr. Salim performed protein level gene silencing assays with propargyl or folic acid modified siRNAs (Figure 24).[11] The most active siRNAs after carrier-free transfection carried a folic acid linker that replaced position 9, or both 9 and 10 of the sense strand. Despite the small size of the linker (approximately one nucleotide long), omitting a second nucleotide did not inhibit activity; perhaps due to the high flexibility of the modification. To better understand the impact of these modifications, assays were performed with propargyl or folic-acid modified siRNAs which replace a single central or the two terminal 3' end nucleotides (Table 2).

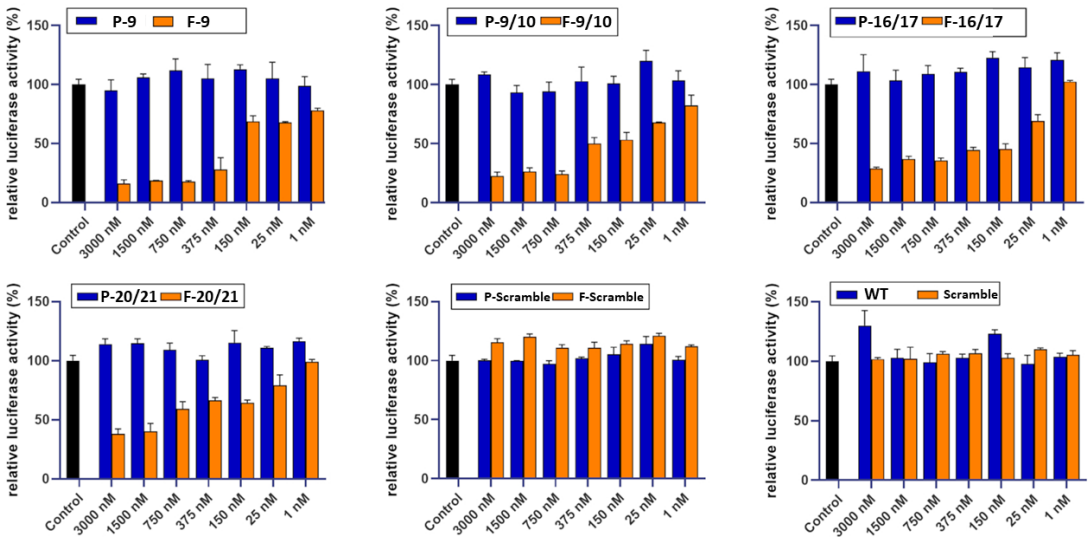

Figure 24: Reduction in antisense or sense strand target mRNA expression for siRNAs bearing a propargyl or folic acid linker on the sense strand, performed by Dr. Salim. The nucleotide(s) replaced by the propargyl (P-#) or folic acid (F-#) linker are indicated on each graph. Expression was measured in HeLa cells 24 hr after transfection. Mean ± SEM values of independent triplicates are shown.

Table 2. Propargyl and folic acid siRNAs used in this study.

siRNA	Sequence and Location of Modification	Modification
WT[a]	5' CUUACGCUGAGUACUUCGAtt 3' 3' ttGAAUGCGACUCAUGAAGCU 5'	N/A
P10	5' CUUACGCUG*****GUACUUCGAtt 3' 3' ttGAAUGCGACUCAUGAAGCU 5'	Propargyl
F10	5' CUUACGCUG*****GUACUUCGAtt 3' 3' ttGAAUGCGACUCAUGAAGCU 5'	Folic Acid
P20/21	5' CUUACGCUGAGUACUUCGA***** 3' 3' ttGAAUGCGACUCAUGAAGCU 5'	Propargyl
F20/21	5' CUUACGCUGAGUACUUCGA***** 3' 3' ttGAAUGCGACUCAUGAAGCU 5'	Folic Acid

[a] The top and bottom strands correspond to the sense and antisense strand, respectively. Deoxynucleotides indicated with lower case.
* Indicates modification location

Assays were performed on siRNA carrying propargyl and folic acid modifications at either position 10 (P10 and F10) or 20 (P20/21 and F20/21) of the sense strand (Figure 25). Notably, the 3' terminal modification removes both thymidine residues, truncating the sense strand by one nucleotide. Despite having the same backbone, the impact of the propargyl modification does not predict the impact of the folic acid modification for either modification location tested. P1 reaches 74% to 97% antisense silencing at 800 pM to 4 nM, respectively, while F1 is only capable of 47% to 65% antisense silencing at the same concentrations. Both P10 and F10 modifications limited sense strand activity, with a maximum of silencing of 43% seen at 800 pM with P10. The small size of the propargyl linker is not likely to interrupt recognition of the adjacent phosphodiester bond, allowing cleavage of the sense strand when oriented as the passenger strand. However, the large size and charge of folic acid is likely to impart electrical or spatial constraints to strand

positioning within Ago2. The dissimilarity of these modifications was even more evident when comparing P20/21 and F20/21. The placement of a 3' propargyl modification in P20/21 substantially increased sense strand activity while limiting antisense strand activity. At 800 pM and 4 nM, the antisense and sense strand were roughly equal in potency. However, a dramatic shift in strand activity balance was observed upon the addition of folic acid. The antisense strand of F20/21 had surprisingly high potency; comparable to wildtype. The high antisense activity was accompanied by the dramatic inhibition of the sense strand, with statistically significant silencing of 31% only at 4 nM. Although 3' modifications are often well tolerated by RISC machinery[12], the folic acid moiety may be involved in hydrogen bond interactions with nearby nucleobases, or base stacking as seen phenyl groups.[13] This could substantially increase the thermodynamic stability of the end, preventing uptake. Alternatively, the size and charge of folate may play a steric or electrostatic role in limiting strand activity.

In conclusion, the proximal, triazole linked folic acid provides a benefit for strand activity at the sense strand 3' terminal, but not at position ten. Additionally, the backbone used for the propargyl linker is not the primary contributor to the selection effects observed, as the propargyl linker itself was a poor predictor for the folic acid modifications. These findings are of interest for decisions regarding the location of conjugated moieties for siRNA.

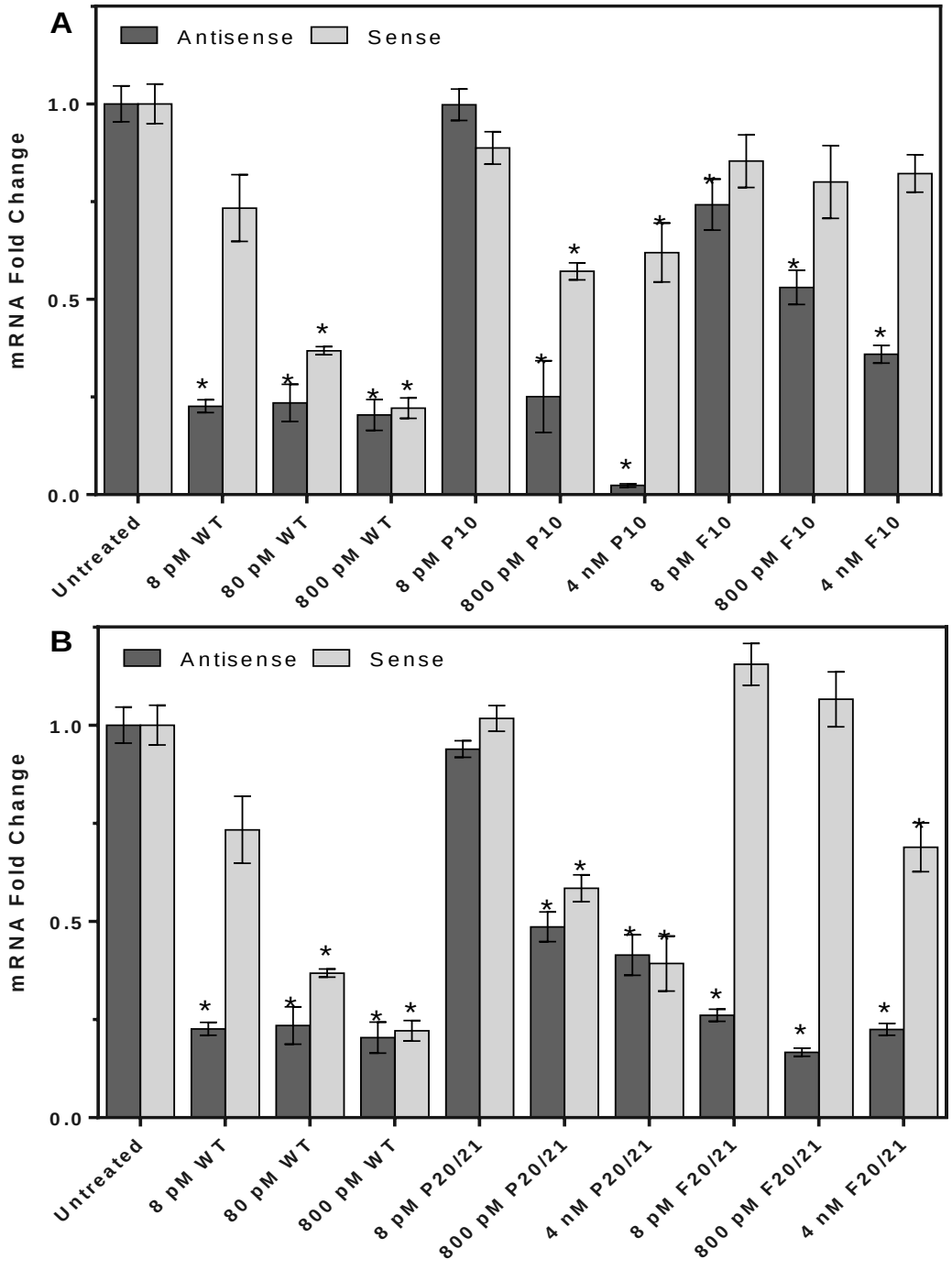

Figure 25: Reduction in antisense or sense strand target mRNA expression for siRNAs bearing a propargyl (P) or folic acid (F) linker within the central region (A) or 3' end (B) of the sense strand. Expression was measured in HeLa cells 24 hr after transfection. Mean ± SEM values of independent triplicates are shown. (*) indicates a statistically significant difference ($p < 0.05$) between the untreated and treated sample.

III.III **Cubane Modified siRNAs**

The cubane molecule is of great interest, both from an organic chemistry and therapeutic approach. It is thermodynamically unstable and highly strained; however, no kinetically viable path exists for its decomposition at physiological temperatures.[14] Importantly, the cubane is of pharmaceutical interest as it can act as a bioisostere of benzene. Much like benzene, the cubane holds significant potential as a robust scaffold, but is preferred for its biological stability and absence from inherent toxicity. Therefore, siRNA may greatly benefit from the incorporation from such a molecule. To introduce a cubane to siRNA (Figure 26), Dr. Kouta Tsubaki synthesized a cubane diol precursor for phosphoramidite coupling, performed by Dr. Hammill.

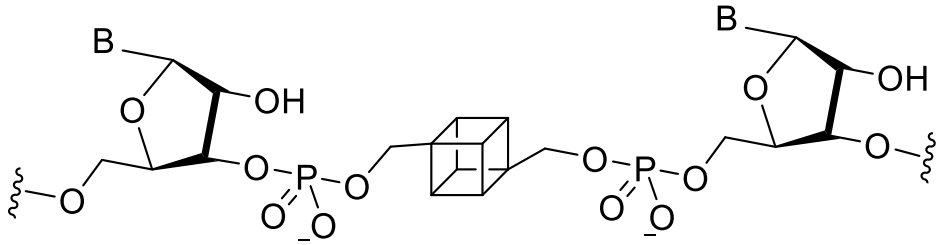

Figure 26: The cubane linker in RNA. The cubane has similar functionality to a benzene but carries less inherent toxicity.

Most modifications that are structurally unique from natural nucleotides are associated with reduced siRNA potency, and luciferase assays (performed by Dr. Salim) revealed that the cubane is no exception. When placed on the antisense or sense strand, the IC_{50} was reduced from 7.7 to 52 fold, with the most dramatic loss in potency seen with a centrally located antisense modification (Figure 27, A).[15] When placed on both the antisense and sense strand, the IC_{50} was reduced by up to 213 fold (Figure 27, B). Modifications near the 3' end were least impactful, while central modifications lead to the most dramatic loss in activity.

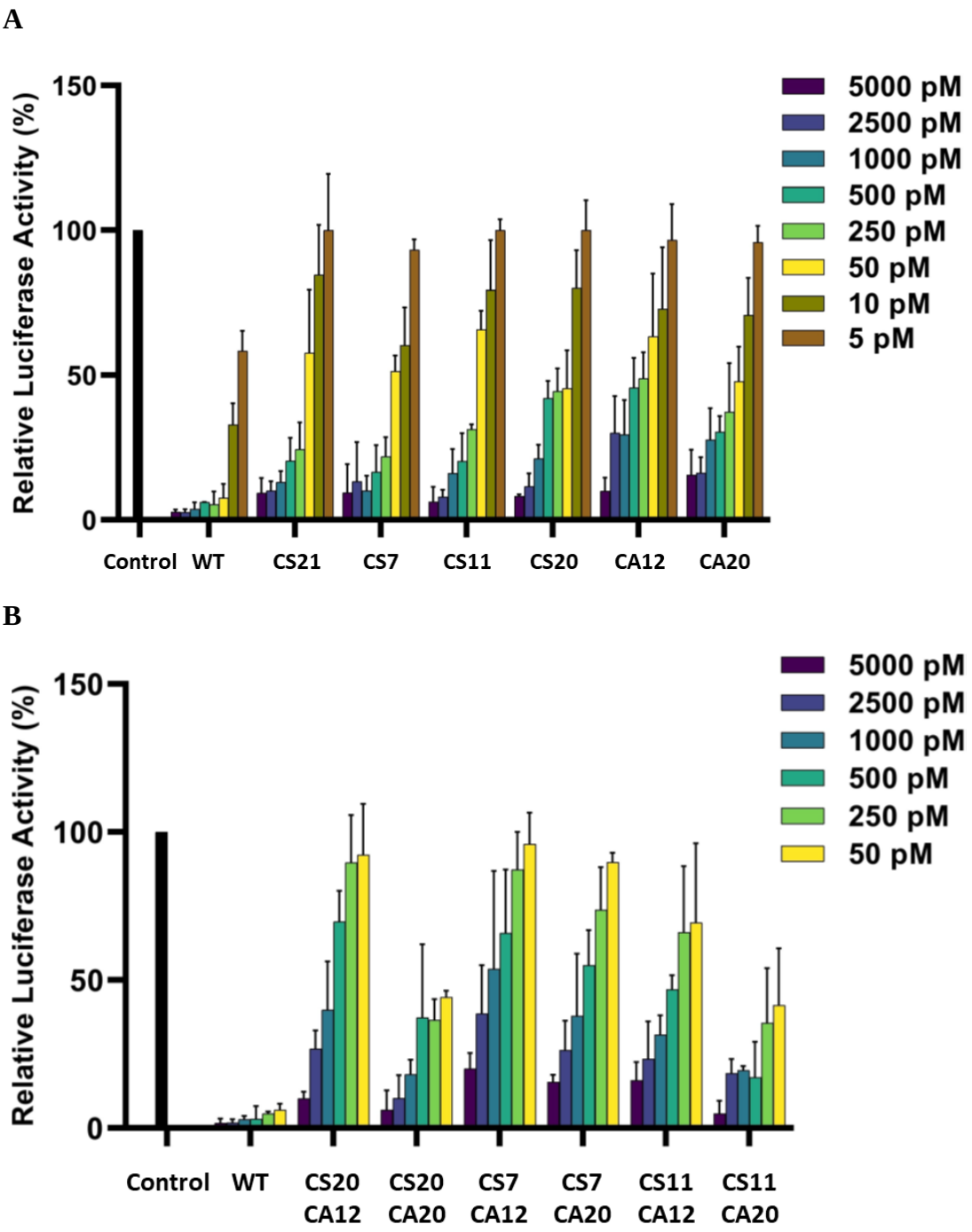

Figure 27: Reduction in antisense or sense strand target mRNA expression for siRNAs bearing a cubane linker (C) on the antisense (A#) or sense strand (S#) (top, A), or both strands (bottom, B), performed by Dr. Salim. The nucleotide position replaced by the linker is indicated as a number from the 5' end. Expression was measured in HeLa cells 24 hr after transfection. Mean ± SEM values of independent triplicates are shown.

Table 3: Cubane modified siRNAs used in this study.

siRNA	Sequence and Location of Cubane
WT[a]	5' CUUACGCUGAGUACUUCGAtt 3' 3' ttGAAUGCGACUCAUGAAGCU 5'
CS7	5' CUUACG*UGAGUACUUCGAtt 3' 3' ttGAAUGCGACUCAUGAAGCU 5'
CS11	5' CUUACGCUGA*****UACUUCGAtt 3' 3' ttGAAUGCGACUCAUGAAGCU 5'
CA12	5' CUUACGCUGAGUACUUCGAtt 3' 3' ttGAAUGCG*CUCAUGAAGCU 5'
CS7:A12	5' CUUACG*UGAGUACUUCGAtt 3' 3' ttGAAUGCG*CUCAUGAAGCU 5'
CS7:A20	5' CUUACG*UGAGUACUUCGAtt 3' 3' *GAAUGCGACUCAUGAAGCU 5'
CS11:A20	5' CUUACGCUGA*UACUUCGAtt 3' 3' *GAAUGCGACUCAUGAAGCU 5'

[a] The top and bottom strands correspond to the sense and antisense strand, respectively. Deoxynucleotides indicated with lower case.
* Indicates modification location

To further our understanding of the role that the cubane has on siRNA, and predict where the loss in activity occurs, strand activity assays were performed on select siRNAs (Table 3). As expected, the addition of cubane modifications reduced siRNA potency at the mRNA level (Figure 28). Sense strand modifications, as seen with CS7 and CS11, were effective at limiting sense strand activity. A central sense strand cubane modification (CS11) completely abolished sense strand activity while facilitating up to 90% antisense knockdown at 5000 pM. Fittingly, the cubane was not well tolerated in the central region of the antisense strand (CA12, CS7:A12) and resulted in the inactivation of siRNA. In contrast, antisense modifications at the 3’ end were well tolerated. The modification in CS7

and CS11 were each combined with a 3’ cubane to create CS7:A12 and CS7:A20. These siRNAs had comparable potency to those bearing the single sense strand modification and exhibited desirable antisense vs sense strand activity.

The ability to measure both the antisense and sense strand activity of cubane modified siRNAs identified that, in the locations tested, the cubane will not result in increased uptake of the non-modified strand. This was exemplified by CA12, as no sense strand activity was measured at the high concentration of 5000 pM, indicating poor recognition siRNA structure itself. However, the location of the modification is critical. Placing the cubane at position 7 of the sense strand (CS7) effectively eliminates sense strand activity, but at a slightly higher penalty to antisense potency than when placed at position 11 (CS11). This is somewhat surprising as a central modification is more likely to impact the position of the passenger strand phosphodiester bond relative to the nuclease active site. Notably, the addition of the 3’ cubane on the antisense strand had a more impactful inactivating effect when added to a sense strand cubane at position 11 than 7, as seen by CS11:A20 and CS7:A20. These findings exemplify the benefits for characterizing the impact that chemical modifications have on strand activity and can reveal mechanisms behind reduced activity.

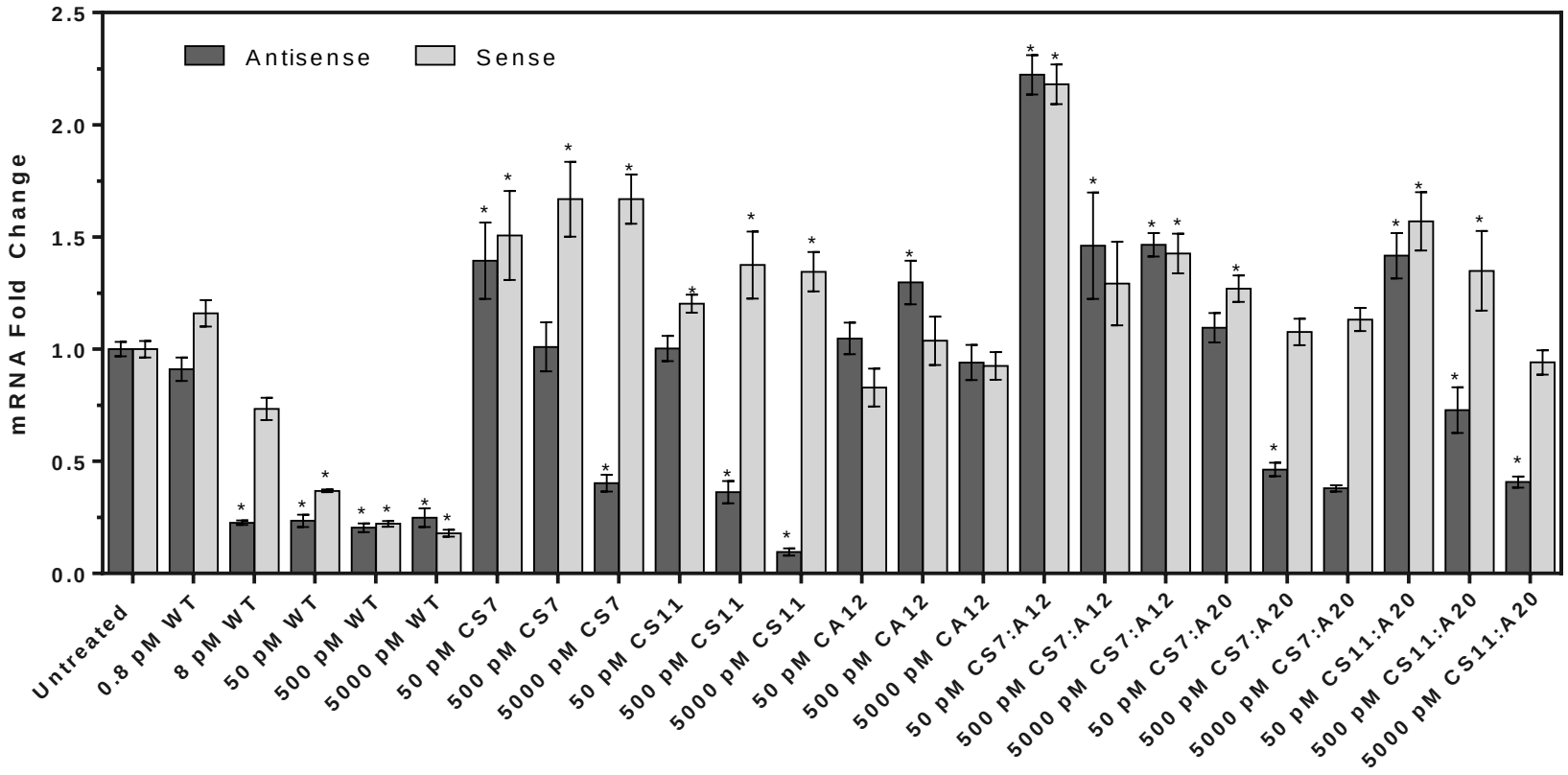

Figure 28: Reduction in antisense or sense strand target mRNA expression for siRNAs bearing an azobenzene linker on the antisense strand, sense strand, or both strands. Expression was measured in HeLa cells 24 hr after transfection. Mean ± SEM values of independent triplicates are shown. (*) indicates a statistically significant difference ($p < 0.05$) between the untreated and treated sample.

III.IV **Phenylethyl Phosphate Modified siRNAs**

Phosphate backbone modifications have been instrumental in the development of siRNA therapeutics for their ability to resist nuclease degradation. The most widely used chemical modification in marketed oligonucleotide therapeutics is the phosphorothioate. While the replacement of a non-bridging oxygen with a sulfur atom provides excellent nuclease resistance with low toxicity, the persisting negative charge of the backbone remains and prevents cell entry through the phospholipid bilayer. Therefore, a neutral backbone modification that is both tolerated within the RISC and provides nuclease resistance is highly desirable. Towards this goal, phenylethyl dinucleotide triesters were developed by Dr. Tsubaki for incorporation the synthesis of phenylethyl phosphotriester (PP) modified siRNA (Figure 29).

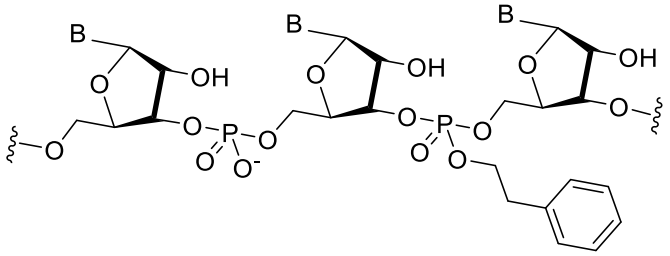

Figure 29: The natural (left) and phenylethyl phosphate linker (right) in RNA. The phenylethyl phosphate is a hydrophobic, neutral backbone modification.

The dinucleotide phosphoramidites were developed as deoxyuridine or deoxythymidine dimers, thus limiting their placement within the siRNA to UU repeats. The modification was therefore placed directly after position 2, 15, or 20 by Dr. Hammill. The PP modification was generally well tolerated at all locations tested in siRNA and provided nuclease resistance (performed by Dr. Salim; Figure 30).[16] To further investigate the utility of this modification, strand activity assays were performed on selected siRNAs (Table 4).

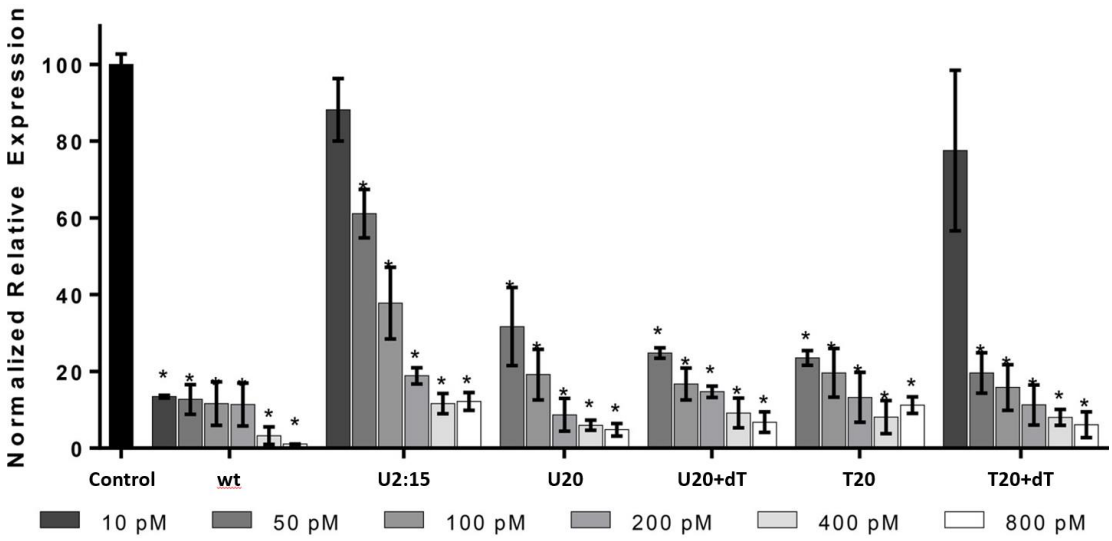

Figure 30: Reduction in normalized firefly luciferase protein expression for siRNAs bearing a phenylethyl phosphotriester linker on the sense strand, performed by Dr. Hammill. U indicates a linker placed between two deoxyuridine nucleotides, T indicates a linker placed between two deoxythymidine nucleotides. The number that follows indicates the location(s) of the modified phosphate on the sense strand. For two of the siRNAs, an additional deoxythymidine (+dT) was placed at the 3' end of the sense strand. (*) indicates a statistically significant difference ($p < 0.05$) between the untreated and treated sample.

Table 4: Phenylethyl phosphotriester modified siRNAs used in this study.

siRNA	Sequence and Location of Modifications
WT[a]	5' CUUACGCUGAGUACUUCGAtt 3' 3' ttGAAUGCGACUCAUGAAGCU 5'
U2:15	5' Cu*uACGCUGAGUACu*uCGAtt 3' 3' ttGAAUGCGACUCAUGAAGCU 5'
U20	5' CUUACGCUGAGUACUUCGAu*u 3' 3' ttGAAUGCGACUCAUGAAGCU 5'
U20+dT	5' CUUACGCUGAGUACUUCGAu*ut 3' 3' ttGAAUGCGACUCAUGAAGCU 5'

[a] The top and bottom strands correspond to the sense and antisense strand, respectively. Deoxynucleotides indicated with lower case.
* Indicates modification location

Little to no improvement in strand activity was seen for U20 or U20+dT, which carry the modification only at the 3' end of the sense strand (Figure 31). However, when the PP

was placed at position 2 and 15 (U2:15), antisense activity reached a maximum potency of 75% silencing by 200 pM with the sense strand only reaching a statistically insignificant silencing of 13% at the same concentration. At four times the concentration (800 pM), there is still a clear difference in activity between the two strands. Taken together, the PP modification is tolerated within the antisense and sense strand but do not have a dramatic impact on strand activity, suggesting that other hydrophobic triester modifications will likely be well tolerated in siRNA.

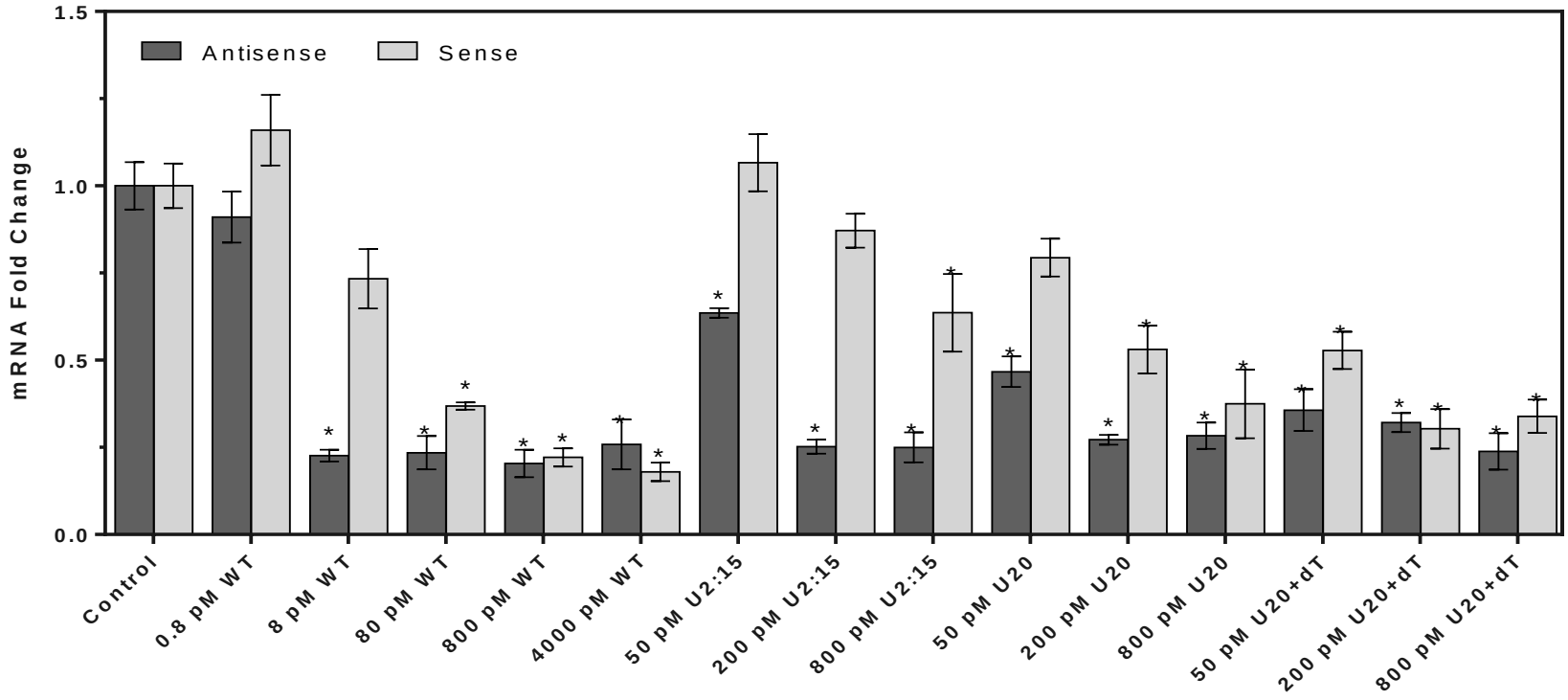

Figure 31: Reduction in antisense or sense strand target mRNA expression for siRNAs bearing a phenylethyl phosphotriester linker on the sense strand. Expression was measured in HeLa cells 24 hr after transfection. Mean ± SEM values of independent triplicates are shown. (*) indicates a statistically significant difference ($p < 0.05$) between the untreated and treated sample.

III.V **Hydrophobic Phosphate Modified siRNAs**

Expanding on previous work with the phenylethyl phosphate triester modification, Dr. Tsubaki developed three more hydrophobic triester modifications. These contain either one (H1), two (H2), or three (H3) hydrophobic octadecyloxy groups bound to a phosphate triester backbone (Figure 32). Like previous work, the hydrophobic triesters were prepared as dinucleotides which limits their placement to UU repeats within siRNA. The long hydrophobic octadecyloxy group used in these dinucleotides are similar in length to lipids within the phospholipid bilayer, theoretically facilitating hydrophobic interactions with the cell membrane.

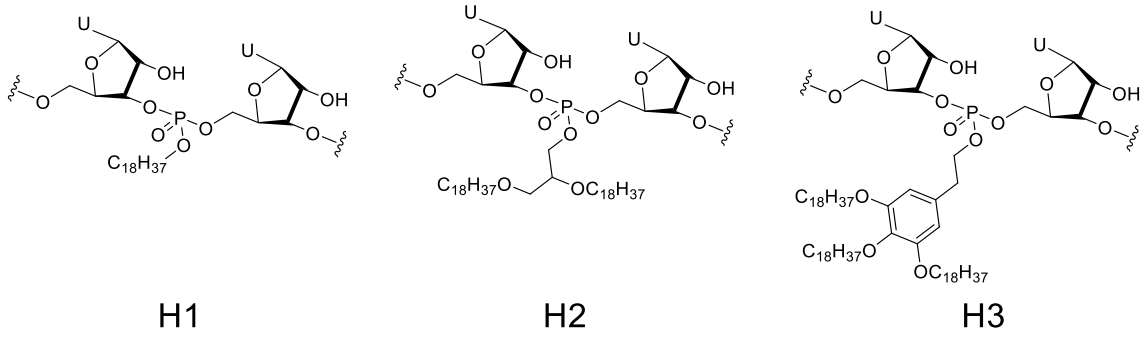

Figure 32: Three novel hydrophobic triester phosphate backbone modifications.

The H1 and H2 modification replaced phosphodiester linkages number 2, 15 and 20 of the sense strand; however, SARS-CoV-2 pandemic-related interruptions resulted in only linkage number 20 of the sense strand being replaced with H3 (siRNAs assembled by Dr. Hammill). Dual luciferase assays were performed by Dr. Salim to evaluate siRNA potential with or without a transfection reagent. Carrier-assisted uptake of siRNA identified high tolerance for the H2 and H3 modification at the positions tested, and moderate tolerance for the H1 modification (Figure 33). The H1 and H2 modifications facilitated efficient cellular uptake in the absence of a transfection carrier (Figure 34). H1 at position 2 or 15 was the most effective at facilitating carrier-free gene silencing. Interestingly, the H3 modification did not permit uptake.

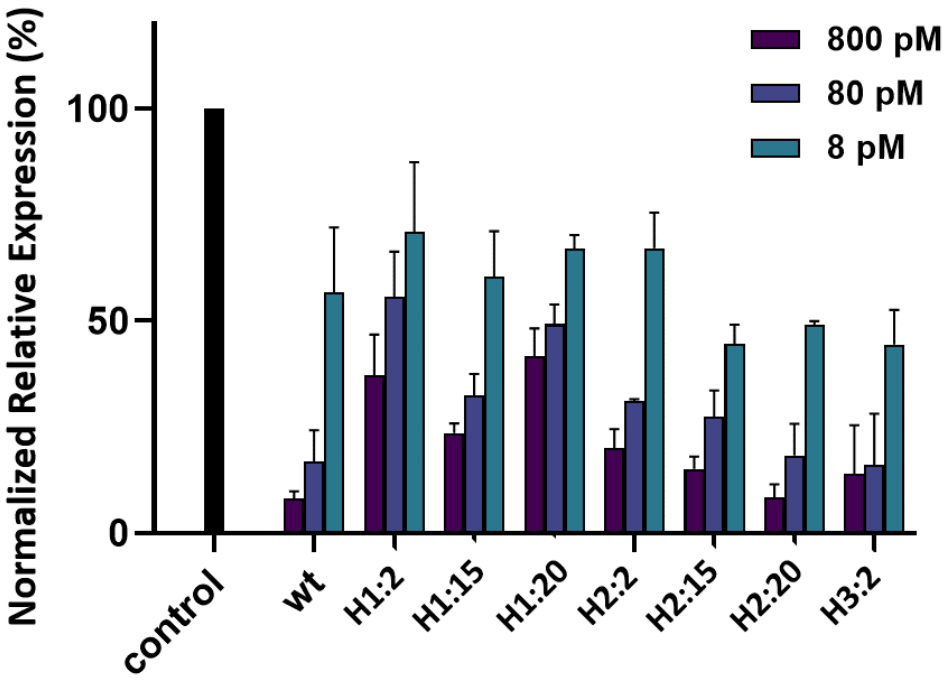

Figure 33: Reduction in normalized firefly luciferase protein expression for transfected siRNAs bearing hydrophobic phosphate triester backbone modifications, performed by Dr. Salim. H1, H2, and H3 refer to modifications described in Figure 32. The number that follows indicates the location(s) of the modified phosphate.

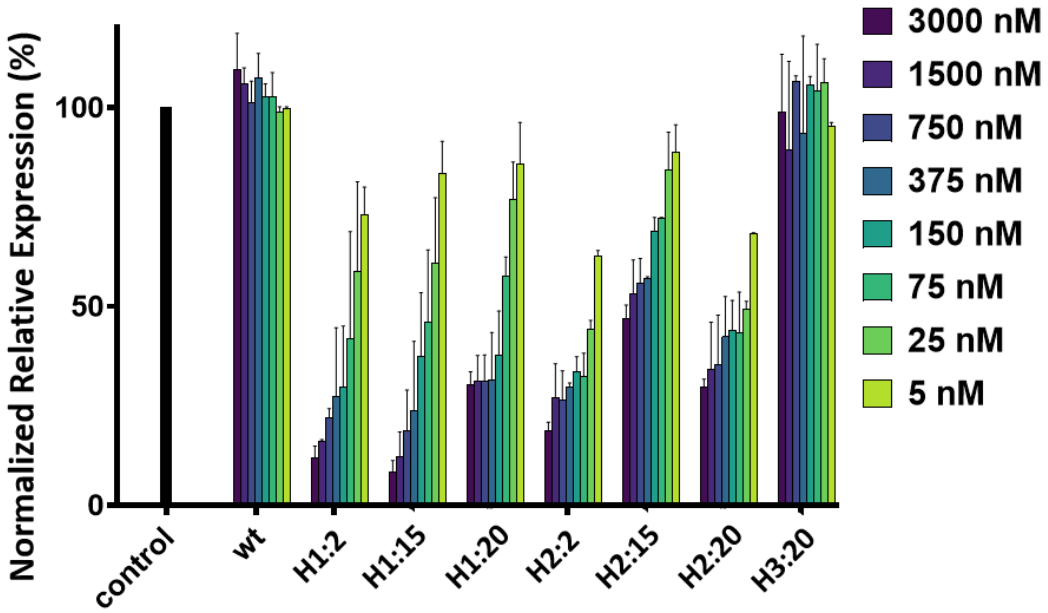

Figure 34: Reduction in normalized firefly luciferase protein expression for carrier-free delivery of siRNAs bearing hydrophobic phosphate triester backbone modifications, performed by Dr. Salim. H1, H2, and H3 refer to modifications described in Figure 32. The number that follows indicates the location(s) of the modified phosphate.

Although the polyanionic macromolecular structure of RNA prevents diffusion past the cellular membrane, hydrophobic interactions between the triester modifications and the lipid membrane are likely to anchor the siRNA into the membrane. From there, two methods of cell entry are theorized. The anchoring may be sufficient to enable diffusion past the cell membrane, as polyanionic macromolecules have been shown to achieve cellular entry when sufficient hydrophobicity is present.[17] Alternatively, the oxtoxy backbone modifications, which resemble the hydrophobic tails of phospholipids, may be recognized by cellular flippase or scramblase pumps to undergo translocation from the outer to the inner leaflets of the membrane.[18] It is also possible that the octadecyloxy groups are recognized by cellular/intracellular trafficking mechanisms and gain entry via endocytosis as seen with lipid siRNA conjugates.[19]

siRNAs with carrier-free delivery functionality were selected for strand activity assays, as described in Table 5. Importantly, the Lipofectamine 2000 carrier was used for these assays to control for variations due to uptake mechanisms. The H1 modification facilitated slightly higher antisense activity than the H2 modification at each position tested (Figure 35). Strand activity was not heavily impacted by the hydrophobic phosphate triester modifications, but position 15 was the most effective for H1, while position 2 was the most effective for H2. H2:2 was the only hydrophobically modified siRNA tested to completely inactivate the sense strand at the concentrations tested.

These results suggest that increasing hydrophobicity or steric hinderance on the phosphate backbone is sufficient to inhibit activity. These findings agree with the phenylethyl phosphate triester modifications, indicating that an overall high tolerance exists for small hydrophobic phosphate modifications. Multiple H1 modifications, such as

at position 2 and 15, may increase inhibition of the strand as seen for the phenylethyl phosphate triester.

Table 5: Hydrophobic phosphate triester modified siRNAs used in this study.

siRNA	Sequence and Location of Modifications
WT[a]	5' CUUACGCUGAGUACUUCGAtt 3' 3' ttGAAUGCGACUCAUGAAGCU 5'
H1:2	5' CU*UACGCUGAGUACUUCGAtt 3' 3' ttGAAUGCGACUCAUGAAGCU 5'
H1:15	5' CUUACGCUGAGUACU*UCGAtt 3' 3' ttGAAUGCGACUCAUGAAGCU 5'
H1:20	5' CUUACGCUGAGUACUUCGAU*U 3' 3' ttGAAUGCGACUCAUGAAGCU 5'
H2:2	5' CU*UACGCUGAGUACUUCGAtt 3' 3' ttGAAUGCGACUCAUGAAGCU 5'
H2:15	5' CUUACGCUGAGUACU*UCGAtt 3' 3' ttGAAUGCGACUCAUGAAGCU 5'
H2:20	5' CUUACGCUGAGUACUUCGAU*U 3' 3' ttGAAUGCGACUCAUGAAGCU 5'

[a] The top and bottom strands correspond to the sense and antisense strand, respectively. Deoxynucleotides indicated with lower case.
* Indicates modification location

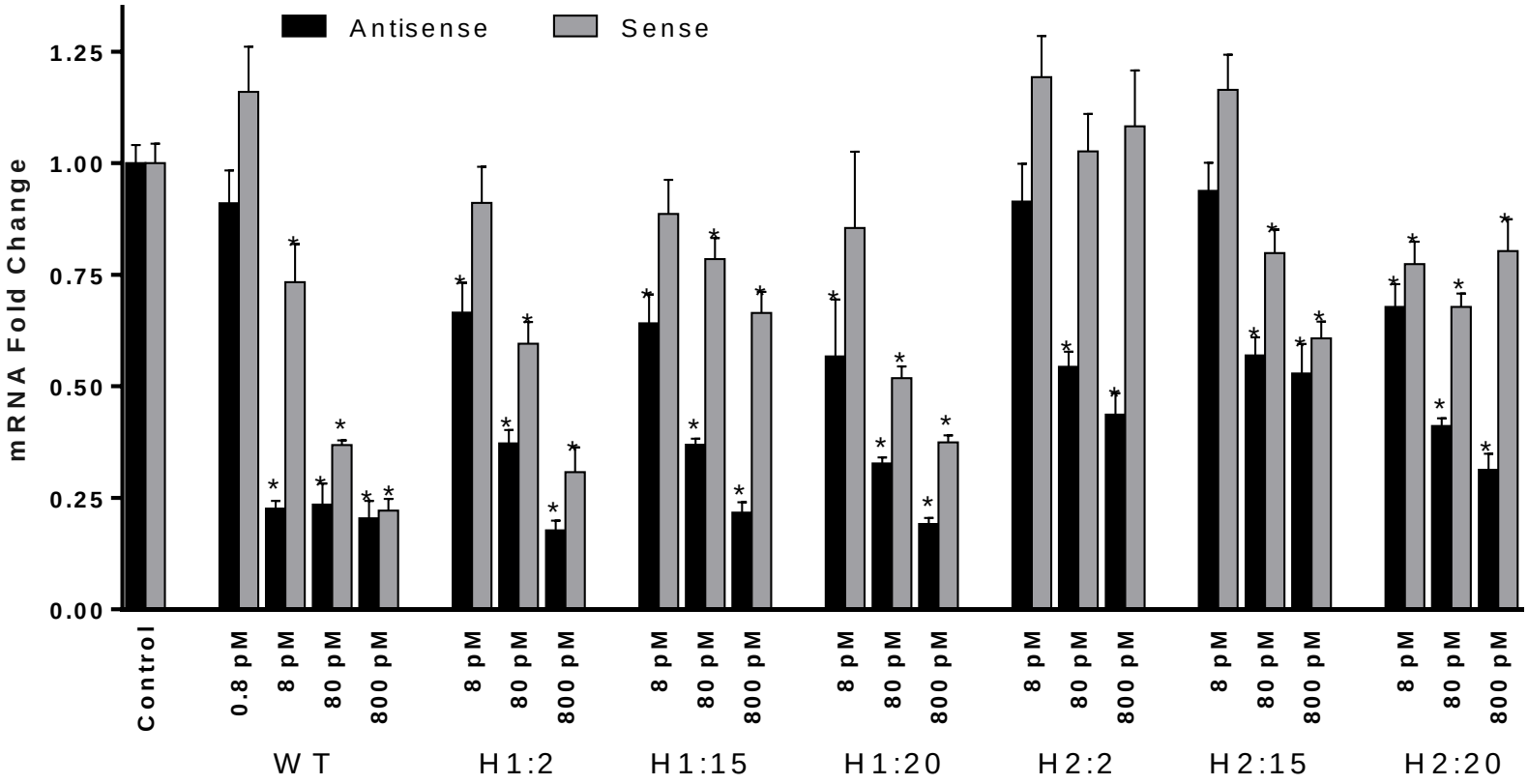

Figure 35: Reduction in antisense or sense strand target mRNA expression for siRNAs bearing a hydrophobic phosphate triester linker on the sense strand. Expression was measured in HeLa cells 24 hr after transfection. Mean ± SEM values of independent triplicates are shown. (*) indicates a statistically significant difference ($p < 0.05$) between the untreated and treated sample.

III.VI **References**

1. Hammill, M. L., Isaacs-Trépanier, C. & Desaulniers, J.-P. siRNAzos: A New Class of Azobenzene-Containing siRNAs that Can Photochemically Regulate Gene Expression. *ChemistrySelect* 2, 9810–9814 (2017).

2. Sato, M., Kinoshita, T., Takizawa, A. & Tsujita, Y. Photoinduced conformational transition of polypeptides containing azobenzenesulfonate in the side chains. *Macromolecules* 21, 1612–1616 (1988).

3. Anosova, I. et al. The structural diversity of artificial genetic polymers. *Nucleic Acids Res*. 44, 1007–1021 (2015).

4. Hammill, M. L., Patel, A., Alla, M. A. & Desaulniers, J.-P. Stability and evaluation of siRNAs labeled at the sense strand with a 3′-azobenzene unit. *Bioorg. Med. Chem. Lett*. 28, 3613–3616 (2018).

5. Hammill, M. L., Islam, G. & Desaulniers, J.-P. Reversible control of RNA interference by siRNAzos. *Org. Biomol. Chem*. 18, 41–46 (2019).

6. Hammill, M. L., Islam, G. & Desaulniers, J.-P. Synthesis, Derivatization and Photochemical Control of ortho-Functionalized Tetrachlorinated Azobenzene-Modified siRNAs. *ChemBioChem* (2020).

7. Foster, D. J. et al. Advanced siRNA designs further improve in vivo performance of GalNAc-siRNA conjugates. *Mol. Ther*. 26, 708–717 (2018).

8. Yuan, Z., Wu, X., Liu, C., Xu, G. & Wu, Z. Asymmetric siRNA: new strategy to improve specificity and reduce off-target gene expression. *Hum. Gene Ther*. 23, 521–532 (2012).

9. Cheung, A. et al. Targeting folate receptor alpha for cancer treatment. *Oncotarget* 7, 52553–52574 (2016).

10. Dohmen, C. et al. Defined folate-PEG-siRNA conjugates for receptor-specific gene silencing. *Mol. Ther. Acids* 1, e7 (2012).

11. Salim, L., Islam, G. & Desaulniers, J.-P. Targeted delivery and enhanced gene-silencing activity of centrally modified folic acid–siRNA conjugates. *Nucleic Acids Res.* 48, 75–85 (2020).

12. Chernolovskaya, E. L. & Zenkova, M. A. Chemical modification of siRNA. *Curr Opin Mol Ther* 12, 158–167 (2010).

13. Nakano, S., Uotani, Y., Uenishi, K., Fujii, M. & Sugimoto, N. Site-Selective RNA Cleavage by DNA Bearing a Base Pair-Mimic Nucleoside. *J. Am. Chem. Soc*. 127, 518–519 (2005).

14. Li, Z. & Anderson, S. L. Pyrolysis chemistry of cubane and methylcubane: The effect of methyl substitution on stability and product branching. *J. Phys. Chem*. A 107, 1162–1174 (2003).

15. Hammill, M. L. et al. Building siRNAs with cubes: synthesis and evaluation of cubane-modified siRNAs. *ChemBioChem* (2021).

16. Tsubaki, K. et al. Synthesis and Evaluation of Neutral Phosphate Triester Backbone-Modified siRNAs. *ACS Med. Chem. Lett*. (2020).

17. Abou Matar, T. & Karam, P. The role of hydrophobicity in the cellular uptake of negatively charged macromolecules. *Macromol. Biosci.* 18, 1700309 (2018).

18. Hankins, H. M., Baldridge, R. D., Xu, P. & Graham, T. R. Role of flippases, scramblases and transfer proteins in phosphatidylserine subcellular distribution. *Traffic* 16, 35–47 (2015).

19. Biscans, A. et al. Diverse lipid conjugates for functional extra-hepatic siRNA delivery in vivo. *Nucleic Acids Res.* 47, 1082–1096 (2019).

Chapter IV.

Synthesis and Characterization of Phosphorofluoridate Modified siRNA

IV.I **Phosphorofluoridates**

Monofluorophosphate esters are highly toxic gases, borne from the search for nerve gas agents during World War II.[1,2] For example, the nerve gas Sarin is a monofluorophosphate ester bearing a methyl and isopropoxy group. Sarin is highly toxic, with an oral LD_{50} of 550 μg/kg.[3] The most well studied phosphorofluoridate ester is diisopropyl phosphorofluoridate, a less toxic (LD_{50} of 6mg/kg) derivative that potently inhibits cholinesterase enzymes.[4] Instead of a chemical weapon, diisopropyl phosphorofluoridate has been investigated for use as a therapeutic and biochemical research tool.[5,6] Therefore, safety is of concern when working with monofluorophosphate esters and care must be taken in considering possible side reactions.

More recently, the success of solid phase oligonucleotide chemistry in the 1980's led to widespread research into alternative building blocks and methods for DNA/RNA synthesis, including nucleoside fluorophosphates. Multiple approaches to the synthesis of DNA and RNA fluorine-substituted phosphate derivates have been described[7-12]; however, no reports exist for their impact on oligonucleotide therapeutics. Therefore, widely applicable fluorinated phosphoramidite reactants for solid state oligonucleotide synthesis are of interest for oligonucleotides therapeutics. In this research, fluorinated phosphoramidites were investigated for the addition of a 5' phosphorofluoridate on siRNA termini.

IV.II **General Methods**

Solvents were purchased from Sigma-Aldrich. Tetrahydrofuran and triethylamine were dried on a Pure-Solv 400 solvent purification system (Innovative Technology (China) Ltd.). Column chromatography was performed using Silicycle Siliaflash P60 according to

standard chromatographic protocols.[13] NMR spectra were obtained on a Bruker Avance III HD 500 MHz NMR Spectrometer (^{1}H: 400 MHz, ^{31}P: 162 MHz, ^{13}C: 101 MHz, and ^{19}F: 377 MHz). Spectrum analysis was performed using ACD/NMR Processor (Advanced Chemistry Development, Inc.). LC/MS chromatograms were performed by Afrodet Giorgees using LC-QTOF on an Agilent 6545 QTOF-MS after separation on a Zorbax Eclipse Plus C18 1x100 mm 1.8-Micron Agilent column with an Agilent 1260 Infinity Binary Pump. The mobile phase was 0.6 ml/min of 5% ACN in 5 mM ammonium acetate pH 7 buffer. Tuning was done in negative mode, mass range 3200 m/z, extended dynamic range 2 GHz, high resolution mode. Sample concertation was 0.01 O.D/µl with injection volume of 20 µl. Data was analyzed using Agilent Technologies MassHunter Workstation Qualitative Analysis Software (Qual. 10.0).

IV.III **Synthesis of Phosphorofluoridates**

The synthesis of phosphorofluoridates can be achieved through replacing aryloxy groups bound to a phosphoramidite with a fluoride anion.[9] To achieve an aryloxy substituted phosphoramidite, aryloxy groups can be readily bound to commercially available starting materials, *N,N*-diisopropylaminodichloro-phosphine, *O*-(2-cyanoethyl) *N,N,N',N'*-tetraisopropylphosphoro-diamidite **1**, or *O*-(2-cyanoethyl) *N,N*-diisopropylchlorophosphoramidite **4.**[9] This can be achieved through an S_N2 substitution of a chlorine or activated diisopropylamine group in basic or acidic conditions, respectively. Ionic fluorine can then perform another S_N2 substitution using tetrabutylammonium fluoride (TBAF) to afford their fluorinated counterparts. A mono- or di-fluorinated phosphoramidite can then be coupled to the 5' hydroxyl of a growing oligonucleotide through standard coupling conditions. Based on work by Dąbkowski and Tworowska[9],

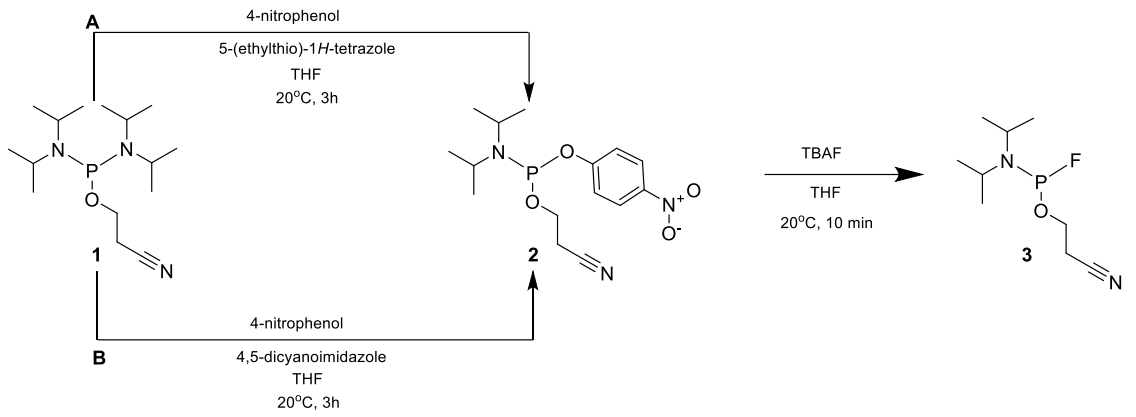

*Figure 36: Proposed scheme for synthesis of 3-(((diisopropylamino) fluorophosphaneyl)oxy)propanenitrile (**3**) via activation by 5-(ethylthio)-1H-tetrazole (A) or 4,5-dicyanoimidazole (B). Note: this does not describe the optimal conditions found through this research.*

proposed schemes for the synthesis of 3-(((diisopropylamino) fluorophosphaneyl)oxy)propanenitrile **3** (Figure 36) and 1,1-difluoro-*N*,*N*-diisopropyl phosphanamine **6** (Figure 37) are described. Both 5-(ethylthio)-1*H*-tetrazole (5-ETT; from Sigma-Aldrich) and 4,5-dicyanoimidazole (DCI; from TCI Chemicals) were evaluated for activating the diisopropylamine leaving group for the synthesis of 2-cyanoethyl (4-nitrophenyl) diisopropylphosphoramidite **2**. 5-ETT has a pKa of 4.3, and has become a standard coupling reagent used for rapid, high yield phosphoramidite synthesis in the mid 1990's[14]; however, DCI is a less acidic (pKa of 5.2), more soluble alternative that may react slower than 5-ETT. With the presence of two diisopropylamine leaving groups, a slower reaction may be beneficial to prevent di-substitution.

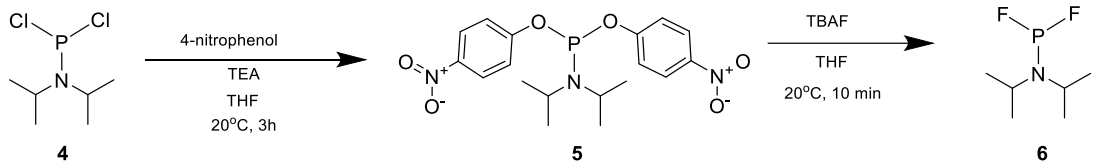

*Figure 37: Proposed scheme for synthesis of 1,1-difluoro-N,N-diisopropyl phosphanamine (**6**). Note: this does not describe the optimal conditions found through this research*

Proposedly, once the phosphoramidites **3** and **6** are prepared, standard phosphoramidite chemistry can be used to couple the molecule at the 5' hydroxyl through a condensation reaction, followed by oxidation, to transform the tricoordinated phosphorous compounds to tetracoordinated phosphorofluoridates.

IV.IV **Preparation of Phosphorofluoridates**

IV.IV.I Preparation of 2-cyanoethyl (4-nitrophenyl) diisopropyl phosphoramidite (2)

Initial attempts to synthesize **2** resulted in limited yield (under 50%) with a significant 4-nitrophenol disubstituted side product. Two approaches to improving yield were hypothesized. Firstly, by eliminating the activator, as 4-nitrophenol may be sufficiently acidic to activate the leaving group. Secondly, quenching the reaction with triethylamine once the starting material is consumed would deactivate diisopropylamine groups and increase stability of the product. Indeed, these adjustments improved yield to 63% with significantly reduced time compared to the proposed scheme. The ideal conditions are described here.

In a flame dried 100 ml round bottom flask, a stirred mixture of 2.5 mmol 3-((bis(diisopropylamino)phosphaneyl) oxy)propanenitrile **1** (Toronto Research Chemicals) in 25 ml dry THF was treated with 1.05 equivalents (2.6 mmol) of 4-nitrophenol under argon gas. Upon addition of 4-nitrophenol, the mixture turns yellow, and the production of a soluble black side product slowly formed. The reaction was monitored by TLC (dichloromethane) using UV light and $KMnO_4$ staining. Once the starting material was consumed (30 minutes), 1 ml of dry triethylamine was added to quench the reaction and dried on a rotary evaporator at 30 °C to yield a yellow oil. The oil was purified by silica

gel chromatography, using a mobile phase of neat dichloromethane with a product R_f of 0.7. Solvent removal afforded the colourless oil 2-cyanoethyl (4-nitrophenyl) diisopropylphosphoramidite **2** in 63% yield. Rapid purification during gel chromatography is essential, as the acidic silica degrades the product and the use of triethylamine in the mobile phase is not possible due to co-elution of other compounds. Nuclear magnetic resonance (NMR) spectra of the product agree with previous reports (Appendix C1).[2] ^{1}H NMR ($CDCl_3$, 400 MHz): Shift (ppm) 8.17 (d, J=8.6 Hz, 2H), 7.13 (d, J=8.8 Hz, 2H), 3.95 (t, J=3.9 Hz, 2H), 3.69-3.79 (m, 2H), 2.70 (t, J=6.2 Hz, 2H), 1.25 (d, J=6.8 Hz, 6H), 1.17 (d, J=6.8 Hz, 6H). ^{31}P NMR ($CDCl_3$, 162 MHz): Shift (ppm) 147.5 (quin, J=17.6 Hz).

IV.IV.II Preparation of 3-(((diisopropylamino)fluorophosphaneyl)oxy) propanenitrile (3)

In a flame dried 50 ml round bottom flask, a stirred mixture of 1.85 mmol 2-cyanoethyl (4-nitrophenyl) diisopropylphosphoramidite **2** in 10 ml dry THF was treated with 1 equivalent of 1.0 M TBAF in THF (1.85 ml; 1.85 mmol) under argon gas. The solution instantly turned yellow, and after several minutes, the tetra-n-butylammonium para-nitrophenolate salt crashed out of solution. The reaction was monitored by TLC (dichloromethane) under UV light and staining with KMnO4. Once the starting material was consumed (10 minutes), the solution was filtered, rinsed with dry THF, and dried on a rotary evaporator at 30 °C. The residue was purified by silica gel chromatography, with a mobile phase of neat dichloromethane with a product R_f 0.70 to afford the clear oil 3-(((diisopropylamino) fluorophosphaneyl)-oxy)propanenitrile **3** in 80% yield. Rapid purification during gel chromatography is essential. Nuclear magnetic resonance (NMR) spectra agree with previous reports (Appendix C2).[2] ^{1}H NMR ($CDCl_3$, 400 MHz): Shift

(ppm) 3.93 - 4.02 (m, 2H), 3.62 - 3.74 (m, 2H), 2.68 (td, J=6.4, 1.8 Hz, 2H), 1.23 (d, J=8.6 Hz, 6H), 1.24 (d, J=8.6 Hz, 6H). ^{31}P NMR ($CDCl_3$, 162 MHz): Shift (ppm) 155 (d, J=1117.0 Hz). ^{19}F NMR ($CDCl_3$, 377 MHz): Shift (ppm) 77.9 (d, J=1118.5 Hz).

IV.IV.III Preparation of bis(4-nitrophenyl) diisopropylphosphoramidite (5)

In a flame dried 100 ml round bottom flask, a mixture of 6 equivalents 4-nitrophenol (24 mmol) and 10 equivalents of triethylamine (5.57 ml) was added to 25 ml THF under argon gas. In a separate flame dried 20 ml vial, a mixture of 4 mmol 1,1-dichloro-N,N-diisopropylphosphanamine **4** (TCI Chemicals) in 10 ml dry THF was prepared. This solution was slowly added to the 4-nitrophenol/TEA solution over 60 seconds (highly reactive). The reaction was monitored by TLC (45:5:1 acetone:ethyl acetate:glacial acetic acid) under UV light and stained with KMnO4. Acetic acid was included in the TLC mobile phase to protonate and retard obscuring compounds on the TLC. Once the starting material was consumed (within 2.5 h), the solution was filtered to remove the triethylammonium hydrochloride salt and dried on a rotary evaporator at 30 °C. The residue was purified by silica gel chromatography, with a mobile phase of 2:3 hexanes:dichloromethane and product R_f of 0.6. Solvent removal afforded white crystals at 73% yield. Rapid purification during gel chromatography is essential. Proton and phosphorous NMR agreed with previous reports (Appendix C3).[2] ^{1}H NMR ($CDCl_3$, 400 MHz): Shift (ppm) 8.15 - 8.19 (m, 4H), 7.12 - 7.17 (m, 4H), 3.85 (dquin, J=11.4, 6.8 Hz, 2H), 1.20 - 1.27 (m, 12H). ^{31}P NMR ($CDCl_3$, 162 MHz): Shift (ppm) 143.8 (t, J=11.7 Hz).

IV.IV.IV Attempted Preparation of 1,1-difluoro-*N*,*N*-diisopropyl phosphanamine (6)

This product was not successfully isolated due to poor stability. Several attempts to make this product indicated a successful reaction, and NMR spectra of crude reaction mixtures suggest the presence of **6** (Appendix C4); however, any attempts at purification were unsuccessful. The following describes reaction conditions that afforded a crude product.

Prepare 2.2 equivalents of 1M TBAF in THF by stirring 3Å molecular sieves under argon gas for 1 hour. A stirred mixture of 0 °C 150 nmol bis(4-nitrophenyl) diisopropyl phosphoramidite (**5**) in 2.5 ml dry THF was prepared in a 25 ml flame dried round bottom flask. To this mixture, the TBAF dry was added dropwise over 60 seconds. After 10 minutes, the reaction was filtered and dried on a rotary evaporator. Quantitative proton and carbon NMR spectra suggested a low relative abundance of **6** compared to the tetrabutylammonium salt suggesting low product conversion. No aromatic protons were identified, meaning that filtration effectively removed 4-nitrophenol. Several phosphorous shifts were identified. Fluorine NMR did not identify a significant peak associated with tetrabutylammonium fluoride in $CDCl_3$ (-129 ppm).[15] Instead, two doublets were present at -73.2 ppm and -70.1 ppm, as well as a triplet in the ^{31}P spectrum, suggesting the presence of two fluorine atoms bound to a phosphorous. Purification using silica gel, liquid-liquid extraction, or precipitation proved unsuccessful due to rapid degradation. Notably, no literature reports exist for the isolation of **6**.

IV.V **Coupling, Oxidation, Cleavage, and Deprotection**

RNA was synthesized on an Applied Biosystems 394 DNA/RNA synthesizer using 1.00 μM cycles kept under argon at 55 psi using β-cyanoethyl 2'-*O*-TBDMS protected phosphoramidites. These phosphoramidites, reagents, and solid supports were purchased from Chemgenes Corporation and Glen Research. Both commercial and phosphorofluoridate phosphoramidites were dissolved in anhydrous acetonitrile to a concentration of 100 mM. Coupling reagents include acetic anhydride/pyridine/THF (Cap A), 16% N-methylimidazole in THF (Cap B), 0.25 M 5-ETT in ACN (activator), 0.02 M iodine/pyridine/H_2O/THF (oxidation solution), and 3% trichloroacetic acid/dichloromethane. Activated phosphoramidite coupling occurred over a period of 999 seconds. Antisense and sense strands were synthesized using 1.00 μM dT solid supports, while 10mer oligos were synthesized using 1.00 μM Universal III solid supports.

For synthesis of phosphorofluoridate modified RNA, manual or automatic coupling was performed, with manual coupling proving most effective. Automatic coupling followed standard synthetic procedures for phosphoramidites. Manual coupling was performed by preparing 250 μl of 100 mM **3** in anhydrous ACN under argon gas in a flame dried vial. The phosphoramidite was activated using 250 μl of 250 mM 5-ETT in anhydrous ACN, quickly mixed and loaded into a 1 ml syringe. With an empty syringe inserted into the opposite end of the solid support column, the 500 μl activated phosphoramidite solution was syringed through the column several times over a period of 10 minutes. The column was then washed with anhydrous ACN. The coupling and wash process was repeated twice more to achieve highest possible conversion. To oxidize the 5' phosphorofluoridite to a

phosphorofluoridate, 500 µl of oxidation solution was applied to the column for 60 seconds then washed with ACN.

Cleavage of oligonucleotides from their solid supports was performed using 1 ml of 1:1 40% w/v methylamine in H_2O and 33% w/v methylamine in ethanol for 1 hr at room temperature. This solution was transferred to a 1.5 ml microcentrifuge tube and incubated overnight at room temperature to remove cyanoethyl protecting groups. Solvent was evaporated using a Genevac miVac Centrifugal Concentrator (Fisher Scientific) evaporator and resuspended in a mixture of 100 µl DMSO and 125 µl triethylamine trihydrofluoride and incubated for 3 hours at 65 °C to remove the 2'-*O*-TBDMS protecting groups. Triethylamine trihydrofluoride was removed using a miVac evaporator overnight. Oligonucleotides were then precipitated with -70 °C 125 mM sodium acetate in EtOH and washed twice with -70 °C ethanol. Desalting of 21mers was performed thrice using Millipore Amicon MWCO 3000 spin columns.

IV.VI **Purification and siRNA Preparation**

Oligonucleotides were HPLC purified using a Vydac 218MS 5µm C18 4.6 mm x 150 mm reverse phase column (HiChrom) on a Waters 1525 binary HPLC pump with a Waters 2489 UV/Vis detector controlled by Empower 3 software. Conditions were 5 to 20% ACN gradient in 0.1M aqueous triethylammonium acetate pH 7 over 30 minutes. Peaks were collected, dried on a miVac evaporator, suspended in ultrapure H_2O, and evaluated via electrospray ionization tandem mass spectrophotometry. High purity antisense (Appendix C5) and sense (Appendix C6) strand samples with the desired product mass were used for siRNA annealing. These were 6771.92 g/mol (measured 6772.02 g/mol) for the antisense and 6685.86 g/mol (measured 6685.90 g/mol) for the sense strand (Appendix C7).

Equimolar quantities of RNAs were annealed by heating RNA to 95 °C for 2 minutes in binding buffer (75.0 mM KCl, 50.0 mM Tris-HCl, 3.00 mM $MgCl_2$, pH 8.30) and slowly cooling the samples to 35 °C. For circular dichroism (CD) analysis, 1.0 OD of siRNA was annealed in sodium phosphate buffer (90.0 mM NaCl, 10.0 mM Na_2HPO_4, 1.00 mM EDTA, pH 7.00). CD spectroscopy was performed on a Jasco J-815 CD at 25 °C with a screening rate of 20.0 nm/min and a 0.20 nm data pitch. Only samples with a spectra that correspond to A-form helixes were used for further analysis.

IV.VII **Protein Silencing**

The phosphorofluoridate modification is a close analogue to the natural phosphate and should fit well in the Ago2 binding pocket; however, the fluorine may alter binding within the pocket. siRNAs bearing the phosphorofluoridate at the 5' end of the antisense strand, sense strand, or both strands, can be easily characterized via the dual luciferase assay (Table 6). Starting at either 405 pM (wildtype) or 1215 pM (modified siRNA), concentrations were diluted seven times by a factor of 3 until reaching a final concentration of 0.55 pM (wildtype) or 1.66 pM (modified siRNA). These concentrations were selected due to preliminary experiments suggesting a slightly lower potency for the modified siRNA. Each modified siRNA had an approximately 10-fold reduction in potency, regardless of where the modification was placed (Figure 38 and 39). The greatest loss in potency was for PF1, which carries a single 5' phosphorofluoridate on the antisense strand, suggesting a minor inhibitory effect due to the modification. Further investigations would be required to determine whether this modification is accepted into Ago2, cleaved and replaced with a natural phosphate, or both.

Table 6: Phosphorofluoridate modified siRNAs used in this study.

siRNA	Sequence and Location of Modifications
WT[a]	5' CUUACGCUGAGUACUUCGAtt 3' 3' ttGAAUGCGACUCAUGAAGCU 5'
PF-AS	5' CUUACGCUGAGUACUUCGAtt 3' 3' ttGAAUGCGACUCAUGAAGCU* 5'
PF-SS	5' *CUUACGCUGAGUACUUCGAtt 3' 3' ttGAAUGCGACUCAUGAAGCU 5'
PF-ASS	5' *CUUACGCUGAGUACUUCGAtt 3' 3' ttGAAUGCGACUCAUGAAGCU* 5'

[a] The top and bottom strands correspond to the sense and antisense strand, respectively. Deoxynucleotides indicated with lower case.
* Indicates modification location

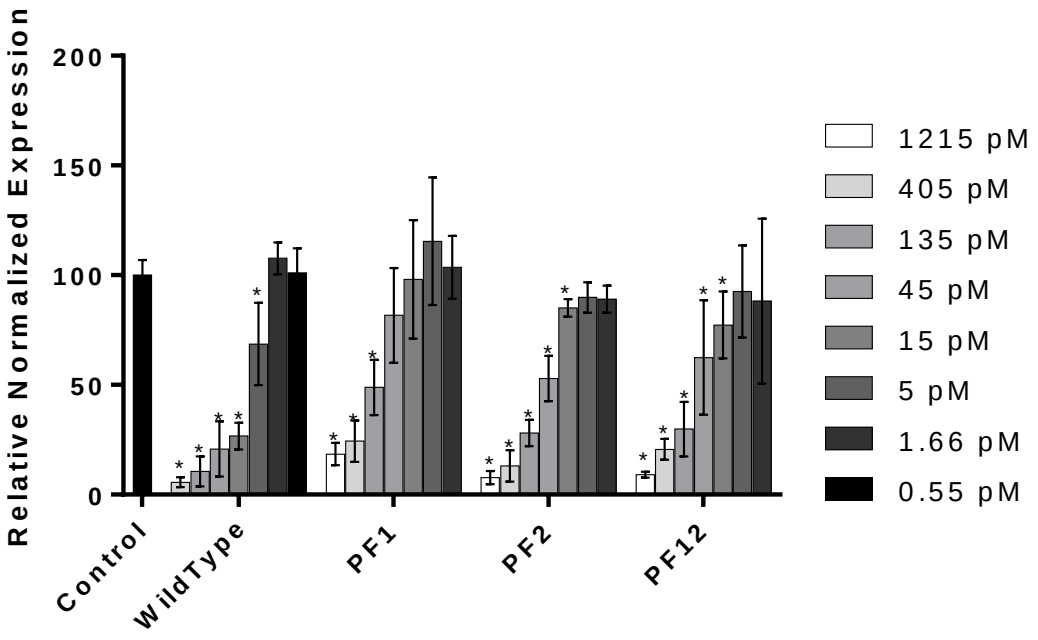

Figure 38: Reduction in normalized firefly luciferase protein expression for siRNAs bearing a 5' phosphorofluoridate on the antisense (PF1), sense (PF2), or both strands (PF12). Mean ± SEM values of independent triplicates are shown. (*) indicates a statistically significant difference ($p < 0.05$) between the untreated and treated sample.

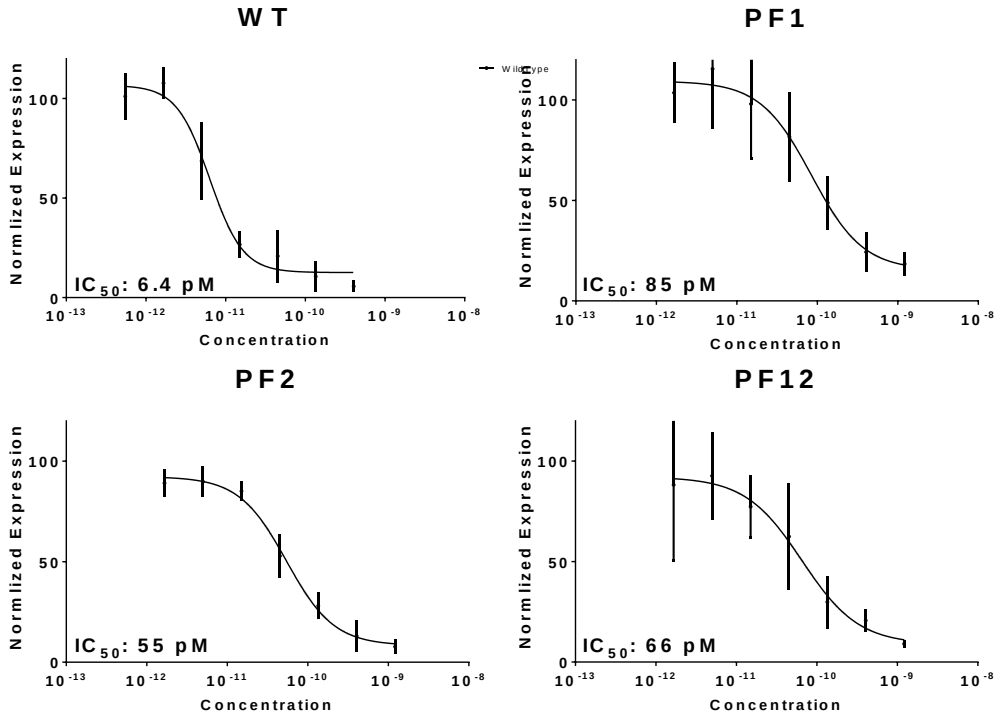

Figure 39: Dose response curves for reduction in firefly luciferase protein expression for siRNAs bearing a 5' phosphorofluoridate on the antisense (PF1), sense (PF2), or both strands (PF12).

IV.VIII **References**

1. Chemical Warfare Service TDMR 832, *Edgewood Arsenal,* Apr. (1944).

2. Lindahl, C. B., & Tariq M. Fluorine Compounds, Inorganic, Phosphorus. *Kirk-Othmer Encyclopedia of Chemical Technology* (2000).

3. Registry of Toxic Effects of Chemical Substances, Vol. II, NIOSH, *U.S. Department of Health, Education, and Welfare, Washington, D.C.*, pp. 667, 686 (1977).

4. Stamper, R. L., Lieberman, M. F. & Drake, M. V. CHAPTER 27 - Cholinergic drugs. in (eds. Stamper, R. L., Lieberman, M. F. & Drake, M. V. B. T.-B.-S. D. and T. of the G. (Eighth E.) 420–430 (Mosby, 2009). doi:https://doi.org/10.1016/B978-0-323-02394-8.00027-9.

5. Grutzendler, J. & Morris, J. C. Cholinesterase inhibitors for Alzheimer's disease. *Drugs* 61, 41–52 (2001).

6. Hoskin, F. C., Rosenberg, P. & Brzin, M. Re-examination of the effect of DFP on electrical and cholinesterase activity of squid giant axon. *Proc. Natl. Acad. Sci. U. S. A.* 55, 1231 (1966).

7. Michalski, J. & Dabkowski, W. New chemistry and stereochemistry of tricoordinate phosphorus esters containing phosphorus–fluorine bond. *Comptes Rendus Chim*. 7, 901–907 (2004).

8. Dabkowski, W. & Tworowska, I. Synthesis of 2′-deoxynucleosid-3′-yl-N, N-diisopropylaminophosphorfluoridites. A new class of stable PIII nucleotides containing a P-F bond. *Tetrahedron Lett*. 36, 1095–1098 (1995).

9. Dąbkowski, W. & Tworowska, I. Novel phosphitylating reagents containing a phosphorus–fluorine bond and their application in efficient synthesis of phosphorofluoridates and phosphorofluoridothionates. *J. Chem. Soc. Perkin Trans*. 1 2462–2469 (2001).

10. Dabkowski, W., Michahki, J. & Cramer, F. Oligonucleotide phosphorofluoridates and fluoridites. in *Protocols for Oligonucleotides and Analogs* 245–260 (Springer, 1993).

11. Aldersley, M. F., Joshi, P. C., Schwartz, H. M. & Kirby, A. J. The reaction of activated RNA species with aqueous fluoride ion: a convenient synthesis of nucleotide 5′-phosphorofluoridates and a note on the mechanism. *Tetrahedron Lett*. 55, 1464–1466 (2014).

12. Dabkowski, W. & Tworowska, I. Synthesis of phosphorofluoridates and phosphorofluoridothioates via the phosphoramidite approach. *Org. Biomol. Chem*. 3, 866–874 (2005).

13. Still, W. C., Kahn, M. & Mitra, A. Rapid chromatographic technique for preparative separations with moderate resolution. *J. Org. Chem*. 43, 2923–2925 (1978).

14. Wright, P., Lloyd, D., Rapp, W. & Andrus, A. Large scale synthesis of oligonucleotides via phosphoramidite nucleosides and a high-loaded polystyrene support. *Tetrahedron Lett.* 34, 3373–3376 (1993).

15. Ben, H.-J. et al. Synthesis, crystal structure, enhanced photoluminescence properties and fluoride detection ability of S-heterocyclic annulated perylene diimide-polyhedral oligosilsesquioxane dye. *J. Mater. Chem. C* 5, 2566–2576 (2017).

Chapter V.

Conclusions and Future Directions

V.I **Conclusions and future directions**

This dissertation set out to accomplish two primary goals: (1) to develop a method to measure both antisense and sense strand activity of siRNA, and (2) to characterize novel chemical modifications for their impact on strand specific activity.

The first goal was achieved through the adaptation of the Dual Luciferase Assay from Promega. This assay relies on two expression vectors, pGL3-Control and pRLSV40, which transcribe distinct luciferase enzymes from the SV40 promoter whose abundance can be uniquely measured via bioluminescence. The commonly used siRNA sequence (5'-UCG AAG UAC UCA GCG UAA GdTdT-3') targets the mRNA transcript from the pGL3-Control derived luciferase.[1-13] To create an mRNA target for the sense strand with similar expression and secondary structure, the antisense target sequence in pGL3-Control was replaced with the reverse compliment sequence through a unique application of the NEBuilder HiFi Assembly (Gibson Assembly) to create pGLR3. Disruption of the protein sequence rendered the mutant luciferase non-functional; however, transcript cleavage offers a valuable measure of strand activity. Combining antisense mRNA cleavage and protein silencing data provides new insights into the mechanisms behind the impacts of chemical modifications.

Apart from a string of 21 bp, the pGL3-Control and pGLR3 derived luciferase transcripts are identical, providing relatively few options for primer design. For confidence in assay design, multiple primer pairs were designed and evaluated to ensure high specificity between targets. Wildtype (unmodified) siRNA was used to validate the assay and identified higher silencing potency for the antisense sense strand compared to the sense strand. This was expected, as the siRNA sequence encourages antisense strand uptake

through low thermodynamic stability and the presence of an A or U at the 5' terminus.[14-16] Furthermore, scramble siRNA was unable to significantly alter expression of either target, confirming that the siRNA sequence was responsible for the measured decrease in mRNA.

The second goal was achieved through employment of this strand activity assay to measure the impact of numerous chemically modified siRNAs. Most of the siRNAs tested were synthesized through the efforts of Dr. Hammill, Dr. Salim, and Dr. Tsubaki. Perhaps unsurprisingly, chemical modifications that replace entire nucleotides with chemically distinct structures, such as the azobenzene, propargyl, triazole-linked folate, and cubane were the most deactivating to their respective strand. These modifications are generally not well tolerated within antisense strands apart from the 3' supplementary region, for which no significant interactions between the RNA and Ago2 have been identified.[17] If placed within the 5' end, seed region, or central region of a strand, these modifications typically lead to the loss of Ago2-phosphate backbone interactions that stabilize the strand. They may also disrupt the canonical A-form RNA duplex structure, important for efficient recognition of siRNA. This likely significantly contributes to the reduced potency seen for the nucleotide-substitution modifications. The only one of these modifications to seem to enhance activity of the associated strand was the 3' propargyl linker (P20/21), and the reasons for this are unclear. Perhaps the positively charged tertiary amine interacts with the anionic backbone or 5' phosphate of the opposite strand, interfering with uptake of the competing strand.

The impact of hydrophobic phosphate triester backbone modifications on strand activity were also explored. Unlike the nucleotide substitution modifications, these modifications do not alter the sugar structure or sugar substituents. Therefore, sugar

puckering is unlikely to be affected and the typical A-form conformation of the duplex should be favored. Indeed, these modifications were well tolerated; however, increasing the number of hydrophobic moieties on the backbone had a deactivating effect. The most impactful sense strand deactivation was identified for the double modified U2:15 siRNA, in which two phenylethyl phosphate modifications were placed within the strand. Hypothetically, the interruption of multiple phosphate backbone interactions may be sufficient to inhibit strand uptake. Notably, the improved strand activity profile was also associated with a small reduction in antisense potency. The mechanisms behind reduced potency for the dual octadecyloxy hydrophobic phosphate modification (H2) are unclear but may be the result of steric constraints with Ago2, interfering with the ideal orientation for target strand hybridization and subsequent cleavage.

With the dependence for a 5' phosphate for RNAi, it's not surprising that some of the most impactful chemical modifications for strand uptake/activity have been 5' terminal modifications such as the 5' morpholino or 5' vinylphosphonate.[18,19] To further expand the chemical modifications investigated within this category, 5' phosphorofluoridate modified siRNAs were developed and investigated. Phosphorofluoridate modifications have been explored within the phosphate backbone, but this is the first report for a 5' terminal phosphorofluoridate.[20,21] Coupling efficiency was low, with multiple coupling treatments required to achieve appreciable yields. With only a single phosphorofluoridate group differentiating the parent compound from the product, purification required substantial HPLC optimization. Unfortunately, a di-substituted phosphorofluoridate was not synthesized as the required phosphoramidite was unstable and isolation was not achievable.

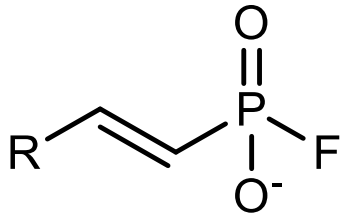

Figure 40: Structure of 5'-(E)-vinylphosphonofluoridate

Dual luciferase assays with phosphorofluoridate modified siRNAs revealed similar, but less potent, activity profiles as wildtype siRNA. Two non-mutually exclusive explanations for this exist. It is possible that Ago2 recognizes the 5' phosphate mimic with slightly less efficiency and incorporates the strand as the guide strand, or the phosphorofluoridate is recognized and hydrolyzed by cellular phosphatases. The resulting primary alcohol is naturally phosphorylated by the Clp1 kinase and subsequently recognized by Ago2.[22,23] If the latter is the case, it is valuable to consider the combination of the 5' vinyl phosphonate with the 5' phosphorofluoridate to create a 5'-(*E*)-vinylphosphonoflouridate (Figure 40). This modification is not a substrate for cellular phosphatases, locking the phosphate mimic in place. To determine whether the phosphorofluoridate is a substrate for cellular phosphatases, a phosphatase assay could be performed via treatment with a phosphatase followed by gel mobility shift analysis on PAGE.

The assay developed in this study was based on the pGL3-Control expression vector; however, Promega has since re-engineered the system. The new pGL4 backbone is meant to reduce anomalous expression and increases the reliability of reporter gene expression.[24] Migrating over to the pGL4 system may provide more consistent gene expression (and 3.7-fold increased expression) over a greater number of cell types, growth stage, and passage number, providing a more robust platform. Importantly, the luciferase gene between

plasmids are identical and the siRNA sequence used in the Desaulniers' lab can be preserved. If a new assay was to be designed, it would also be possible to create a Dual Luciferase Assay-compatible platform that is simultaneously compatible with the Desaulniers' lab siRNA sequence, by moving the target site into the 3'UTR in a two-step process. Firstly, the original target can be removed by introducing multiple silent mutations, thereby maintaining the amino acid sequence while allowing the mRNA to evade detection by the RISC. Secondly, placing the antisense or sense strand within the 3'UTR would still facilitate rapid mRNA degradation upon RISC recognition. This design would effectively measure gene silencing via the Dual Luciferase Assay; however, the antisense and sense target plasmids must be delivered separately (in contrast to the mRNA level assay developed in this thesis).

In conclusion, this dissertation has improved our ability to evaluate the impact of novel chemical modifications and improved our general understanding of the role that different types of modifications play in strand activity. Continued research in this field is essential for limiting off-target effects to develop safe and reliable siRNA therapeutics. This assay can be used by any research group to further investigate novel modifications and improve the mechanistic understanding of chemical modifications on strand activity.

V.II **References**

1. Hammill, M. L., Islam, G. & Desaulniers, J.-P. Reversible control of RNA interference by siRNAzos. *Org. Biomol. Chem*. 18, 41–46 (2019).

2. Salim, L., Islam, G. & Desaulniers, J.-P. Targeted delivery and enhanced gene-silencing activity of centrally modified folic acid–siRNA conjugates. *Nucleic Acids Res.* 48, 75–85 (2020).

3. Elbashir, S. M. et al. Duplexes of 21-nucleotide RNAs mediate RNA interference in cultured mammalian cells. *Nature* 411, 494 (2001).

4. Sardo, C., Craparo, E. F., Porsio, B., Giammona, G. & Cavallaro, G. Improvements in rational design strategies of inulin derivative polycation for siRNA delivery. *Biomacromolecules* 17, 2352–2366 (2016).

5. Chen, Q. et al. Lipophilic siRNAs mediate efficient gene silencing in oligodendrocytes with direct CNS delivery. *J. Control. Release* 144, 227–232 (2010).

6. Hammill, M. L., Isaacs-Trépanier, C. & Desaulniers, J.-P. siRNAzos: A New Class of Azobenzene-Containing siRNAs that Can Photochemically Regulate Gene Expression. *ChemistrySelect* 2, 9810–9814 (2017).

7. Varley, A. J., Hammill, M. L., Salim, L. & Desaulniers, J.-P. Effects of Chemical Modifications on siRNA Strand Selection in Mammalian Cells. *Nucleic Acid Ther*. 30, 229–236 (2020).

8. Tsubaki, K. et al. Synthesis and Evaluation of Neutral Phosphate Triester Backbone-Modified siRNAs. *ACS Med. Chem. Lett*. (2020).

9. Hammill, M. L., Islam, G. & Desaulniers, J.-P. Synthesis, Derivatization and Photochemical Control of ortho-Functionalized Tetrachlorinated Azobenzene-Modified siRNAs. *ChemBioChem* (2020).

10. Hammill, M. L. et al. Building siRNAs with cubes: synthesis and evaluation of cubane-modified siRNAs. *ChemBioChem* (2021).

11. Salim, L., McKim, C. & Desaulniers, J.-P. Effective carrier-free gene-silencing activity of cholesterol-modified siRNAs. *RSC Adv.* 8, 22963–22966 (2018).

12. Zhu, L. & Mahato, R. I. Targeted delivery of siRNA to hepatocytes and hepatic stellate cells by bioconjugation. *Bioconjug. Chem*. 21, 2119–2127 (2010).

13. Lorenzer, C. et al. Targeted delivery and endosomal cellular uptake of DARPin-siRNA bioconjugates: Influence of linker stability on gene silencing. *Eur. J. Pharm. Biopharm*. 141, 37–50 (2019).

14. Tomari, Y., Matranga, C., Haley, B., Martinez, N. & Zamore, P. D. A protein sensor for siRNA asymmetry. *Science* 306, 1377–1380 (2004).

15. Okamura, K., Ishizuka, A., Siomi, H. & Siomi, M. C. Distinct roles for Argonaute proteins in small RNA-directed RNA cleavage pathways. *Genes Dev.* 18, 1655–1666 (2004).

16. Lisowiec-Wąchnicka, J., Bartyś, N. & Pasternak, A. A systematic study on the influence of thermodynamic asymmetry of 5′-ends of siRNA duplexes in relation to their silencing potency. *Sci. Rep*. 9, 2477 (2019).

17. Schirle, N. T. & MacRae, I. J. The crystal structure of human Argonaute2. *Science* 336, 1037–1040 (2012).

18. Kumar, P. et al. 5′-Morpholino modification of the sense strand of an siRNA makes it a more effective passenger. *Chem. Commun.* 55, 5139–5142 (2019).

19. Elkayam, E. et al. siRNA carrying an (E)-vinylphosphonate moiety at the 5′ end of the guide strand augments gene silencing by enhanced binding to human Argonaute-2. *Nucleic Acids Res*. 45, 3528–3536 (2016).

20. Michalski, J. & Dabkowski, W. New chemistry and stereochemistry of tricoordinate phosphorus esters containing phosphorus–fluorine bond. *Comptes Rendus Chim.* 7, 901–907 (2004).

21. Dąbkowski, W. & Tworowska, I. Novel phosphitylating reagents containing a phosphorus–fluorine bond and their application in efficient synthesis of phosphorofluoridates and phosphorofluoridothionates. *J. Chem. Soc. Perkin Trans*. 1 2462–2469 (2001).

22. Weitzer, S. & Martinez, J. The human RNA kinase hClp1 is active on 3′ transfer RNA exons and short interfering RNAs. *Nature* 447, 222 (2007).

23. Weitzer, S. & Martinez, J. hClp1, A Novel Kinase Revitalizes RNA Metabolism. *Cell Cycle* 6, 2133–2137 (2007).

24. Promega. *pGL4 Luciferase Reporter Vectors*. (2020)

Chapter VI.

APPENDICES

Appendix A. **Primers and Plasmids**

A1. Primer Pairs Used in this Study

Primer Name	Sequence	Tm	Product (bp)	Note
Asbml.F	TCGAAGTACTCAGCGTAAGAA TGTCCGTTCGGTTGGCAG	69	5275	Tm for pGL3-Control target is 60 °C for each primer
Asbml.R	CTTACGCTGAGTACTTCGATG ATGTCCACCTCGATATGTGCATC	69		
Seq_F	ACATAAAGAAAGGCCCGGCG	60	183	Sequencing primers for pGLR3
Seq_R	TAGCTTCTGCCAACCGAACG	60		
Luc_qPCR1.F	GAAGAGATACGCCCTGGTTCC	59	193	Universal for firefly luciferase from pGL3-Control or pGLR3
Luc_qPCR1.R	GCCCAACACCGGCATAAAGA	58		
Luc_qPCR2.F	AGATGCACATATCGAGGTGGAC	58	170	Universal for firefly luciferase from pGL3-Control or pGLR3
Luc_qPCR2.R	CTCCGATAAATAACGCGCCC	59		
Luc_qPCR1.F	GAAGAGATACGCCCTGGTTCC	59	209	Universal for firefly luciferase from pGL3-Control or pGLR3
Luc_qPCR2.R	CTCCGATAAATAACGCGCCC	59		
Luc_qPCR2.F	AGATGCACATATCGAGGTGGAC	58	154	Universal for firefly luciferase from pGL3-Control or pGLR3
Luc_qPCR1.R	GCCCAACACCGGCATAAAGA	58		
Rluc_qPCR1.F	GGTAACGCGGCCTCTTCTTA	58	228	For Renilla luciferase from pRLSV40 (reference controll)
Rluc_qPCR1.R	AAATGCCAAACAAGCACCCC	59		
Rluc_qPCR2.F	ATGGTAACGCGGCCTCTTC	59	230	For Renilla luciferase from pRLSV40 (reference control)
Rluc_qPCR1.R	AAATGCCAAACAAGCACCCC	59		
AS_qPCR1.F	ACATATCGAGGTGGACATCACTTAC	58	164	Specific for firefly luciferase from pGL3-Control
Luc_qPCR2.R	CTCCGATAAATAACGCGCCC	59		
AS_qPCR2.F	TCGAGGTGGACATCACTTACGC	61	159	Specific for firefly luciferase from pGL3-Control
Luc_qPCR2.R	CTCCGATAAATAACGCGCCC	59		
SS_qPCR1.F	ATCGAGGTGGACATCATCGAAGTAC	60	160	Specific for firefly luciferase from pGLR3
Luc_qPCR2.R	CTCCGATAAATAACGCGCCC	59		
SS_qPCR2.F	GAGGTGGACATCATCGAAGTACTC	58	157	Specific for firefly luciferase from pGLR3
Luc_qPCR2.R	CTCCGATAAATAACGCGCCC	59		

A2. Plasmids Used in this Study

Plasmid Name	Relevant Features	Source
pGL3-Control	Firefly luciferase reporter vector. Target for the antisense siRNA strand	Promega
pGLR3	Mutant firefly luciferase reporter vector. Target for the sense siRNA strand	This Study
pRLSV40	*Rinella* Luciferase Reporter Vector. Used as a reference control.	Promega

A3. Plasmid Map for pGL3-Control

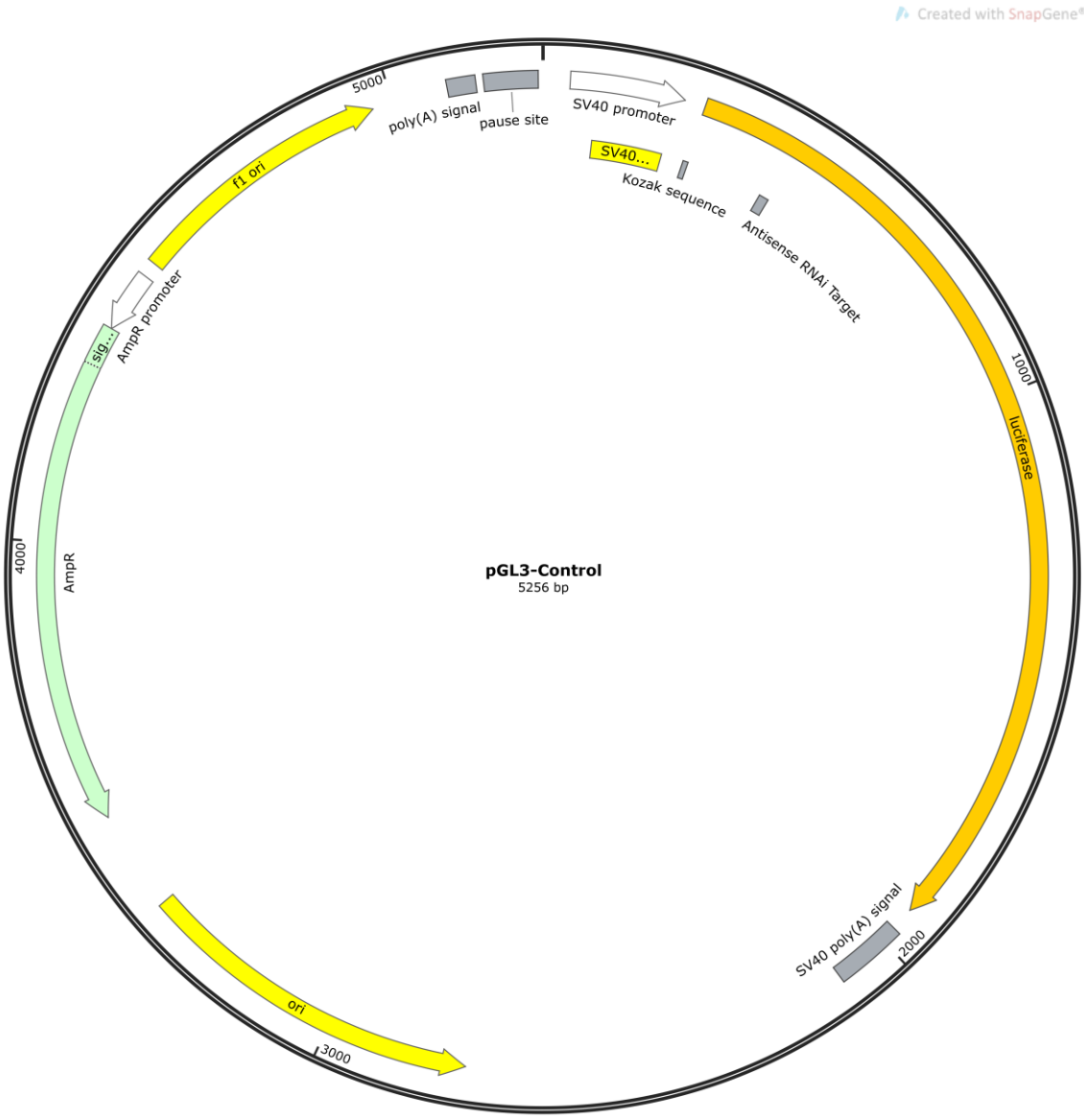

A4. Plasmid Map for pGLR3

A5. Plasmid Map for pRLSV40

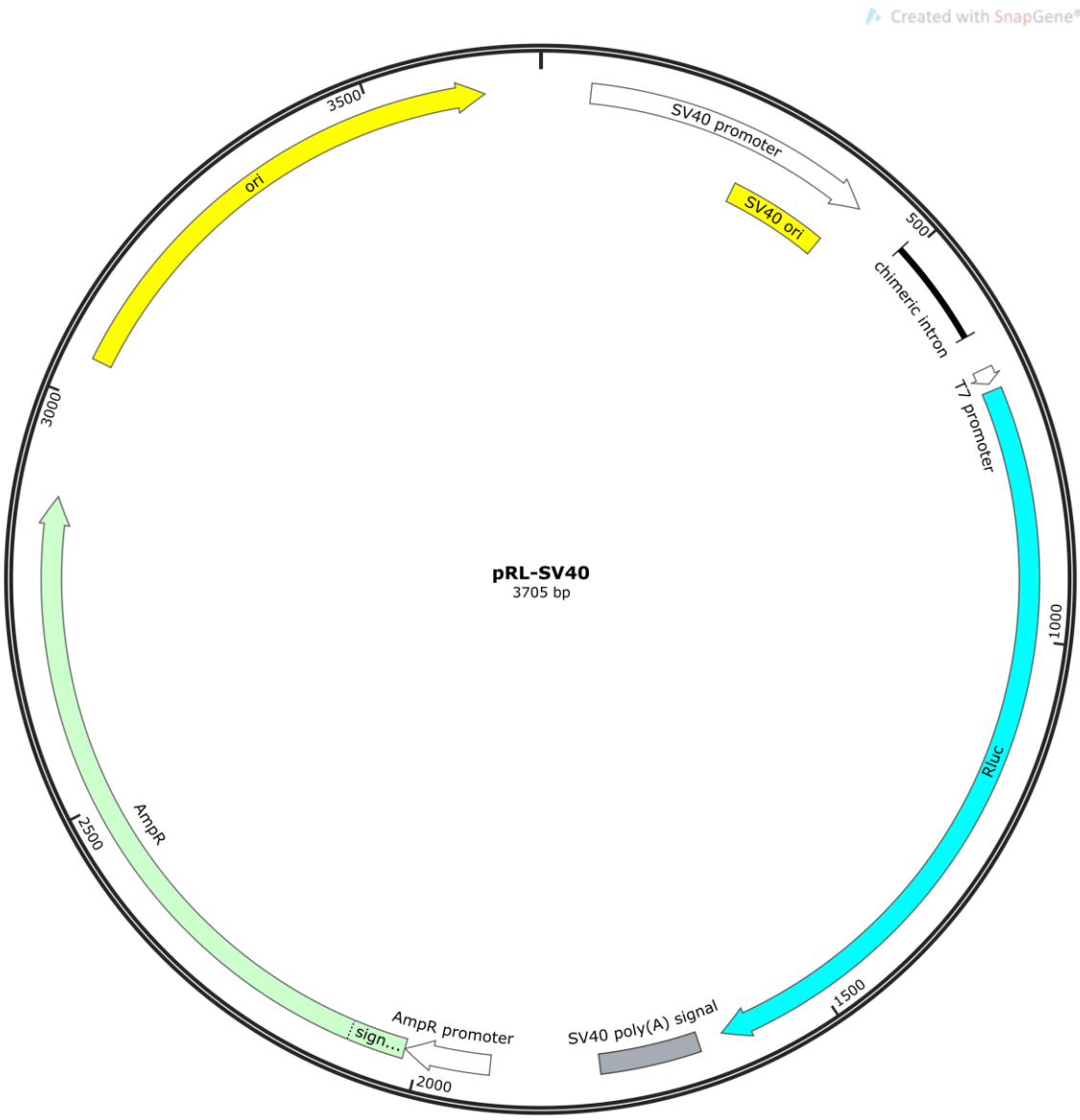

Appendix B. **Standard Curves**

B1. Standard Curve for Firefly Luciferase Expressed from pGL3-Control

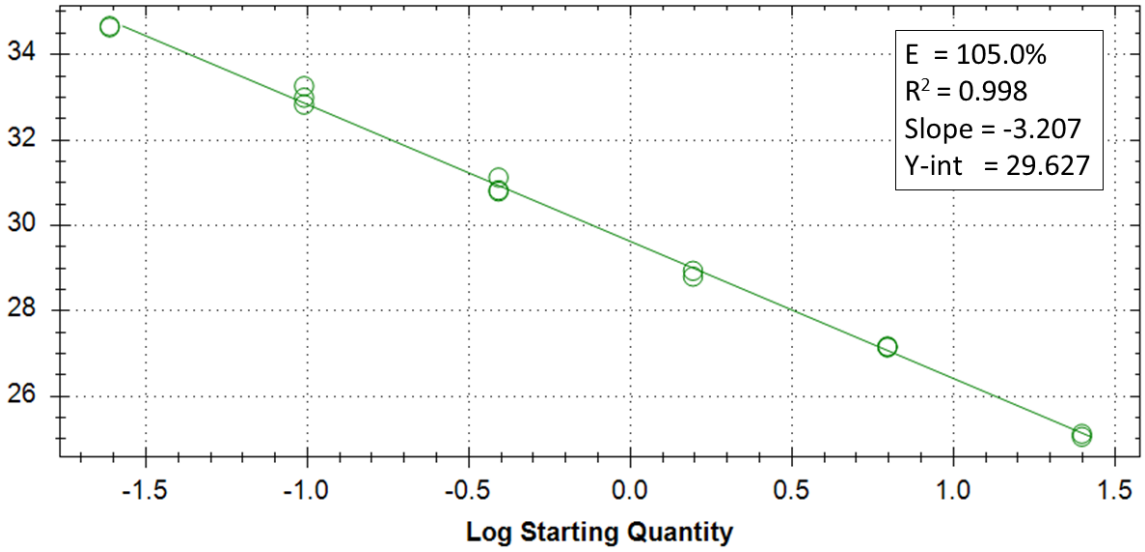

B2. Standard Curve for Mutant Firefly Luciferase Expressed from pGLR3

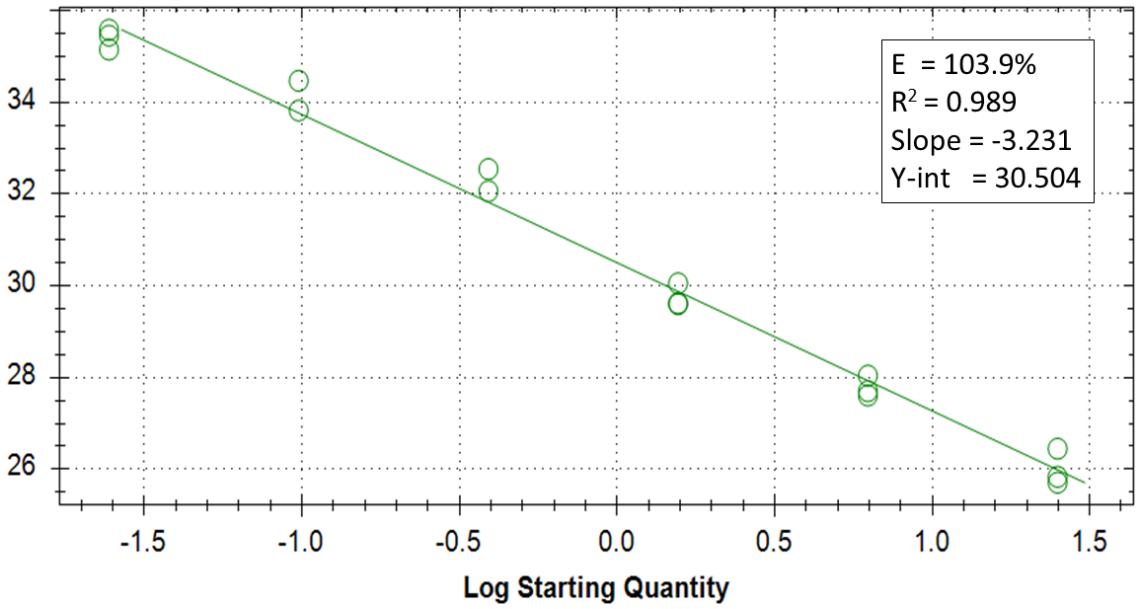

B3. Standard Curve for *Renilla* Luciferase Expressed from pRLSV40

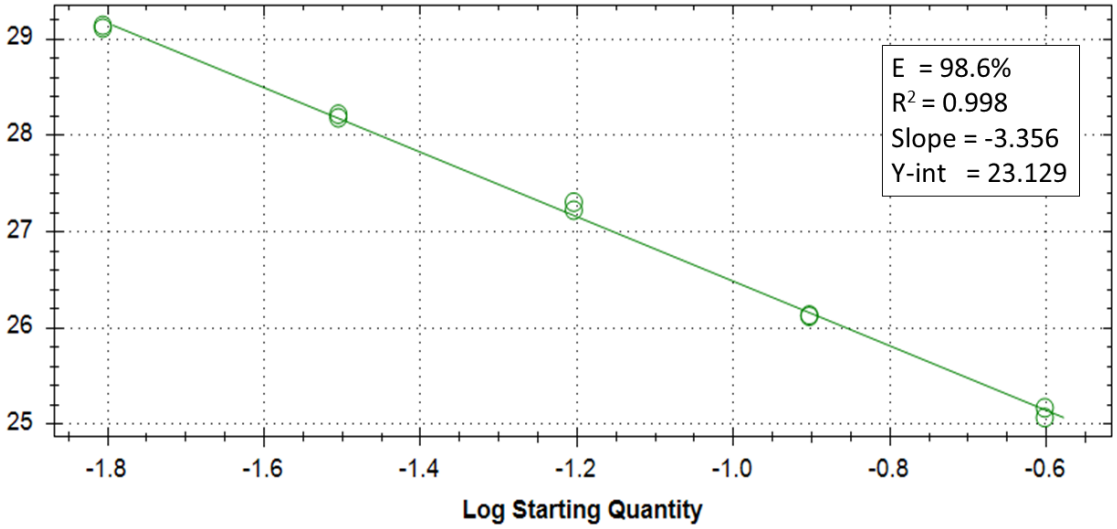

Appendix C. **Spectra of Compounds from Chapter IV**

C1. NMR of 2-cyanoethyl (4-nitrophenyl) diisopropyl phosphoramidite (**2**)

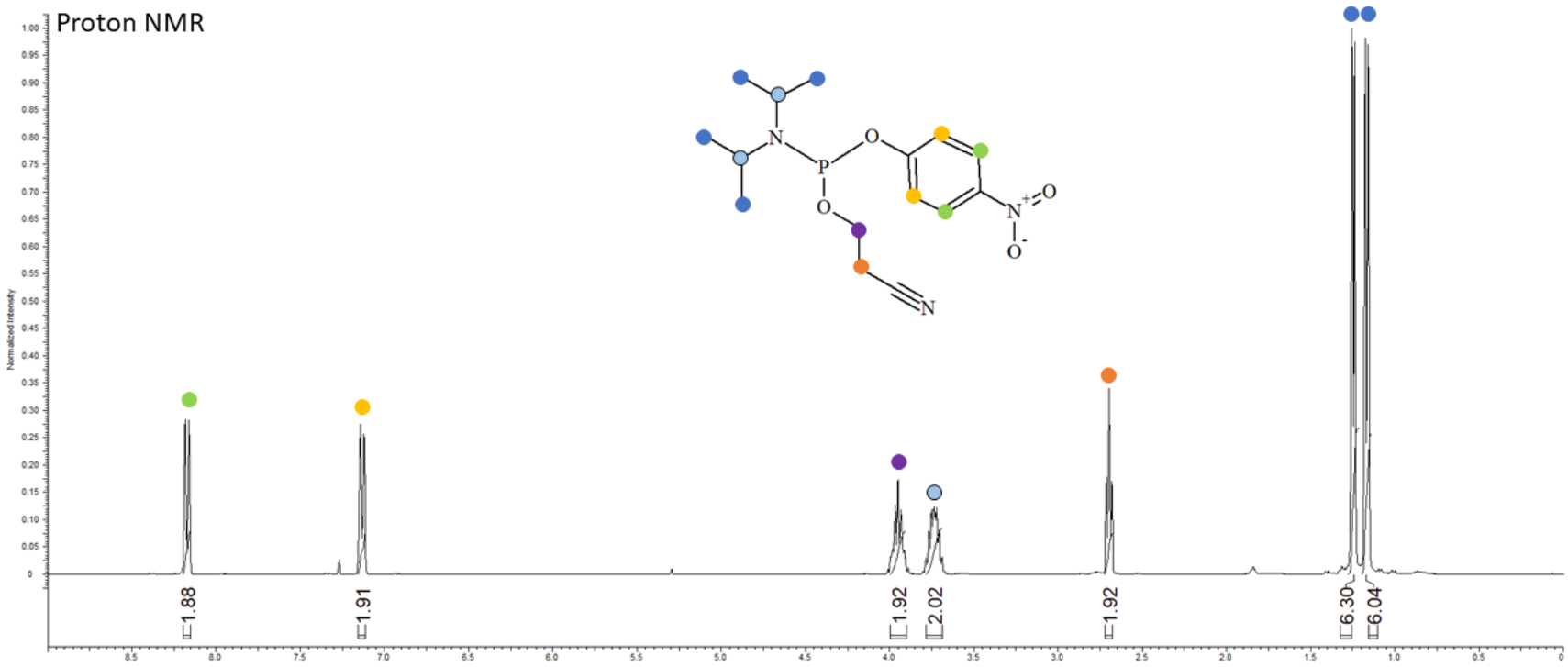

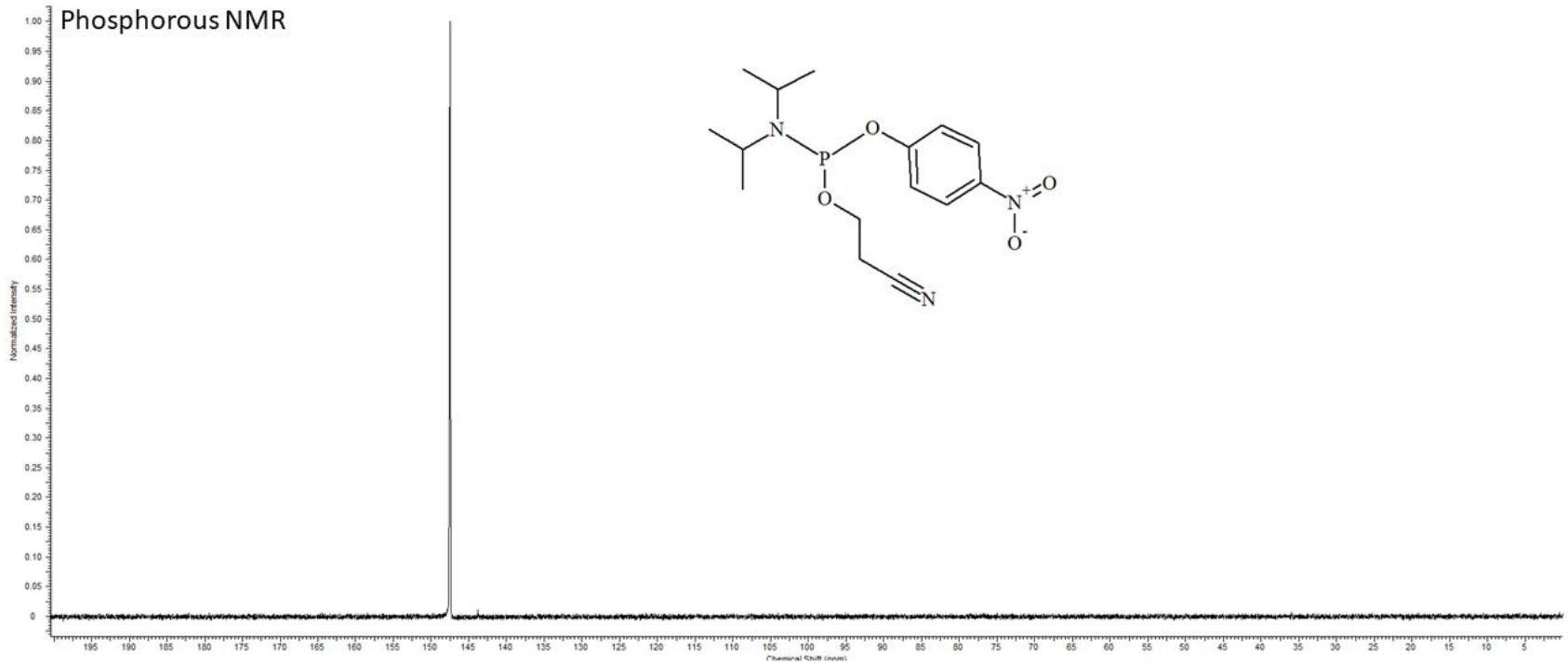
Phosphorous NMR
Normalized Intensity
Chemical Shift (ppm)

C2. NMR of 3-(((diisopropylamino)fluorophosphaneyl)oxy) propanenitrile (**3**)

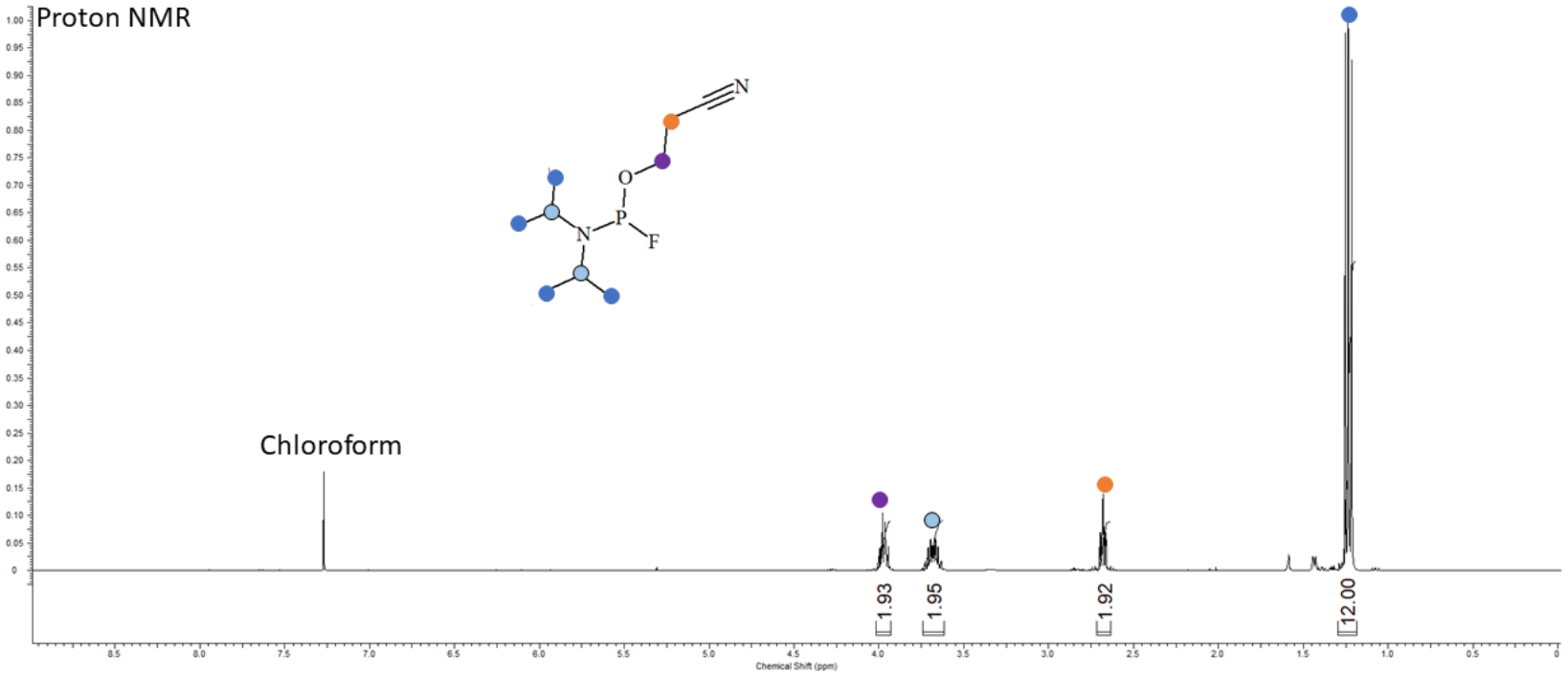

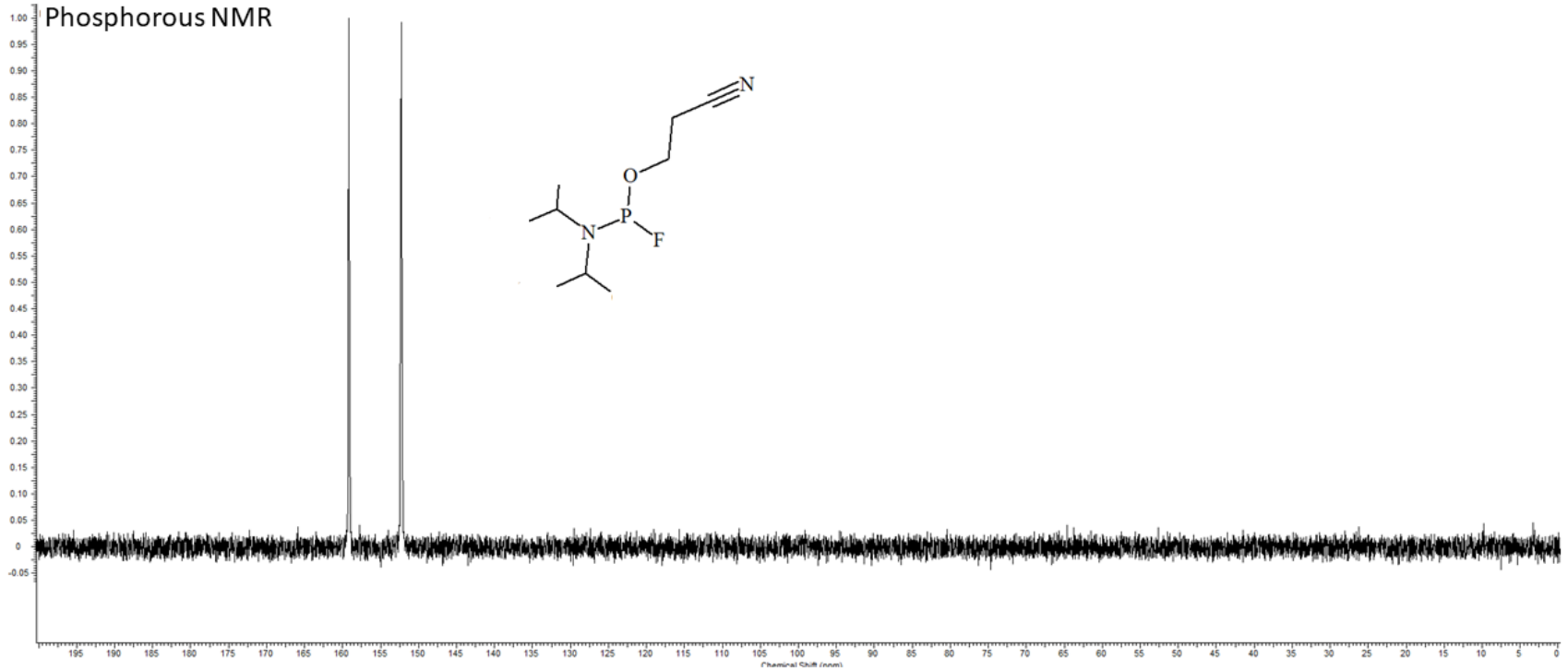
Phosphorous NMR
N
O
P
N
F

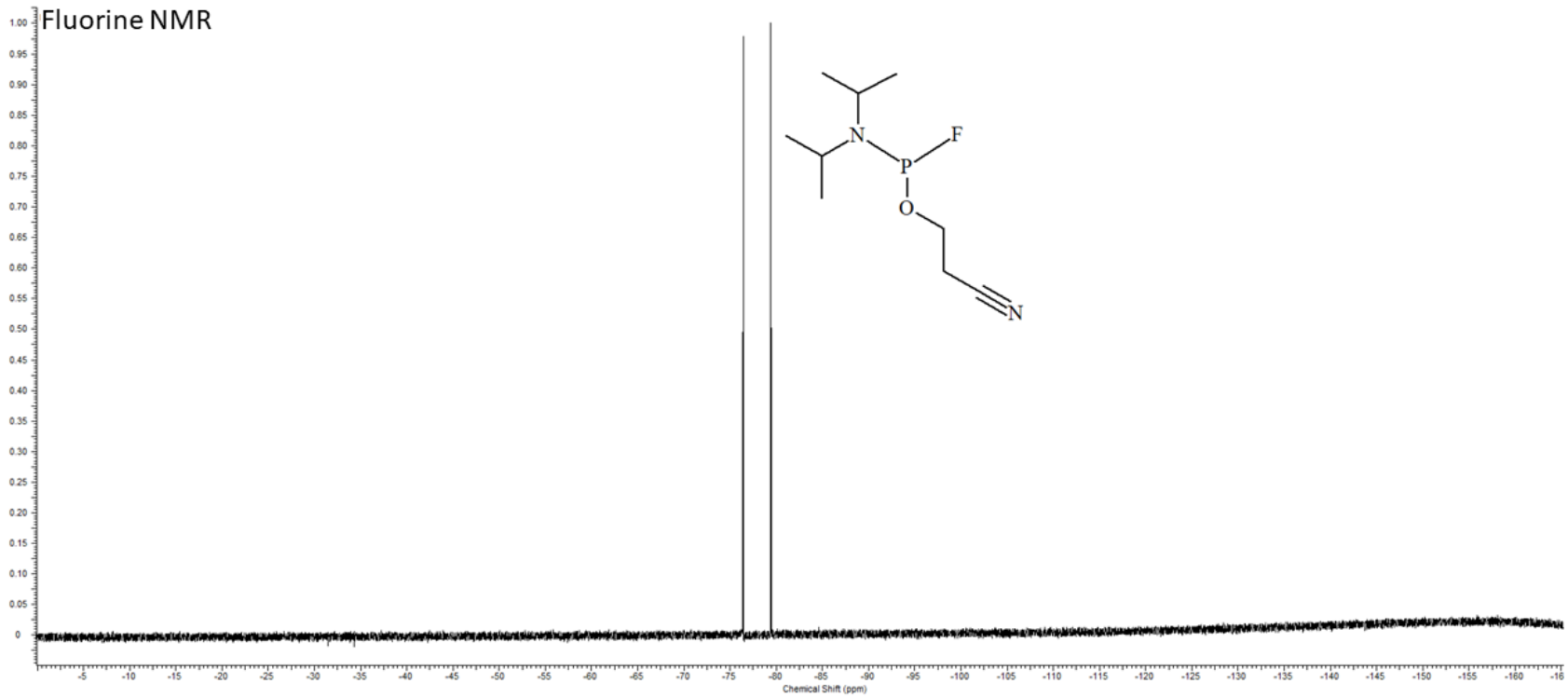
Fluorine NMR
N
F
P
O
N
Chemical Shift (ppm)

C3. NMR of Preparation of bis(4-nitrophenyl) diisopropylphosphoramidite (**5**)

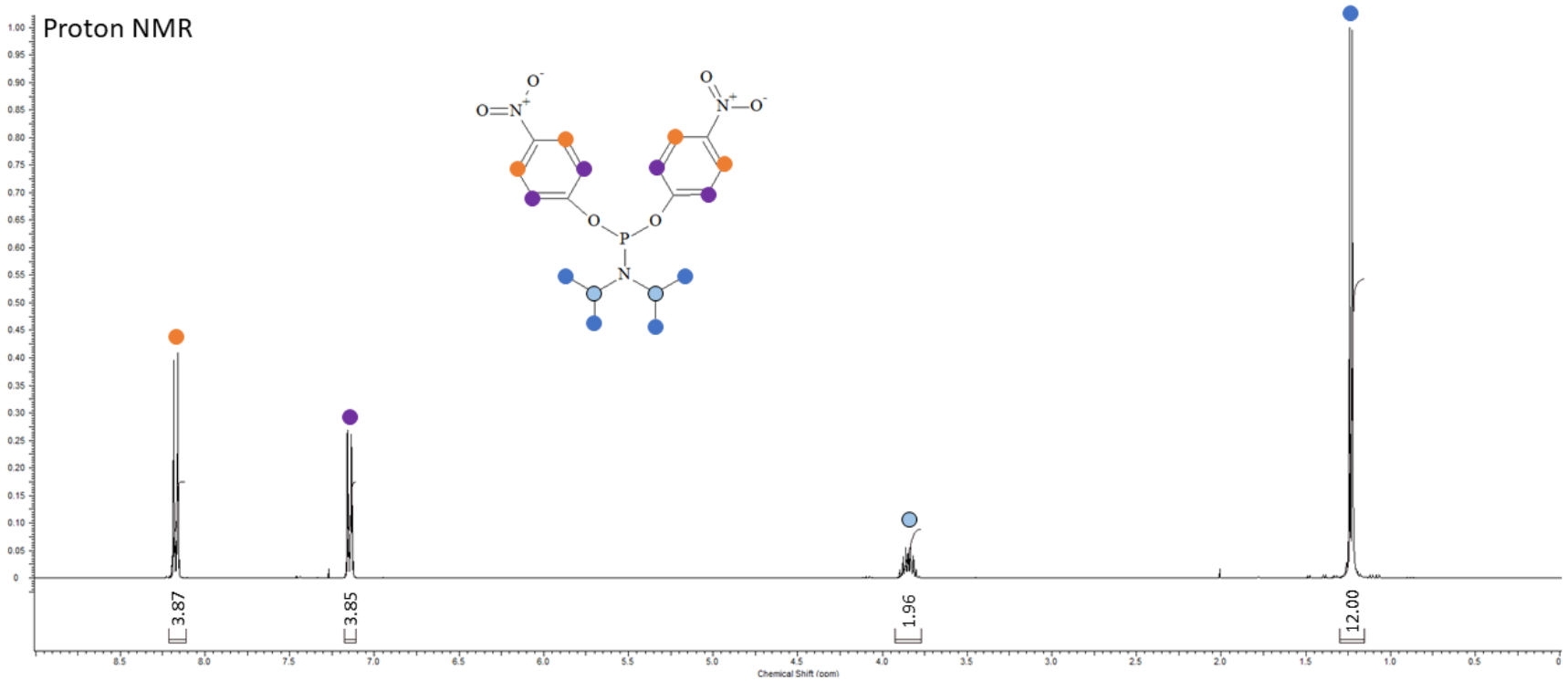

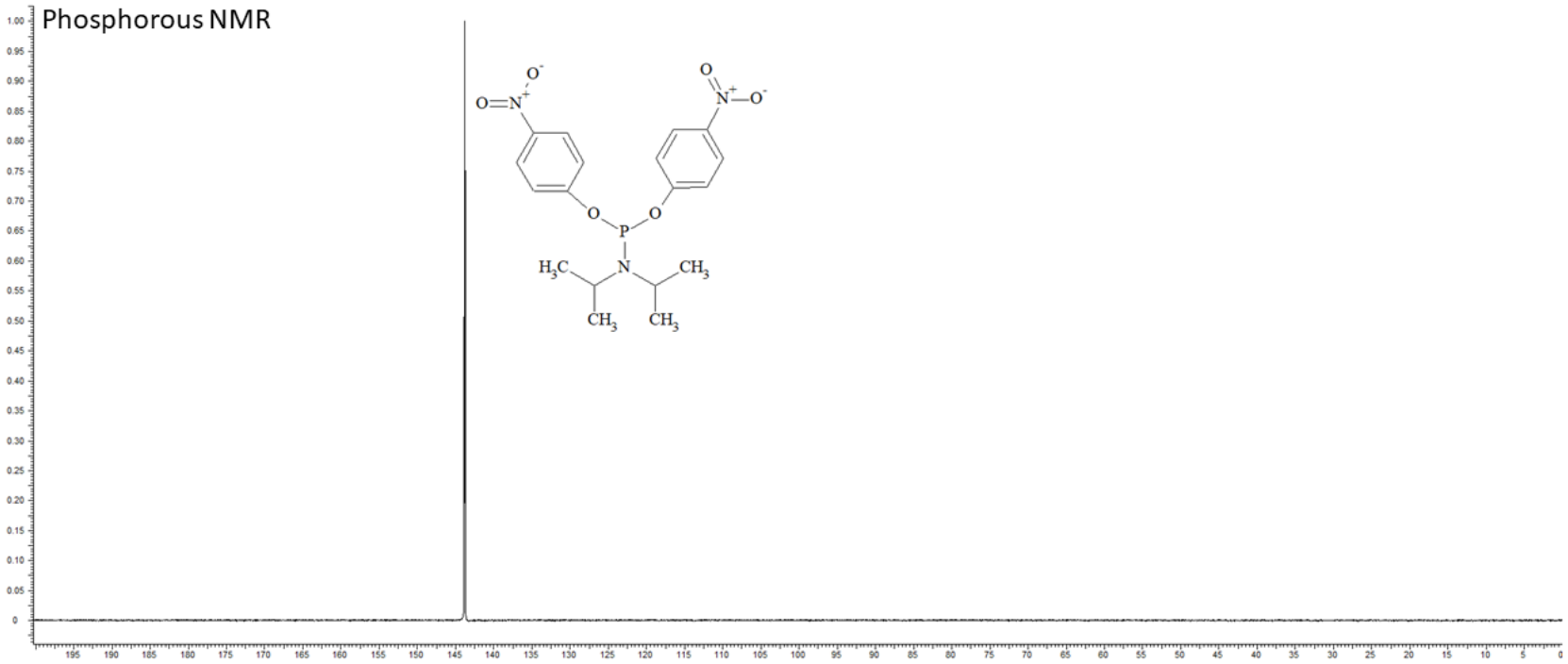
Phosphorous NMR

C4. NMR of 1,1-difluoro-N,N-diisopropyl phosphanamine (**6**)

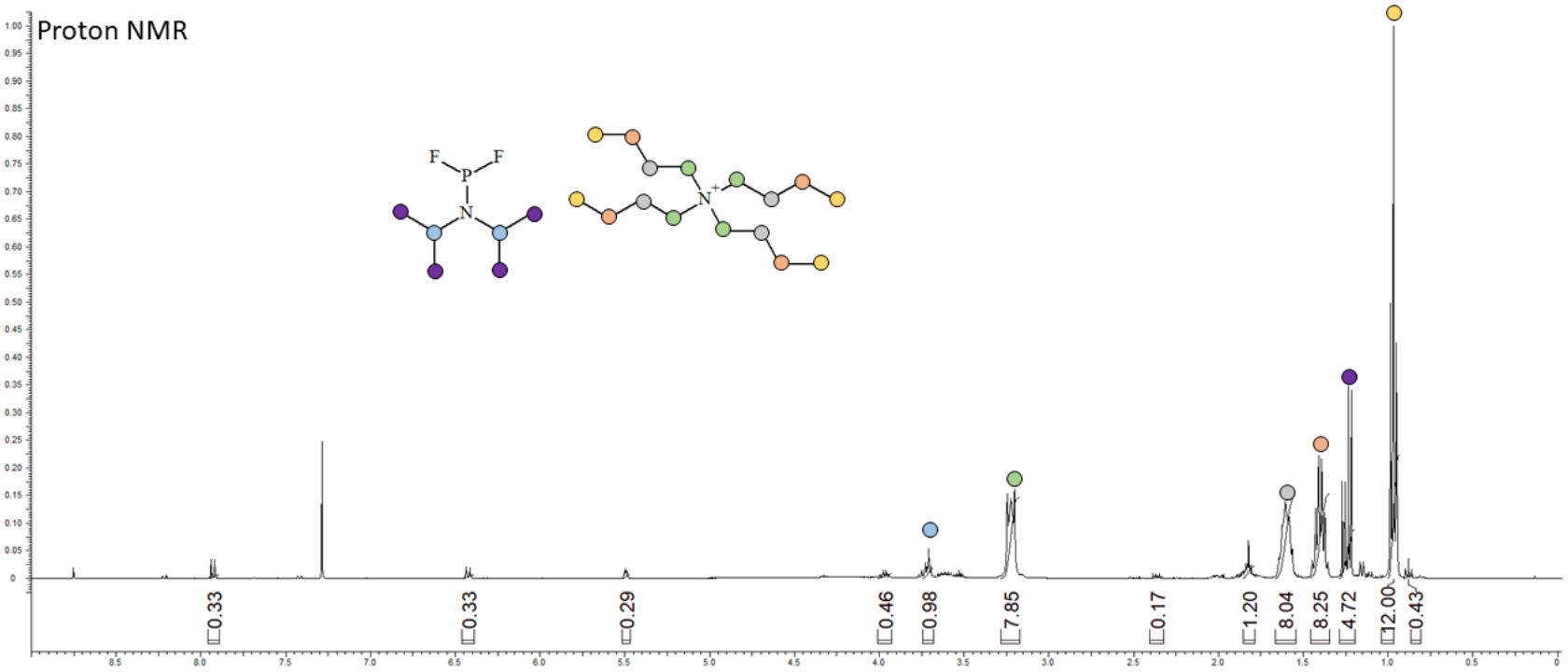

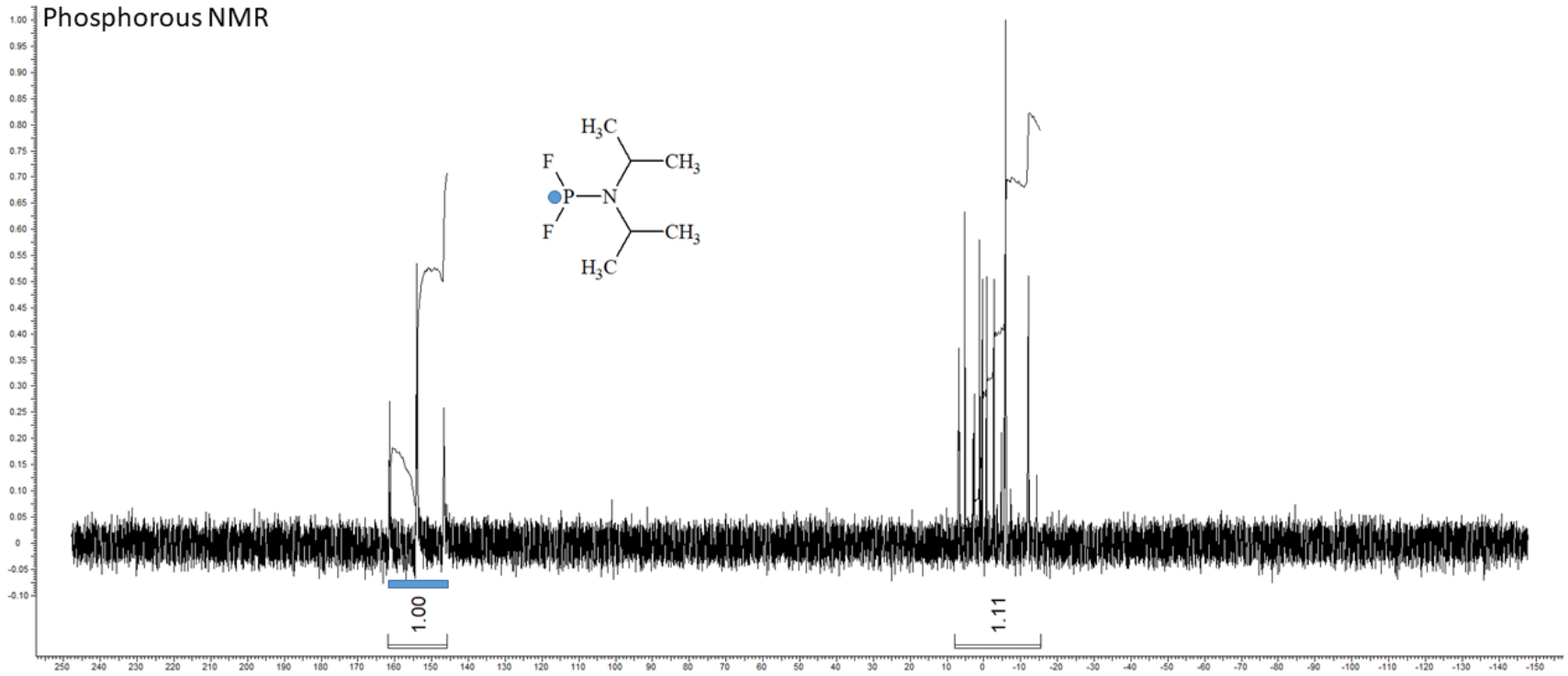
Phosphorous NMR
H3C
CH3
F
P
N
F
CH3
H3C
1.00
1.11

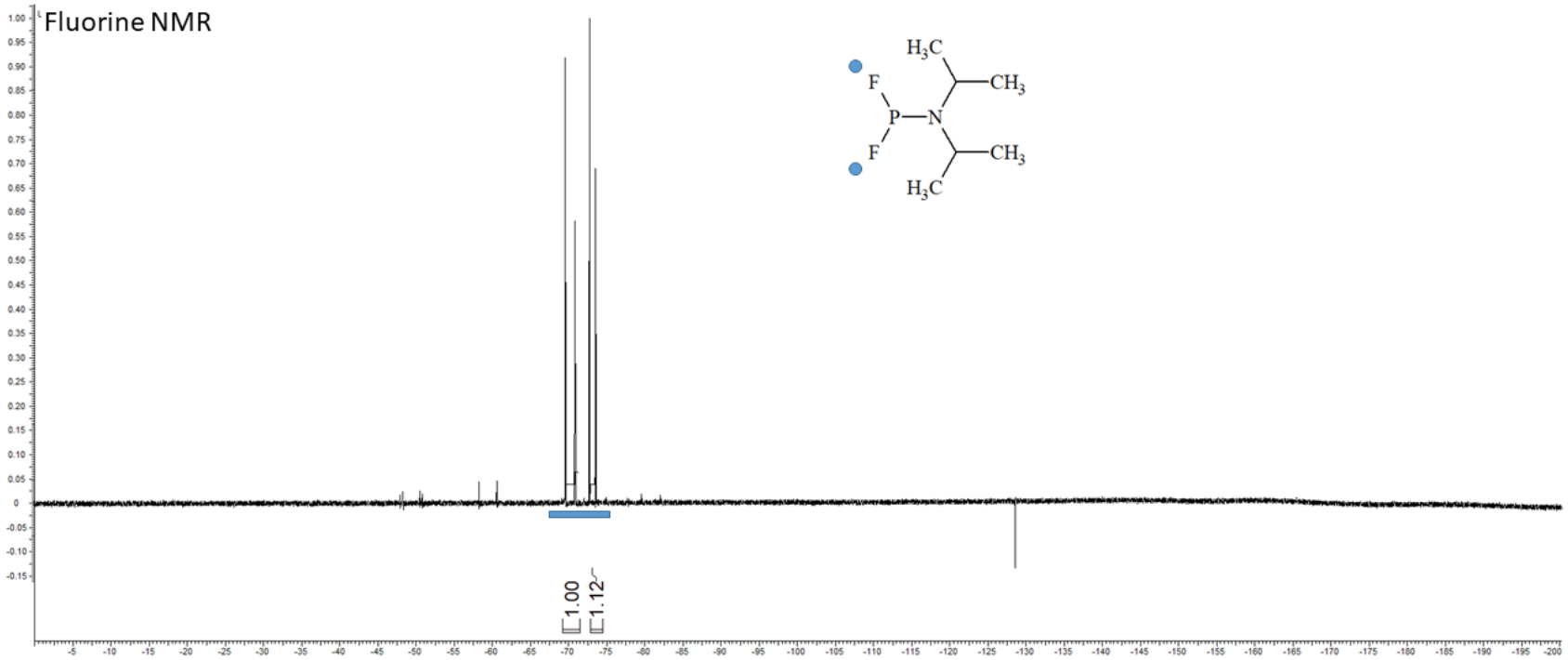
Fluorine NMR
1.00
1.12
F
P
N
F
H_3C
CH_3
CH_3
H_3C

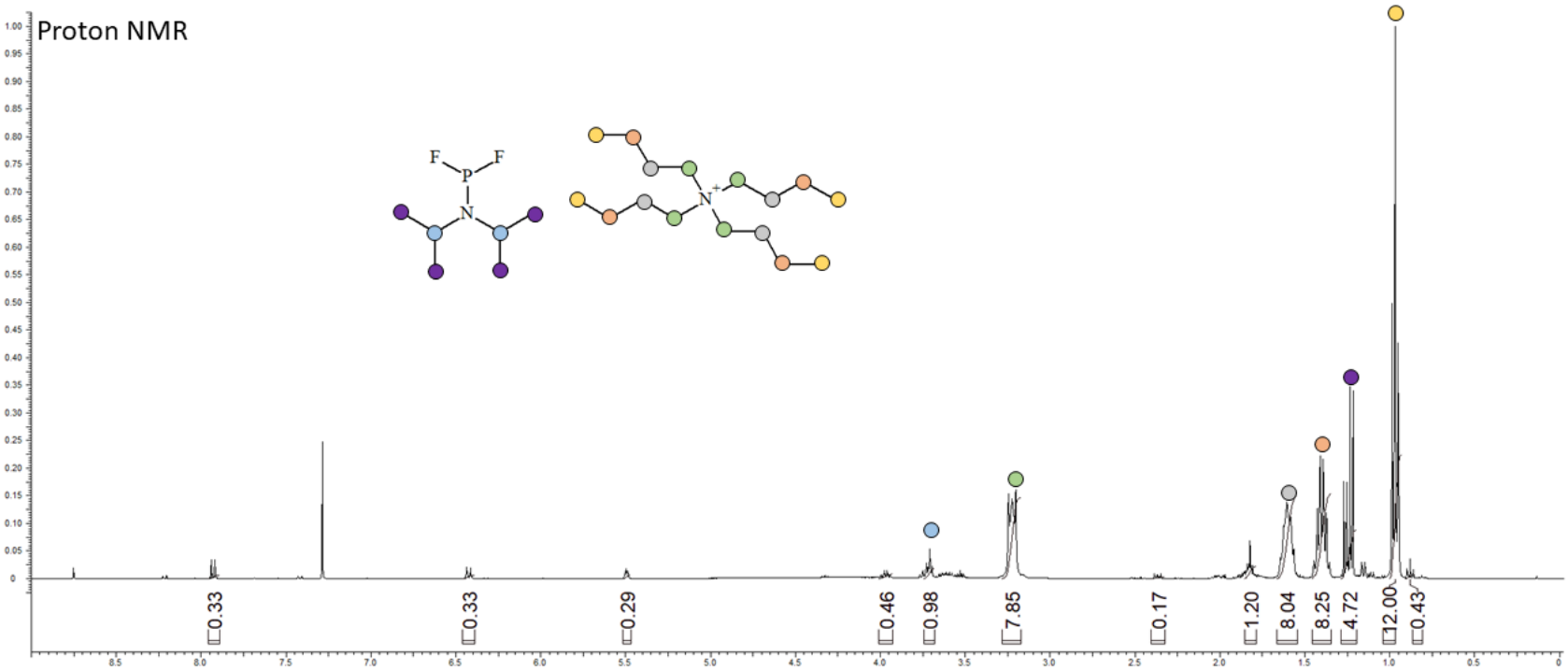
Proton NMR
F
P
F
N
N+
0.33
0.33
0.29
0.46
0.98
7.85
0.17
1.20
8.04
8.25
4.72
12.00
0.43

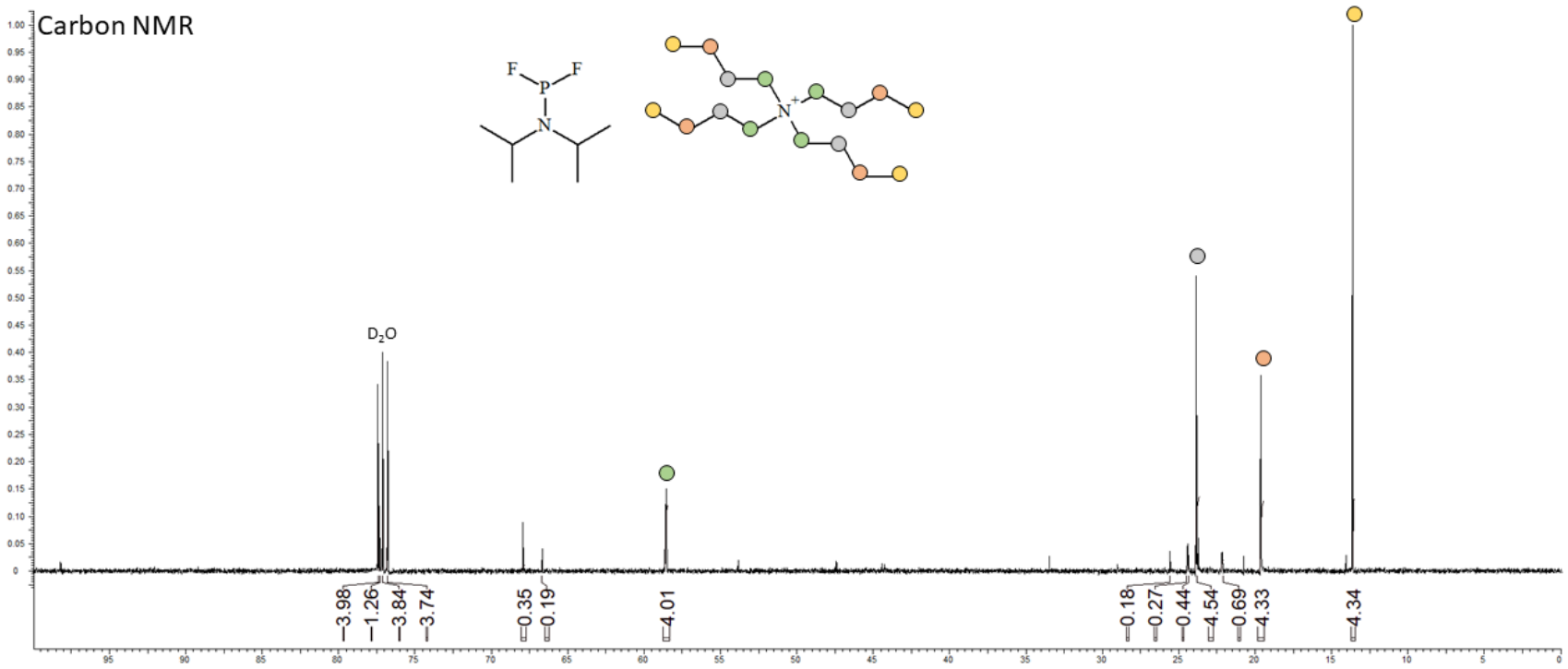
Carbon NMR
F
P
F
N
N+
D2O
3.98
1.26
3.84
3.74
0.35
0.19
4.01
0.18
0.27
0.44
4.54
0.69
4.33
4.34

C5. HPLC Trace of Phosphorofluoridate Modified Antisense Strand

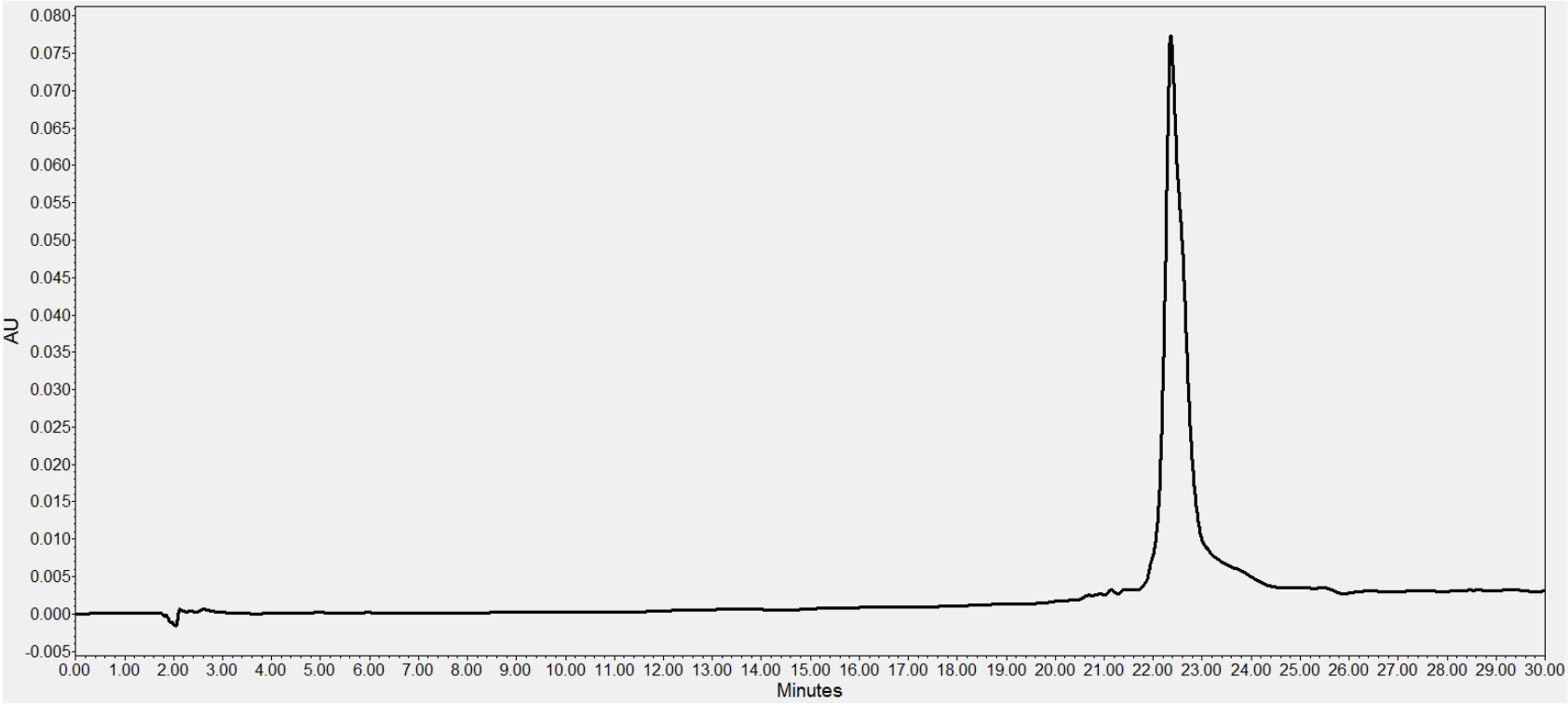

HPLC chromatogram of the phosphorofluoridate modified antisense strand used in siRNA synthesis. Conditions were 5% acetonitrile in 95% 0.1 M triethylammonium acetate pH 7.0 with exponentially increasing acetonitrile up to 20% over 30 minutes. Spectra were processed using Empower 3 software.

C6. HPLC Trace of Phosphorofluoridate Modified Sense Strand

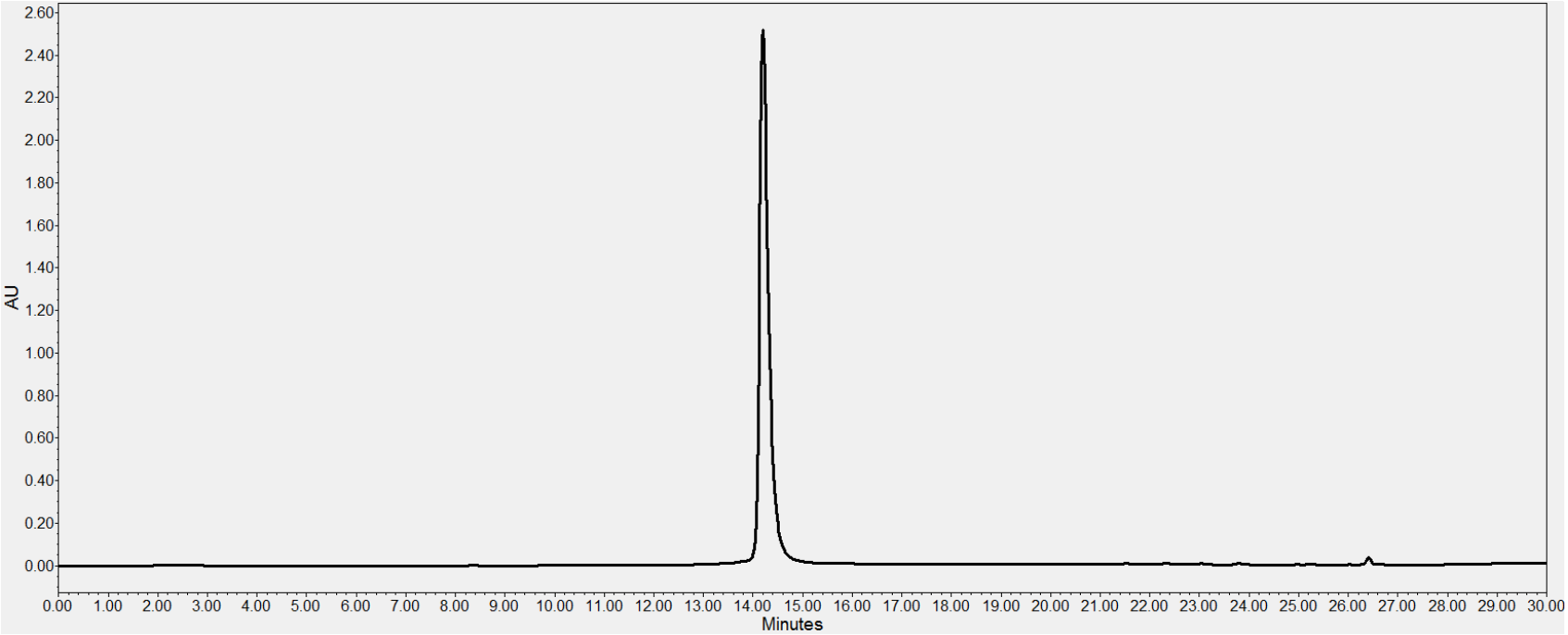

HPLC chromatogram of the phosphorofluoridate modified antisense strand used in siRNA synthesis. Conditions were 5% acetonitrile in 95% 0.1 M triethylammonium acetate pH 7.0 with exponentially increasing acetonitrile up to 100% over 30 minutes. Spectra were processed using Empower 3 software.

C7. Mass Spectrometry Data for Phosphorofluoridate Modified Antisense and Sense Strands